

Chapter 4

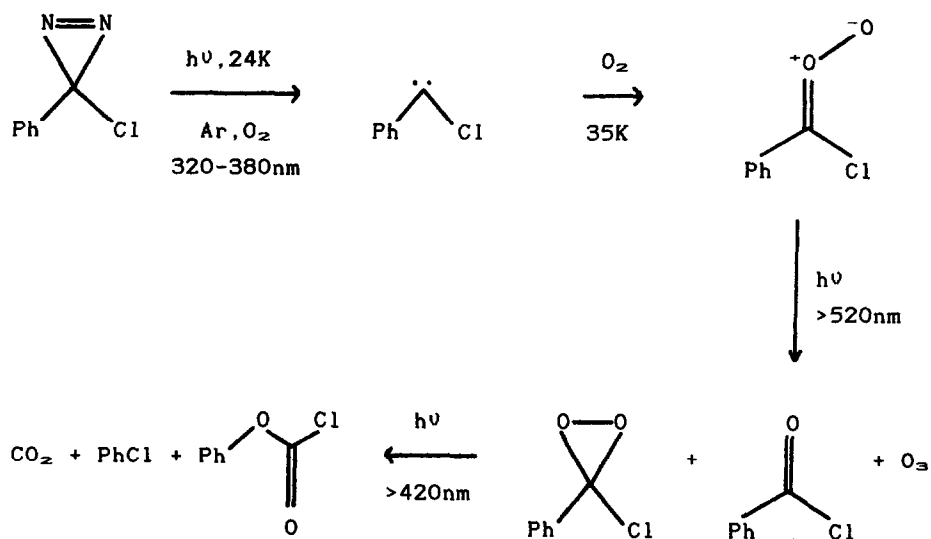
ELEMENTS OF GROUP 4

P.G.Harrison

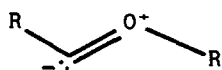
4.1	CARBON	234
4.2	SILICON, GERMANIUM, TIN AND LEAD	264
4.2.1	Transient Intermediates and their Stable Analogues	264
4.2.2	Multiple Bonds Involving Germanium, Tin and Lead	275
4.2.3	Other Low-valent Compounds	294
4.2.4	Molecular Tetravalent Compounds of Silicon and Germanium	313
4.2.5	Structures and Spectroscopy of Tin and Lead Compounds	330
	REFERENCES	347

4.1 CARBON

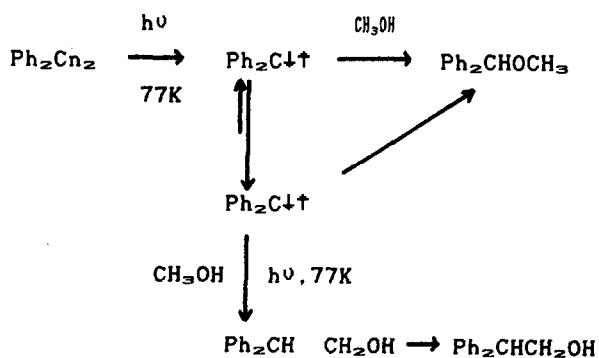
Ab initio quantum mechanical calculations using triple- ζ -plus double polarisation quality basis sets in conjunction with self-consistent-field, two-configuration SCF, and configuration interaction methods show that the three halocarbenes, CHF, CHCl, and CHBr, all have singlet ground states with singlet-triplet separations predicted to be 13.2, 5.4, and 4.1 kcal mol⁻¹, respectively [1]. Two methods are available for the generation of carbenes: the decomposition of the appropriate diazo or diazine derivatives. The diazine method has been employed for the generation of phenylchlorocarbene [2], methoxycarbene [3], and phenoxycarbene [4] in argon or nitrogen matrices at 10K. Warming phenylchlorocarbene in an argon matrix containing oxygen to 35K resulted in the formation of the corresponding yellow-green carbonyl oxide, photolysis of which with visible light gave the corresponding dioxirane, benzoyl chloride, and ozone (Scheme 1). Irradiation of the dioxirane gave mainly phenyl chloroformate



Scheme 1



(1)

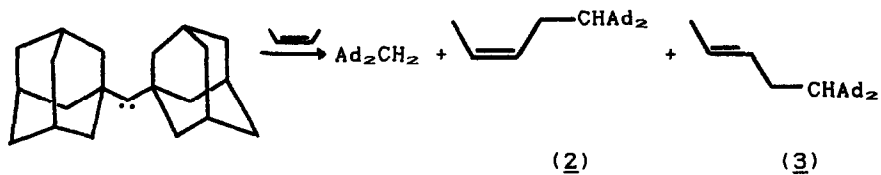
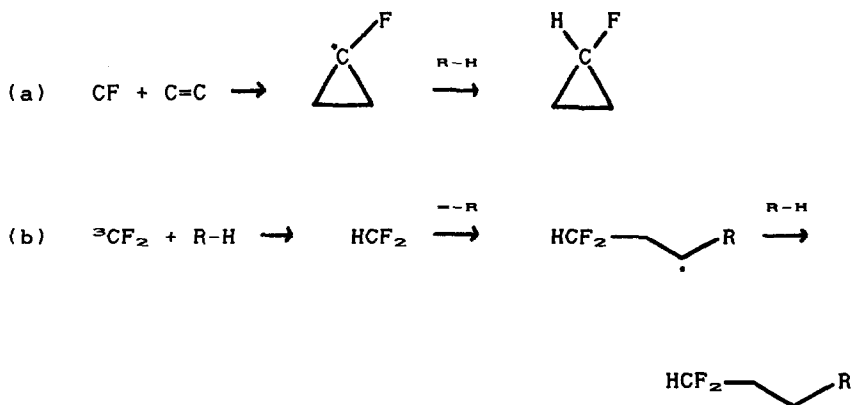
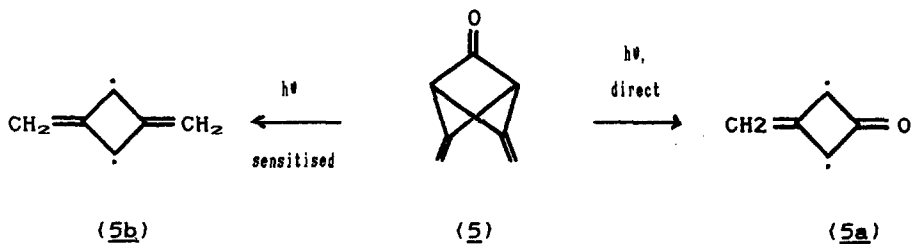
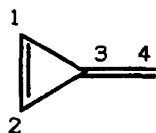


Scheme 2

together with a small amount of chlorobenzene and CO_2 . Deuterium and ^{18}O labelling indicate significant C=O double bond character in methoxychlorocarbene (due to the charge separated form (1)), which exhibits an intense infrared absorption at ca. 1300 cm^{-1} . The data are indicative of two geometric isomers for this carbene, the *cis*-carbene showing a significantly lower C-Cl stretching frequency than the *trans*, consistent with an anomeric interaction. Irradiation of the carbene in argon matrices gives acetyl chloride, ketene, and HCl, whilst in nitrogen small amounts of CO and methyl chloride are also observed. Similar results are also obtained from phenoxycarbene. Photolysis of diphenyldiazomethane in frozen alcoholic matrices affords ground-state triplet diphenylcarbene, which at 77K reacts primarily with alcohols by OH insertion to give ethers [5]. Photolysis produces an excited carbene which reacts with the matrix by hydrogen atom abstraction to give ultimately alcohol-type products (Scheme 2). Raney nickel causes the elimination of N_2 from diazopropane quantitatively at 373K yielding not only propene (cf. the decomposition on quartz wool which requires a temperature of 523K and affords only propane) but also tetramethylethylene in 40% yielding, an observation which lends support to the surface methylene mechanism of the Fischer-Tropsch synthesis [6]. The diazo method has also been used to generate diadamantylcarbene [7] and 1-naphthylcarbene [8]. Irradiation of dry, degassed solutions of diadamantyldiazomethane in *cis*-butene at room temperature leads to the formation of diadamantylmethane together with small amounts of the 1:1 adducts (2) and (3) (Scheme 3). The reactions of 1-naphthylcarbene have been examined by flash photolysis techniques. Generation of the carbene in hydrocarbon solvents leads to the formation of 1-naphthylmethyl radicals. However, in cyclohexane and cyclohexane- d_{12} , the main reaction pathway is carbene insertion into the C-H bond rather than hydrogen-abstraction. The carbene reacts readily with nitriles to yield nitrile ylides, which can also be generated from the corresponding azirine. Reaction with oxygen affords the carbonyl oxide. *Ab initio* calculations have shown that, in contrast to ordinary carbenes, unsaturated carbenes such as $\text{H}_2\text{C}=\text{C}$ ($^1\text{A}_1$) undergo insertion into the O-H bond of water with a non-zero energy barrier ($15.3\text{ kcal mol}^{-1}$ for $\text{H}_2\text{C}=\text{C}$ ($^1\text{A}_1$)).

The correlation effect is also important in determining the barrier height [9]. The univalent species CF appears to be formed as an intermediate in the reaction of arc generated carbon atoms with CF_4 at 77K. When the reactions are carried out in the presence of alkenes as trapping reagents the observed products are fluorocyclopropanes, postulated to arise by addition of CF to the double bond generating cyclopropyl radicals which then abstract hydrogen (Scheme 4(a)), and 1,1-difluoroalkanes. These latter products are postulated to form by reaction of triplet CF_2 (Scheme 4(b)). The addition of CF to alkenes is stereospecific and gives both *cis* and *trans* fluorocyclopropanes with the latter generally predominating [10]. The kinetics and mechanism of the reactions of HCO radicals with unsaturated hydrocarbons have been studied experimentally by the flash photolysis-laser resonance absorption technique in the temperature range 350–510K as well as theoretically in the case of ethylene by *ab initio* SCF MO calculations with double ξ basis sets. The radicals were generated by photolyzing acetaldehyde, and reaction with alkenes and butadiene essentially proceeds via an addition mechanism rather than a hydrogen-atom transfer from HCO to the double bond, which is also energetically favourable. The experimental results are supported by the calculated potential energy surfaces involved in the two possible reaction channels, and in particular that the energy barrier is much higher for the hydrogen atom transfer [11]. The oxygen-methylated carbon monoxide cation, CH_3OC^+ , has been generated in mass spectrometric experiments as a stable (lifetime $>10^{-6}$ s) species in the gas phase. The data was consistent with the structure $\text{CH}_3-\text{O}^+=\text{C}$ [12]. Reaction of $[\text{Fe}(\text{C}_5\text{Me}_5)_2]^+[\text{BF}_4]^-$ with $\text{K}[\text{C}(\text{CN})_3]$ leads to the isolation of $[\text{Fe}(\text{C}_5\text{Me}_5)_2]^+[\text{C}(\text{CN})_3]^-$ as green needle crystals. Crystals comprise independent cations and anions, but there is no evidence for a structure with C_{2v} symmetry corresponding to the $[(\text{NC})_2\text{C}=\text{C}=\text{N}]^-$ resonance form. Infrared and Raman data confirm a D_{3h} structure, which was confirmed by *ab initio* calculations [13].

The reaction between $\text{C}_2\text{H}_5\text{O}^+$ and NH_3 has been investigated by the ion-trapping technique, and the rate constants for three reaction modes were determined. The first gives methanol and protonated methyleneimine via nucleophilic addition of NH_3 to the

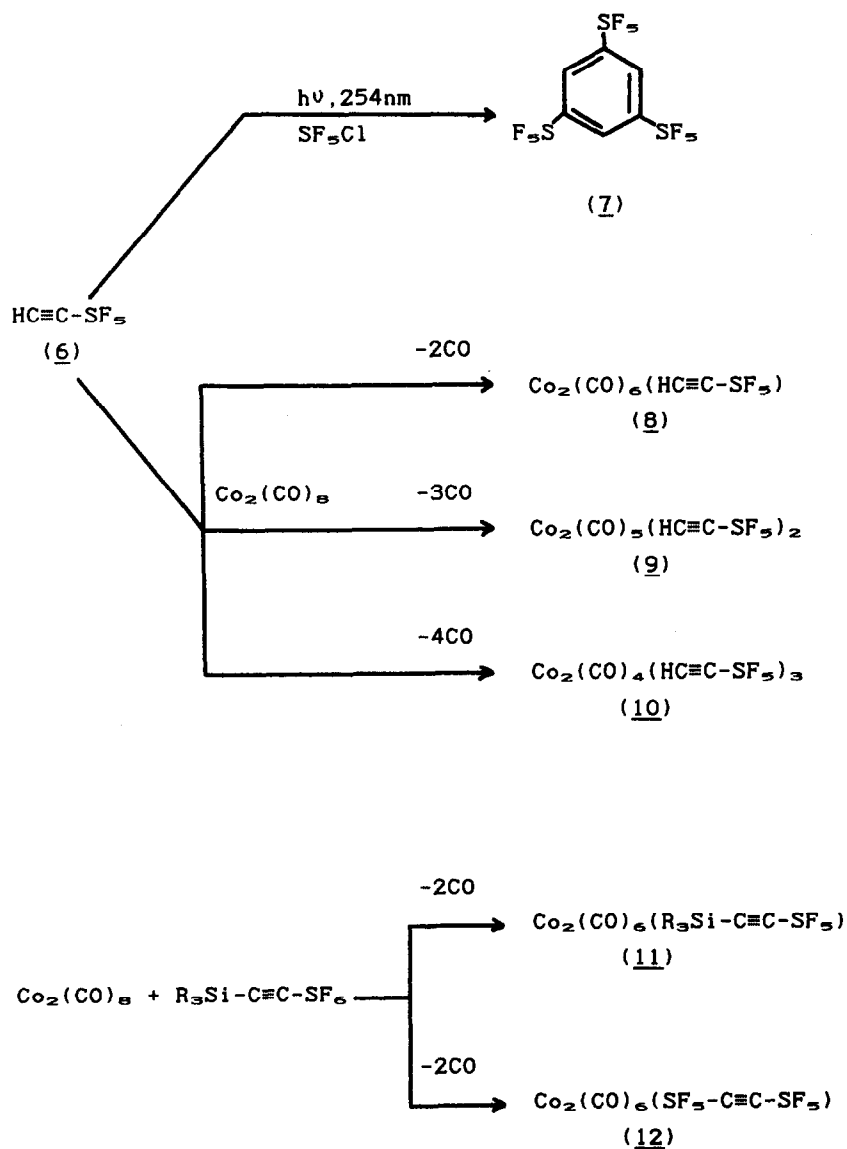
Scheme 3Scheme 4Scheme 5

carbonyl carbon atom followed by a 1,3 proton shift. The other two reactions give formaldehyde and protonated methylamine and the ammonium ion and ethylene oxide [14]. Potential energy profiles of these reactions [14] and also for the S_N2 reactions of OH^- and OOH^- with methyl chloride [15] have been calculated by ab initio methods. The latter reactions are exothermic by 40–50 kcal mol⁻¹ and have the double-well energy surfaces characteristic of gas-phase S_N2 reactions. The results are consistent with experimental observations including the lower reactivity of OOH^- than OH^- in the gas ion. The gas-phase infrared spectrum of the short-lived species formyl cyanide, $CHCOCN$, (obtained by the pyrolysis of methoxyacetonitrile) has been recorded at low resolution and nine of the fundamentals observed [16].

In agreement with experimental data, MNDO calculations show that excited state ($S(1D)$) atomic sulphur inserts into the CH bonds of alkanes such as methane and ethane whereas ground state ($S(3P)$) atomic sulphur does not. Similarly, MNDO calculations offer a reasonable rationalisation for the observed differences in the addition of ground and excited state atomic sulphur to ethylene. Here, the stereoselectivity of the ground state is postulated to result from rapid intersystem crossing rather than from a high methylene rotational barrier in the triplet biradical. Ethenethiol is predicted to result from isomerization of hot thiirane rather than from sulphur insertion into the C–H bond. In addition to acetylene, ground state atomic sulphur is predicted to give thioketocarbene in contrast to thiirene, thioketene and ethynethiol which are predicted to result from reaction of excited state atomic sulphur [17]. The structure of ethylene oxide has been determined at 150 K. In the crystal the molecule is within experimental error an equilateral triangle, with the C–O bond distance being very similar to those in other cyclic ethers whereas the C–C distance somewhat shorter than that found by other methods. MP2/6-31G* calculations predict the same C–O distance, but a longer C–C bond distance. In the crystal lattice, adjacent molecules are connected by short C–H...O contacts [18]. The geometries of fluorinated ethylenes have been optimized at the SCF level with a double- ξ plus polarization function on carbon (DZ+D_C) basis set. The C=C and C–F bond distances for C_2H_4 , $C_2H_2F_2$,

CH_2CF_2 , *cis*- and *trans*-CHFCHF, and C_2F_4 have been optimized at the configuration-interaction level, including all single and double excitations. Good agreement with electron diffraction data was found. The values of $r(\text{C}=\text{C})$ and $r(\text{C}-\text{F})$ decrease with increasing fluorine substitution. Calculated values for the heats of formation of *cis*- and *trans*-CHFCHF are in excellent agreement with experimental data [19]. Microwave spectra, electric dipole moments, and molecular structures have been reported for *cis*- and *trans*-1,2-difluorocyclopropane [20,21], *cis*, *trans*-1,2,3-trifluorocyclopropane [22], and methylenecyclopropene (4a) [23]. All ring bonds in *trans*-1,2-difluorocyclopropane are shorter than the C-C bonds in cyclopropane, but those in the *cis* isomer are longer than those in the *trans* isomer. The orientation of the HCF group with respect to the ring plane is almost the same for both isomers and does not differ significantly from the CH_2 orientation in cyclopropane. The ring bonds in *cis*, *trans*-1,2,3-trifluorocyclopropane are also shortened compared to cyclopropane, with a greater reduction occurring in the two equivalent *trans* ring bonds. The C-F bonds are inequivalent, with longer C-F bonds observed in the HCF moiety exclusively *trans* to neighbouring HCF groups. Analysis of experimental and calculated (MP2/6-31G*) data for (4a) indicates that the dipolar resonance form (4b) constitutes about 20% of the ground state character, but it only contributes a π -delocalization energy comparable to that of 1,3-butadiene. (4a) is concluded to be non-aromatic. The molecular structure of the free allyl radical, produced with 75% relative abundance by vacuum pyrolysis of 1,5-hexadiene at 980°C, has been determined by high-temperature electron diffraction coupled with mass spectrometry. The data are consistent with a planar symmetric geometry with a C-C distance of 1.428(13)Å and a C-C-C angle of 124.6(34)° [24]. Isomeric allyl, 2-propenyl, 1-propenyl, and cyclopropenyl anions and the vinyl anion have been generated in the gas-phase by collision-induced dissociation of the corresponding carboxylate anions using a FT-mass spectrometer. Interconversion of isomers does not occur under the conditions of the experiments. Each ion produces a unique set of products in the bimolecular reaction with N_2O which is characteristic of its structure. The vinylic isomer and cyclopropyl anion exhibit acid-

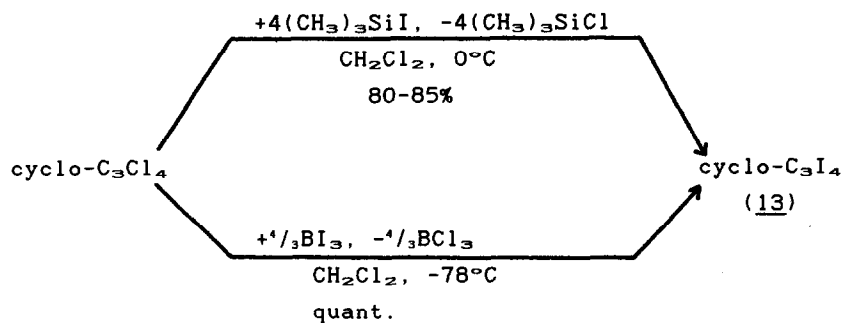
base behaviour which is consistent with their expected high basicities. *Ab initio* MO calculations indicate that propene is more acidic than ethylene at the 2-position but less so at C-1. The vinyl anions and cyclopropyl anion exhibit bent and pyramidal structures, respectively, with relatively high barriers to inversion. The effect of methyl-substitution on both vinyl anion basicity and inversion barriers can be rationalized in terms of charge polarization and hyperconjugative interactions [25]. The lowest energy form of the $C_4H_2^{2+}$ dication has been calculated (at the MP3/6-31G*//HF/6-31G* level) to have a linear ($D_{\infty h}$) structure. The alternative four-membered ring (D_{2h}) structure is 13.3 kcal mole⁻¹ less stable. However, at the MP4SDQ/6-31G*//3-21G level, the linear $C_4H_2^+$ cation ($C_{\infty v}$) is only 3.6 kcal mol⁻¹ more stable than its four-membered ring (C_{2v}) isomer. Despite the very high estimated heat of formation (733 kcal mole⁻¹) for the dication, all the modes of dissociation explored are calculated to be exothermic, the most favourable being dissociation into $C_3H^+ + CH^+$ and into $C_3H_2^+ + C^+$. All the four-membered ring structures show σ -deficient character for the bridging carbon atoms, with the HOMO's being σ orbitals of non-bonding nature with the significant stabilization resulting from 4-centre, 2-electron aromatic π bonding [26]. The direct irradiation of the ketone (5) at 10 K affords the 3-methylenecyclobutanone diradical (5a), whilst a different product, dimethylenecyclobutadiene (5b) is obtained by photolysis in the presence of acetophenone as a sensitizer (Scheme 5) [27]. The mono- and dications of both hydroxyacetylene [28] and aminoacetylene [29] have been characterised by mass spectrometry. The acetylene (6) can be transformed into many other halogeno- and metallo-substituted derivatives (Scheme 6). UV photolysis of (6) produces the cyclic trimer (7), whilst reaction with $Co_2(CO)_8$ affords the complexes (8)-(12)). The crystal structure of (10) shows it to contain a helical six-membered carbon chain as a ligand [30]. *cyclo-C_3I_4* (13) has been synthesised by two different ways (Scheme 7) and can be isolated as a yellow-brown crystalline powder which decomposes violently at 80°C. The properties of (13), eg the formation of (14) and (15) by reaction with excess Me_3SiMe or Me_3SiNMe_2 and spectroscopies data, indicate that it is best formulated as triiodocyclopropenium

Scheme 6

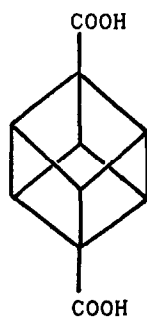
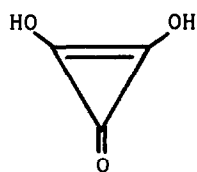
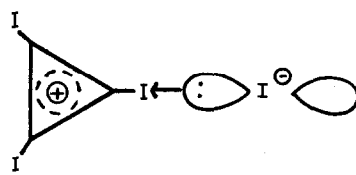
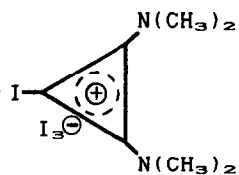
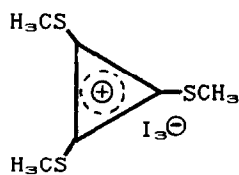
Iodide (18) [31].

Codeposition of lithium atoms and carbon monoxide molecules in an krypton at 12 K leads to the spontaneous formation of numerous products: (i) the mononuclear species $\text{Li}(\text{CO})_n$, with $n = 1, 2, 3$, and >4 , (ii) species with several lithium atoms and one or two CO molecules in which the carbonyl groups are only weakly coupled, and (iii) species identified by stretching modes of either CO single bonds or strongly coupled double bonds and therefore are species in which true chemical bonds are formed between carbonyls [32]. *Ab initio* MO calculations have been carried out on the low stoichiometry complexes and show that the 1:1 Li-CO complex corresponds to a linear ${}^{\infty}\Pi$ state in which the lithium atom faces the carbon end of the carbonyl group. An analogous ${}^{\infty}\Pi$ structure is also predicted for the linear 1:2 (OC-Li-CO) complex, while for the 2:1 (Li-CO-Li) complex two inequivalent linear geometries are found corresponding to ${}^1\Pi$ and ${}^{\infty}\Sigma$ states. In all these complexes large electron transfer toward oxygen occurs, leading to large dipole moments for Li-CO and Li-CO-Li. The bonding in these complexes is described as charge transfer between Li^+ and CO^- [33]. The gas phase hydration of carbon dioxide has also been studied by MO calculations (PFDDO and 4-31G SCF). In the most favourable pathway, H and O of water approach respectively O and C of carbon dioxide, and after the transition state is passed the new OH bond is formed followed by formation of the new CO bond. Deformation energies of CO_2 and H_2O contribute most to the energy barrier; exchange repulsive interactions are also important. No barrier is found for the reaction of HO^- with CO_2 . In this case the deformation energy for CO_2 is smaller than the charge transfer and electrostatic interactions as CO_2 and HO^- react, owing to the extra negative charge. In the reverse reaction, the dehydration of H_2CO_3 , the barrier arises primarily from the loss of interaction energies which may be described as charge transfer and electronic interactions [34].

Free carbonic acid (H_2CO_3) has been generated in the gas phase by thermolysis at ca. 120 and characterised by high resolution mass measurement using a mass spectrometer [35]. Bis(trichloromethyl) carbonate $\text{Cl}_3\text{C-O-CO-CCl}_3$, a stable

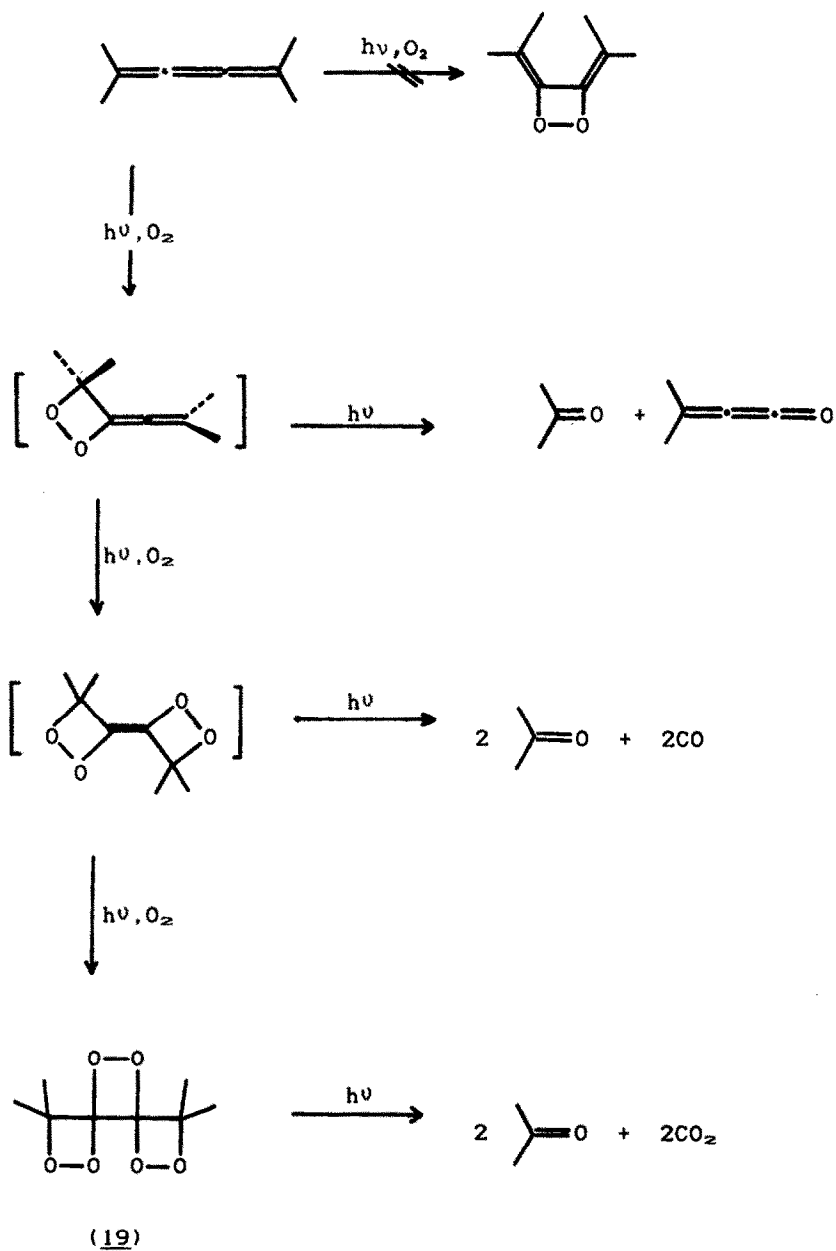


Scheme 7

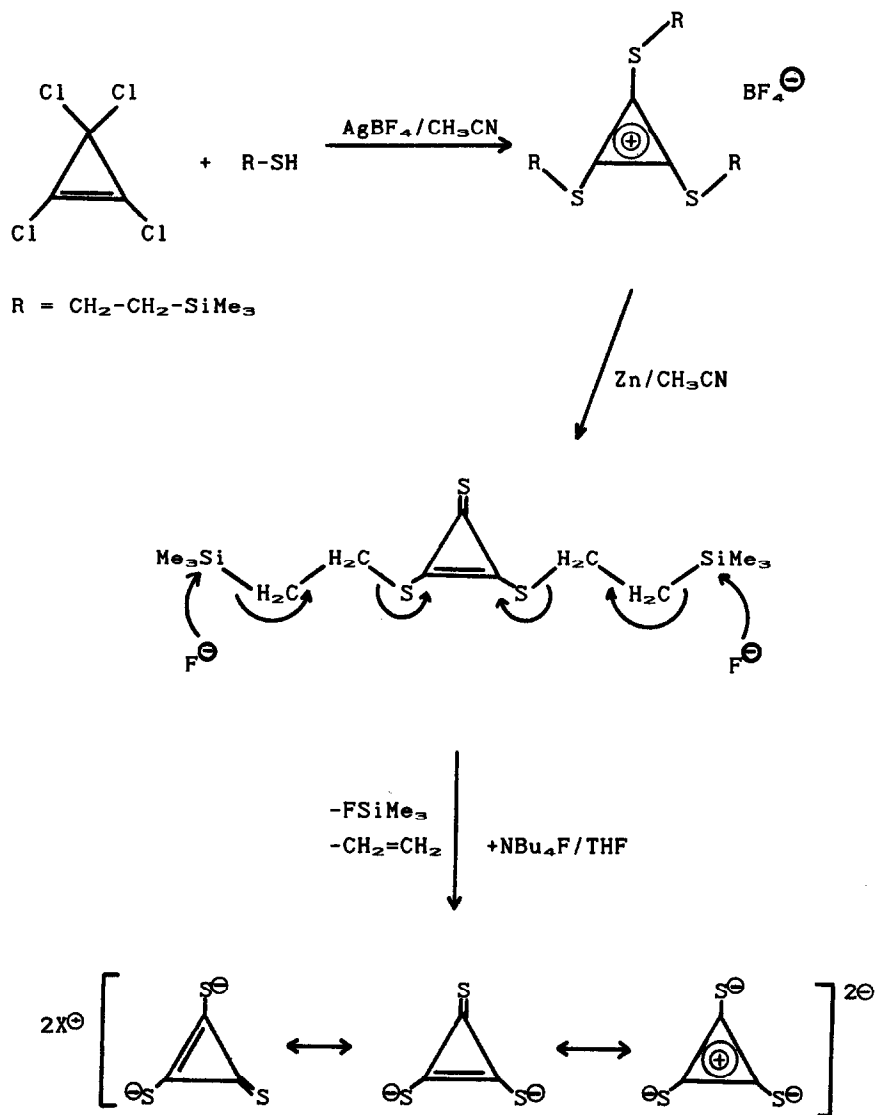


crystalline solid, reacts as three moles of phosgene in the presence of nucleophiles such as pyridine or triethylemine in chloroformylation, carbonylation, chlorination, and dehydration reactions, but is much easier to transport and store than phosgene itself [36]. The structures of two unusual carboxylic acids, deltic acid [37] (17) and 1,4-cubanedicarboxylic acid [38] (18), have been reported. Crystals of the (17) were grown from an alcohol solution of the di-tert-butyl ester, and the structure was found to correspond closely to that proposed previously on the basis of vibrational data. Molecules is situated across a mirror plane in the crystal and has C_{2v} symmetry, and are tied together in strings in a "dimeric" fashion reminiscent of the well-known dimeric carboxylic acid units (eg. the formic acid dimer [39]). Although the molecular geometry is clearly that of 2,3-dihydroxycyclopropen-1-one, the covalent bond lengths show a remarkable degree of conjugation. The high degree of symmetrization is at least in part due to the strong hydrogen bonding in the crystal, and in addition dipolar resonance and ring strain are also important factors influencing the overall geometry of the molecule. (18) exhibits shortened $C(sp^3)-C(sp^2)$ bonds between the cubane and the carboxylic carbon atoms, since the endocyclic C-C-C angles in the rigid cubane framework are compressed to about 90° and the exocyclic angles correspondingly widened to about 125° . The density of (18) is also rather high (1.643 g cm^{-3}), which may also be partly due to the compression of the cubane carbon atoms ensuing from the small bond angles. The photooxidation of 2,5-dimethyl-2,3,4-hexatriene, matrix-isolated in argon at 10K, in the presence of 1-100% gives a variety of oxygen-containing products including the trisdioxetane (19) (Scheme 8). Interestingly, the hexatriene was not totally consumed even after prolonged irradiation in pure oxygen matrices. Rather after a fast initial step, the rate slowed down and finally stopped. Annealing at 40K and cooling back to 10K led to further reactivity demonstrating that the formation of the dioxetanes requires a well-defined orientation of dioxygen molecules relative to the alkene [40].

The trithiodeltate anion (20) has been synthesised by the route shown in Scheme 9, and characterised crystallographically as



Scheme 8



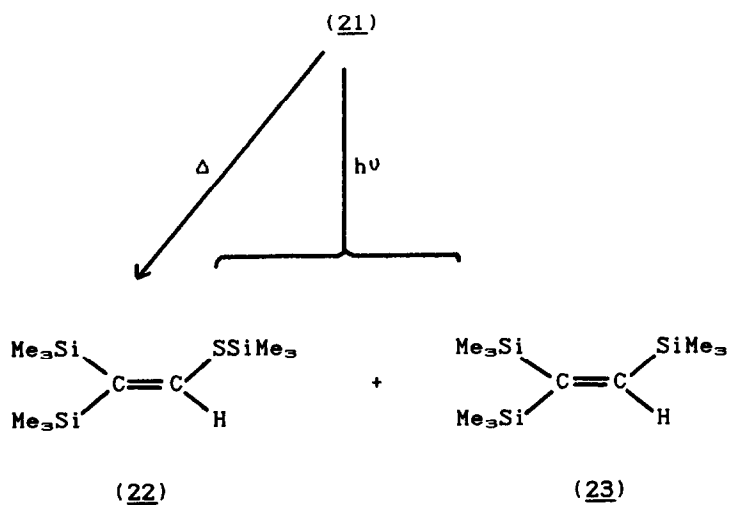
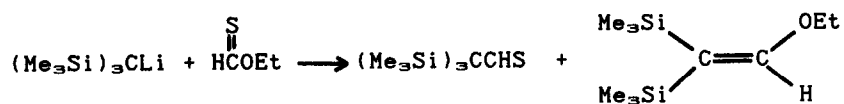
a, X = NBu₄; b, X = Na; c, X = Ph₃MeP

(20)

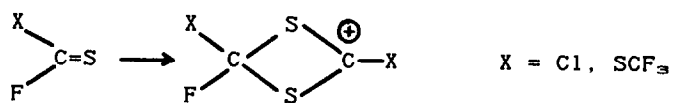
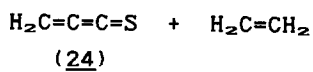
Scheme 9

the disodium salt [41]. Vibrational data are similar to those of the isoelectronic cation of trichlorocyclopropenylum, and are consistent with the planar D_{3h} symmetry structure of the crystallographic study. A stable thioaldehyde (21) has been obtained by the reaction of $(Me_3Si)_3CLi$ with O-ethylthioformate (Scheme 10). (21) is a pink-red crystalline solid which can be stored in a refrigerator for a long time without any decomposition and is stable in air at ambient temperature for at least a week. On heating (80°), (21) isomerizes (rather than oligomerizes) to give the vinyl sulphide (22). Photolysis produces the alkene (23) in addition to (22) [42]. The third member of the cumulenethione series, propadienethione (24) is produced in the pyrolysis of cyclopenteno-1,2,3-thiazole. The dipole moment (2.064(8) Debye) indicates that the molecule is planar with C_{2v} symmetry [43]. Solvolysis of the thiocarbonyl fluorides $XFC=S$ ($X = Cl, SCF_3$) in HF/SbF_5 or FSO_3H/SbF_5 yields the dithietan-2-ylum ions (25) (Scheme 11). Reaction of (25) with fluoride in HF gives the dithietanes (26) [44]. N-Acetimidoyl dithiocarbamic acid exists in the dipolar form, $H_2N^+=CMe-NH-CS_2^-$, in two different planar conformations. Adjacent molecules are linked by hydrogen bonds [45]. N-Acetimidoyl dithiocarbamates react with methyl iodide to produce the new methyl ester of N-acetimidoyl dithiocarbamic acid (27), as well as $MeSC(S)SMe$, $MeSC(S)NH_2$, (28), and other minor products [46].

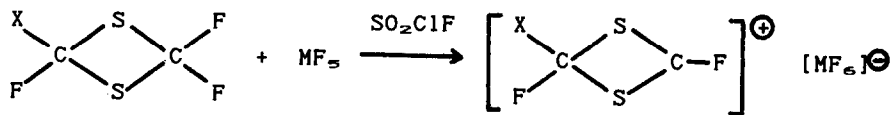
The first vicinal pentaketones have been synthesised (Scheme 12) [47]. Diphenylcarbene undergoes oxidation to benzophenone O-oxide (29) by molecular oxygen in an argon matrix. (29) is more sensitive to irradiation with visible light than diphenyldiazomethane, and hence (29) is only formed in the thermal reaction of oxygen with the carbene. Photolysis of (29) yields diphenyl dioxirane (30) and some benzophenone. The final product is (31) (Scheme 13) [48]. The microwave spectrum of benzyne, generated by the pyrolysis of benzocyclobutene-1,2-dione, has been reported, and indicates that the molecule is planar and of symmetry group C_{2v} [49]. Hexaethynylbenzene (32) has been obtained as a white powder (Scheme 14) which turns brown rapidly in air but only slowly in its absence. Soluble only in more polar solvents such as thf, dme or dmsO, preliminary data show that (32)



Scheme 10

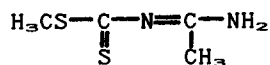


(25)

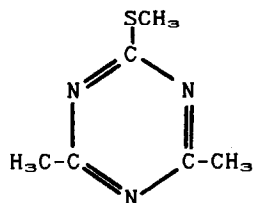
 F_2/HF  $\text{X} = \text{F}, \text{Cl}$ $\text{M} = \text{Sb}, \text{As}$

(26)

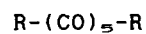
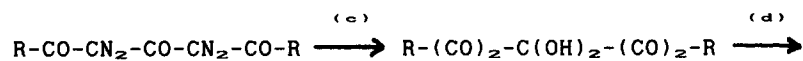
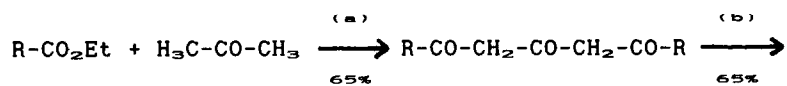
Scheme 11



(27)



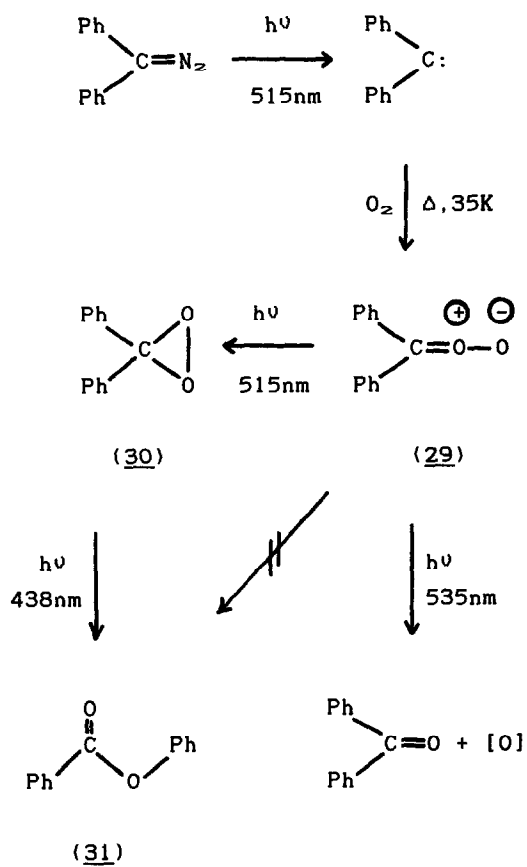
(28)



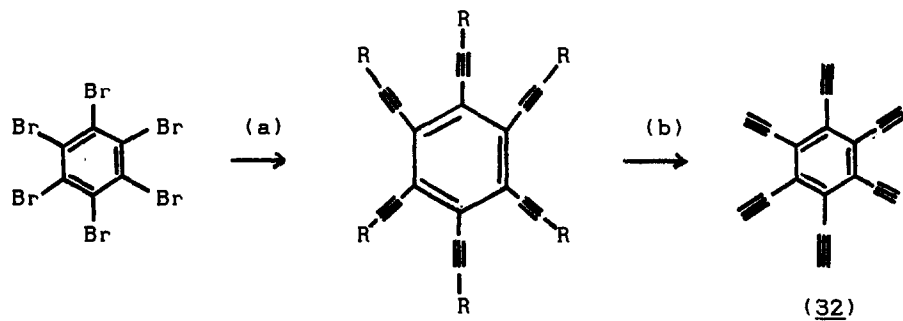
(a) NaH, monoglyme; (b) $p\text{-CH}_3\text{-C}_6\text{H}_4\text{-SO}_2\text{N}_3/\text{Et}_3\text{N}$, CH_3CN ;

(c) $t\text{-C}_4\text{H}_9\text{-OCl}/\text{HCOOH}$; (d) P_2O_5 , CHCl_3 .

Scheme 12



Scheme 13



(a), $R = C(CH_3)_2OH$

(b), $R = Si(CH_3)_3$

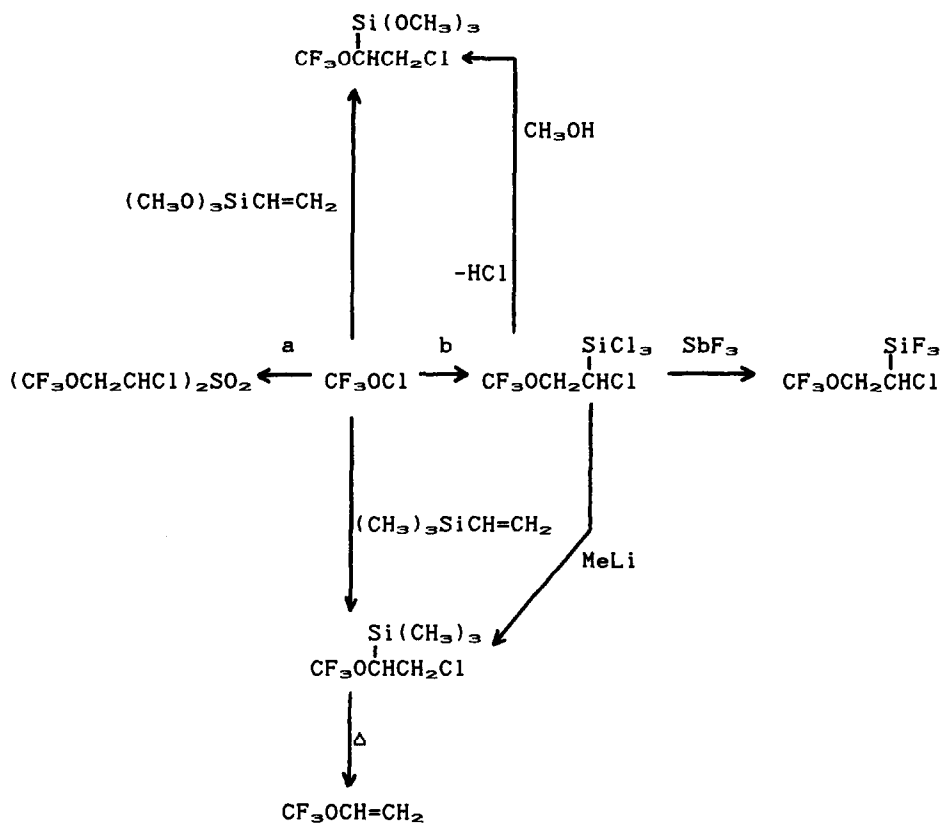
a) $[PdCl_2(PPh_3)_2]$, CuI , PPh_3 (for a only), Et_3N , $RC\equiv CH$;
 (a: 34% ; b: 28%); b) from a: $KOBu^t$, Bu^tOH (undetermined yield);
 from b: $KD.2H_2O$, [18]crown-6, DME, 10min (99%).

Scheme 14

forms complexes with transition metals [50].

The electron affinities of a number of perfluoro aromatic compounds have been determined using a pulsed electron high-pressure mass spectrometer. Data include C_6F_6 (0.52 eV), C_6F_5CN (1.1 eV), $C_6F_5-C_6F_5$ (0.91 eV), $C_6F_5CF_3$ (0.94 eV), $C_6F_5COCH_3$ (0.94 eV), $(C_6F_5)_2CO$ (1.61 eV), and 1,4-(CN) $_2$ C_6F_4 [51]. The salt/molecule reaction technique coupled with matrix isolation has been used to demonstrate the formation of two isomers, *cis* and *trans*, of the $C_2F_3O_2^-$ anion ion-paired with a Cs^+ cation. Infrared data are suggestive of a fluorine-bridged structure for each isomer. On warming, the bridged form rearranges to the more stable $CF_3CO_2^-$ form [52]. Trifluoromethylhypochlorite reacts with substituted alkenes to give mixtures of isomeric ethers. Typical reactions and further transformations of the products are summarised in Schemes 15-17 [53]. Perfluoroalkylfluorosulphates, R_fOSO_2F ($R_f = CF_3CH(CH_3)$, $CF_3C(CH_3)_2$, and $(CF_3)_2CH$), have been synthesized by the reaction of polyfluoro alcohols with sulphuryl fluoride or sulphuryl chloride fluoride, and react with nucleophiles such as amines, polyfluoro alcohols, polyfluoroalkoxides and bromide ion to afford sulphamates, dialkyl sulphates, and polyfluoroalkyl bromides, respectively. In the reaction of $CF_3(CH_2)COSO_2F$ with bromide ion, the polyfluoroalkyl bromide loses hydrogen bromide to give 2, (trifluoromethyl)propene in high yield [54]. Reaction of 2,2,4,4-tetrafluoro-1,3-dithietane and arsenic and antimony pentafluoride affords the stable 2,4,4-trifluoro-1,3-dithietan-2-ylum salts (33) and (34), which can add chloride bromide or iodide to give the corresponding 2,2,4-trifluoro-4-halo-1,3-dithietanes (35) [55]. The structure of two dithietanes have been determined; (33) by crystallography [56], and $(SF_4CF_2)_2$ by electron diffraction [57]. That of bis(pentafluorothio)difluoromethane, $(SF_5)_2CF_2$ has also been determined by electron diffraction [57]. Contrary to other sulphines, Bis(trifluoromethyl)sulphine (36) reacts with amines, alcohols and hydrogen chloride to yield derivatives of the corresponding sulphinic acid (Scheme 18) [58].

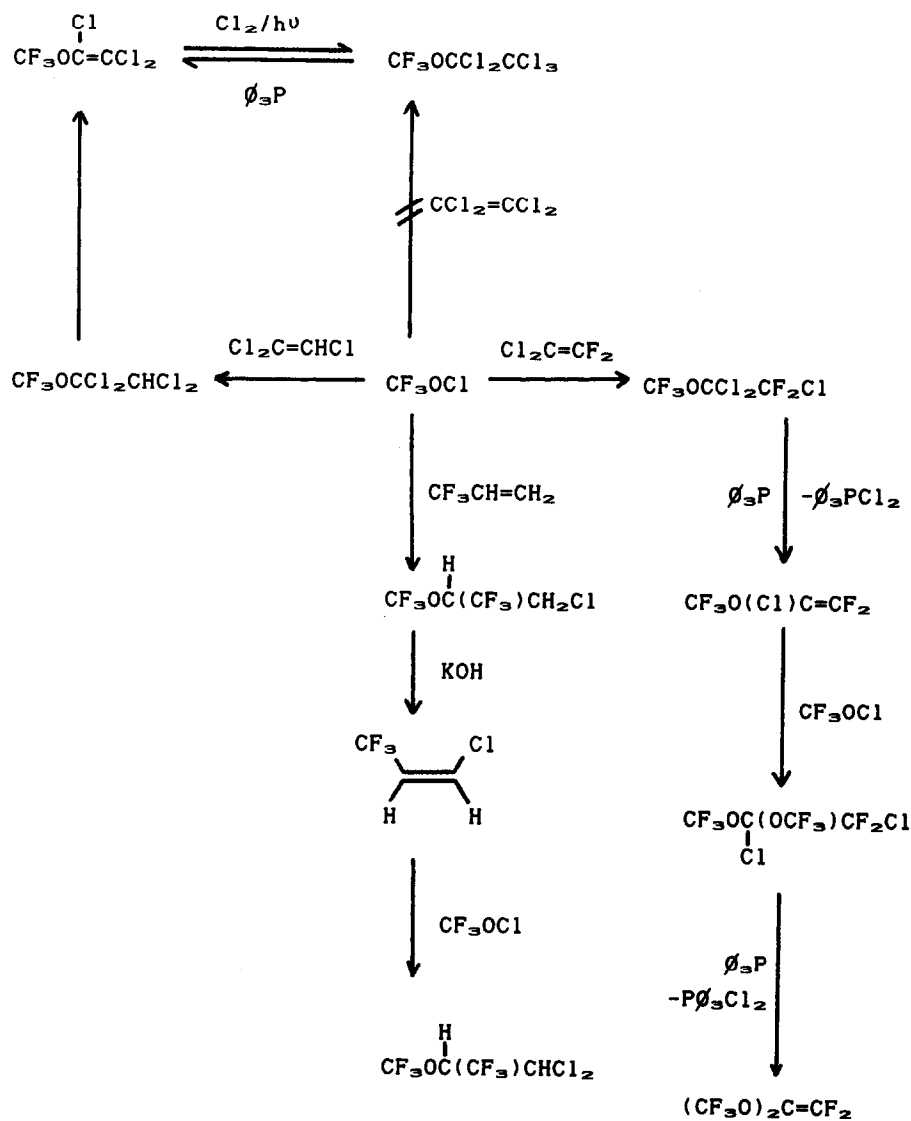
The N-fluorosulphonamides (37)-(39), which are easily prepared in high yield and have excellent stability and good physical properties, are useful selective fluorinating reagents



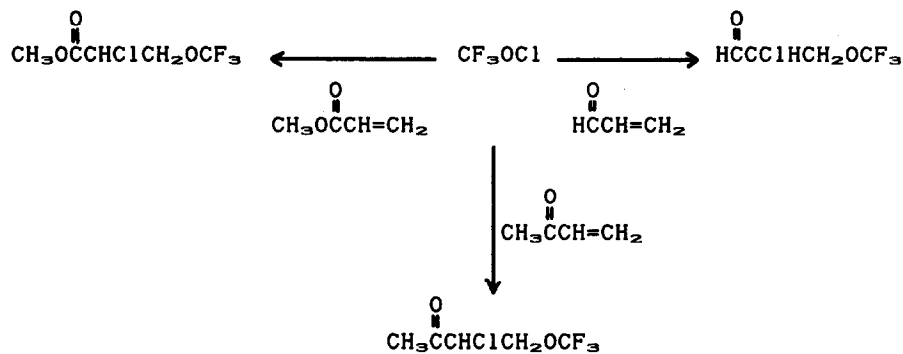
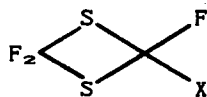
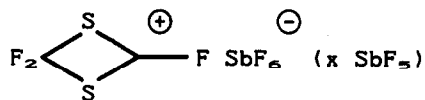
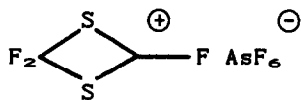
a) = $(\text{CH}_2=\text{CH})_2\text{SO}_2$

b) = $\text{Cl}_3\text{SiCH}=\text{CH}_2$

Scheme 15

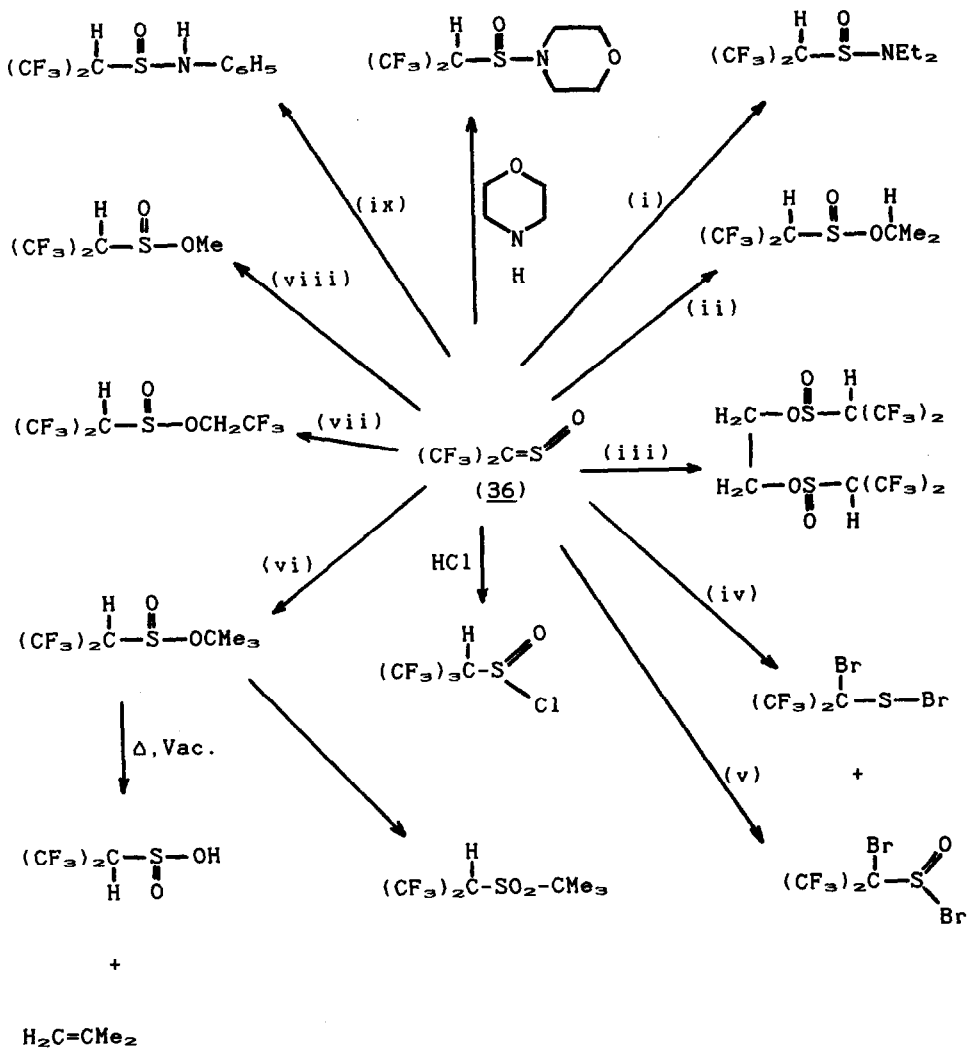


Scheme 16

Scheme 17

X = Cl, Br, I.

(35)



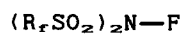
- (i) HNEt_3 ; (ii) Me_2CHOH ; (iii) $\text{HO-CH}_2\text{-CH}_2\text{-OH}$; (iv) HBr ;
 (v) Br_2 ; (vi) $\text{Me}_3\text{C-OH}$; (vii) $\text{CF}_3\text{-CH}_2\text{OH}$; (viii) $\text{CH}_3\text{-OH}$;
 (ix) $\text{C}_6\text{H}_5\text{NH}_2$

Scheme 18

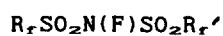
for the replacement of aromatic hydrogen by fluorine at ambient temperature [59]. Reaction of trifluoromethyl isocyanide with trifluoroacetic acid produces N-trifluoromethylformamide, which is surprisingly stable and can be distilled at 116° without decomposition. With hexafluoroacetone, however, only yellow crystals of (40) in which the two five-membered rings are nearly planar (Scheme 19) [60].

The gas phase structure of trifluoroethyldynesulphur trifluoride, $\text{CF}_3\text{-C}\equiv\text{SF}_3$, has been probed by several techniques. Assignment of the vibrational data is mostly simply based on a C_{2v} model with a linear $\text{C-C}\equiv\text{S}$ skeleton, although small deviations cannot be excluded. A linear structure is, however, not compatible with the electron diffraction data, from which the average $\text{C-C}\equiv\text{S}$ angle is determined to be $155(3)^\circ$ for all acceptable models. Ab initio calculations on $\text{HC}\equiv\text{SF}_3$, $\text{FC}\equiv\text{SF}_3$, $\text{CH}_3\text{C}\equiv\text{SF}_3$ and $\text{CF}_3\text{C}\equiv\text{SF}_3$ predict linear carbon using SCF wave functions, but are predicted to bend, albeit to different extents, when electron correlation is included at the MP2 level [61]. All the ring bonds in 1,1,2,2-tetrafluorocyclopropane are found to shorten relative to cyclopropane with the greater reduction occurring in the $\text{C}_1\text{-C}_2$ bond. The FCF and HCH methylene angles are larger than in 1,1-difluorocyclopropane [62]. The very thermally stable, but photosensitive radical, 4,5-bis(trifluoromethyl)-1,3,2-dithiazolyl (41), has been prepared from the corresponding cation. Electron diffraction shows the ring to be planar, and the molecule is paramagnetic in the liquid state at room temperature [63]. The molecular structure and electronic properties of $\text{CF}_3\text{C}\equiv\text{SF}_3$ have been calculated using a double- ξ basis set augmented by sets of polarisation functions on both carbon and sulphur. The lowest energy structure has a short (1.412\AA), polar $\text{C}\equiv\text{S}$ bond and a linear $\text{C-C}\equiv\text{S}$ skeleton, somewhat different from the experimental data which indicates an angle of 171.5° . However, a bent structure with an angle of 171.6° is only 210 cal mole^{-1} higher in energy [64].

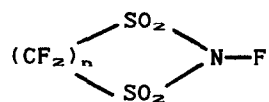
A more convenient synthesis of O=C=C=C=S , by the pyrolysis of (42) (Scheme 20), has been described. The photoelectron spectrum of O=C=C=C=S was also reported [65]. Microwave spectra show that butatrienone, $\text{H}_2\text{C=C=C=O}$, is not kinked in its equilibrium



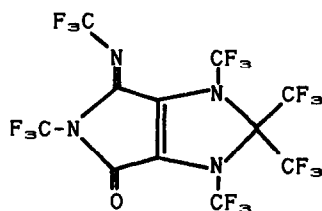
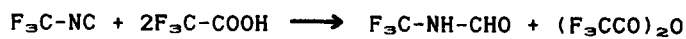
(37)



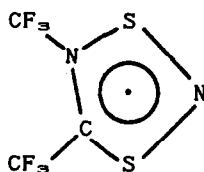
(38)



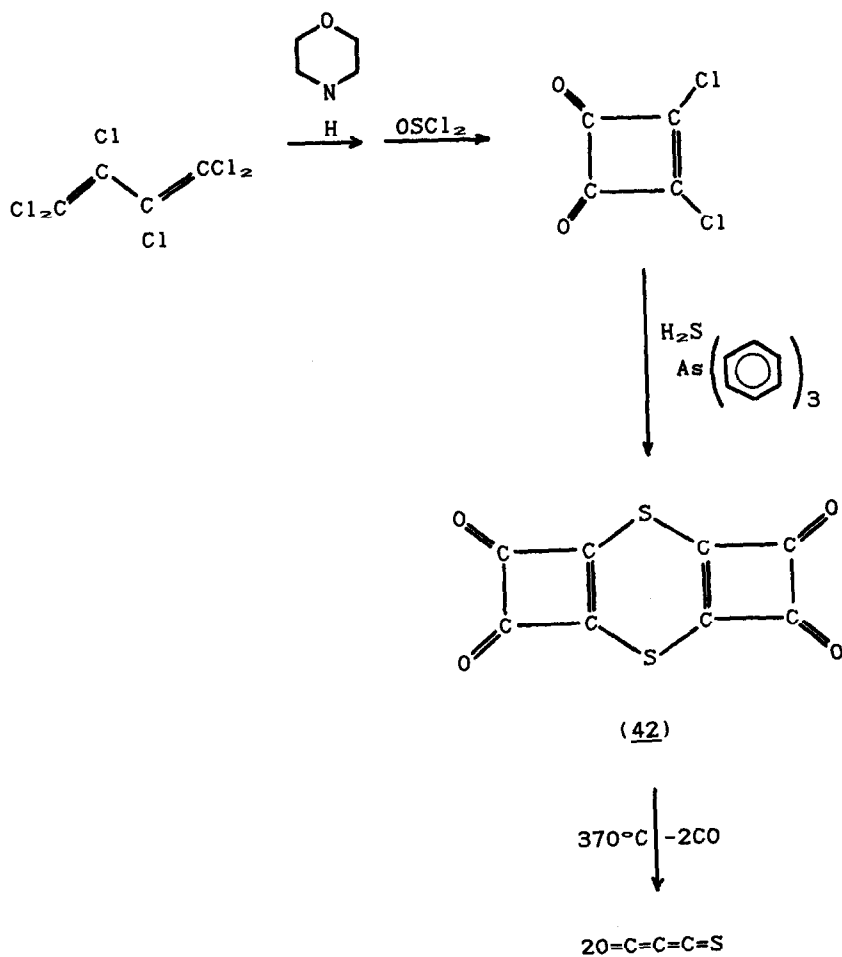
(39)



(40)

Scheme 19

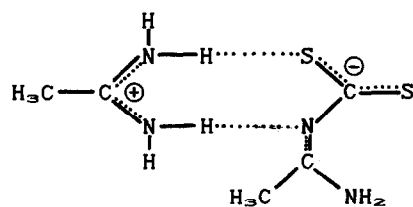
(41)



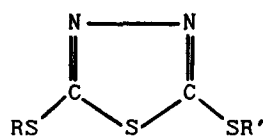
Scheme 20

configuration [66]. The reaction of $\text{H}_2\text{N}-\text{C}(\text{Me})=\text{NH}$ with CS_2 at -15° yields the acetimidium salt of N-acetimidoyl dithiocarbamic acid, $[(\text{H}_2\text{NC}-\text{C}(\text{Me})][\text{S}_2\text{C}=\text{N}-\text{C}(\text{Me})-\text{NH}_2]$, which reacts with metal hydroxides to form the corresponding metal derivatives ($\text{M} = \text{Na}, \text{K}, \text{Rb}, \text{Cs}, \text{Tl}, \frac{1}{2}\text{Pb}, \frac{1}{2}\text{Cd}$) [67]. The structures of these salts have been investigated spectroscopically [68], whilst that of $[(\text{H}_2\text{NC}-\text{C}(\text{Me})][\text{S}_2\text{C}=\text{N}-\text{C}(\text{Me})-\text{NH}_2]$ has been determined by X-ray crystallography [69]. In the crystal, the cation is associated with one anion, which is not planar, by $\text{S}\dots\text{H}-\text{N}$ and $\text{N}\dots\text{H}-\text{N}$ hydrogen bridges forming an eight-membered ring as in (43). Orange coloured N-acetimidoyl dithiocarbamic acid has been prepared by reaction of $[(\text{H}_2\text{NC}-\text{C}(\text{Me})][\text{S}_2\text{C}=\text{N}-\text{C}(\text{Me})-\text{NH}_2]$ in aqueous solution with hydrochloric acid at 0° . The acid, from spectroscopic data, exists in the zwitterionic form $\text{H}_3\text{N}^+\text{C}(\text{Me})-\text{NH}-\text{CS}_2^-$ [70]. Spectroscopic and thermogravimetric data have also been reported for metal N,N'-diphenyl N-formimidoyl dithiocarbamate solvates, $\text{M}[\text{S}_2\text{C}-\text{N}(\text{Ph})-\text{CH}=\text{NPh}]\cdot x\text{L}$ ($\text{L} = \text{water, acetonitrile, dioxane, dms, acetone}$; $\text{M} = \text{Na, K, Rb, Cs, Tl, } \frac{1}{2}\text{Ba, } \frac{1}{2}\text{Pb}$) [71]. In crystals of the potassium salt-dioxane solvate the potassium cation is surrounded by one oxygen, one nitrogen, and three sulphur atoms to form a distorted trigonal bipyramid. The $[\text{S}_2\text{C}(\text{N})\text{N}]$ framework of the anion is planar with the E,E conformation [72]. The potassium salt also reacts with alkyl halides to form the esters $\text{PhN}=\text{CH}-\text{NPh}-\text{CS}-\text{SR}$ ($\text{R} = \text{Me, Et, CH}_2\text{Ph}$) and $(\text{PhN}=\text{CH}-\text{NPh}-\text{CS}-\text{S})\text{CH}_2$ [73]. Reaction of $\text{K}_2[\text{S}_2\text{C}-\text{NH}-\text{NH}-\text{CS}_2]$ or $\text{K}_2[\text{S}_2\text{C}=\text{N}-\text{NH}-\text{CS}-\text{SMe}]$ with H_2Cl affords 2,5-dimethylthio-1,3,4-thiadiazole (44, $\text{R} = \text{R}' = \text{Me}$) as the major product along with a small amount of bis(methylthio)ketazine (45). Reaction of hydrazine with $\text{ClCS}-\text{SPh}$ gives exclusively (44, $\text{R} = \text{R}' = \text{Et}$). With benzyl bromide, $\text{K}_2[\text{S}_2\text{C}=\text{N}-\text{NH}-\text{CS}-\text{SMe}]$ affords a mixture of dibenzyl sulphide, (44, $\text{R} = \text{R}' = \text{CH}_2\text{Ph}$) and (44, $\text{R} = \text{Me, R}' = \text{CH}_2\text{Ph}$) [74]. Hydrazine reacts with carbonyl sulphide in the presence of sodium methoxide to give $\text{Na}_2[\text{SOC}-\text{NH}-\text{NH}-\text{COS}]$, which forms the corresponding methyl ester with methyl iodide [75]. The anion of the N-methyl-N-thioformylcarbamate salt, $[\text{NBu}-n_4][\text{S}_2\text{C}-\text{NMe}-\text{CS}-\text{H}]$, has an essentially planar skeleton [76].

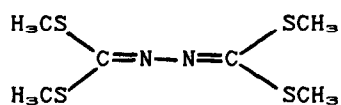
Tetramethylethylenediamine-complexed lithium monothiobenzoate, $(\text{PhCOSLi} \cdot \text{TMEDA})_2$, is dimeric, with an eight-membered ring composed of coplanar carbon, oxygen and sulphur atoms and the lithium atoms



(43)



(44)



(45)

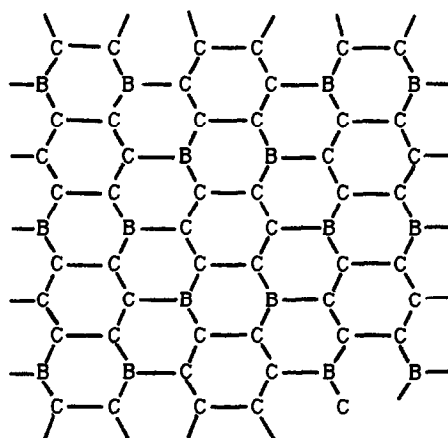


Figure 1. The probable atomic arrangement in a layer of the boron-carbon hybrid BC_{∞} .

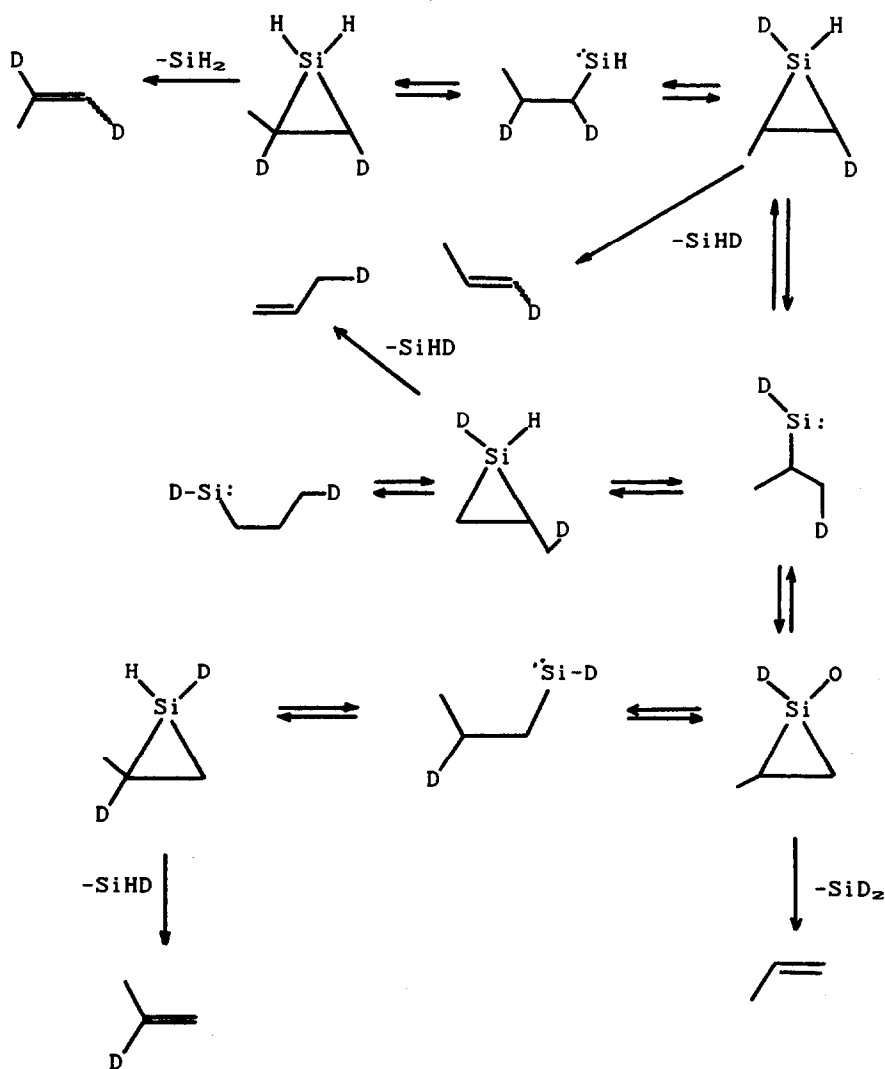
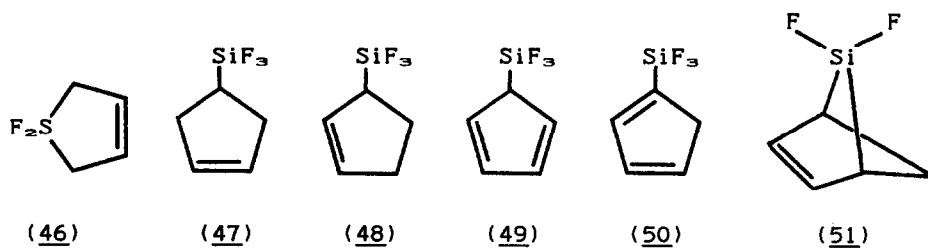
lying above and below this plane in order to reduce excessively angles at oxygen and to accommodate the bulky TMEDA ligands [77].

Extended-Hückel band calculations for patterns of ordered overlayers of hydrogen atoms on unreconstructed graphite (11% coverage) show energy differences as large as 15 kcal mole⁻¹, ascribed primarily to differences in interactions between the hydrogen atoms and graphite rather than direct interactions between hydrogen atoms [78]. The formation of graphite fluoride, (C₆F)_n, from artificial graphite has been investigated. Elemental fluorine is occluded into the particle of fluorinated graphite and distributed in the interface between unreacted graphite and already formed (C₆F)_n. Reaction of fluorine with graphite then occurs in two steps: (i) where both (CF)_n and (C₆F)_n coexist with unreacted graphite, and (ii) when the fluorine content of the product slightly increases in spite of the absence of unreacted graphite [79]. A novel graphite-like material of composition BC₂ has been prepared by the reaction of benzene with boron trichloride at 800°. The probable structure of this material is shown in Figure 1. A similar nitrogen-carbon graphite analogue was obtained from chlorine and pyridine at the same temperature [80]. Intercalation of graphite by SbCl₄F affords various stage products, which are stable in air. Aqueous HCl or KOH removes only pentavalent and no trivalent antimony [81]. Other metal halides which have been intercalated into graphite are SbCl₅, SbCl₄F₂, SbF₅, AsCl₅, SbCl₃, BiCl₃, AlCl₃, GaCl₃, and FeCl₃ [82, 83].

4.2 SILICON, GERMANIUM, TIN AND LEAD

4.2.1 Transient Intermediates and their Stable Analogues.

The gas phase pyrolysis of hexafluorodisilane is a convenient method for the generation of monomeric difluorosilylene. Thus, fast-flow pyrolysis at 670-720° in a mixture with excess 1,3-butadiene affords high yields of the addition product 1,1-difluoro-1-silacyclopent-3-ene (48). The reactions of SiF₄ with halogens have been reinvestigated by both co-condensation and gas-



Scheme 21

phase methods. The former yields a number of fluorohalogenosilanes including mono-, di-, and higher silane derivatives containing SiF, SiF₂ and SiF₃ units. The reactivity towards SiF₂ decreases in the order Cl>Br>I, and, while chlorine and bromine give rise to a number of fluorohalogenosilanes, iodine yields only monosilane derivatives. In contrast, the gas-phase reactions do not proceed to any appreciable extent [84]. A lower limit of $k_2 = 10^8 \text{ M}^{-1} \text{ s}^{-1}$ was estimated for the addition reaction [85]. Several new organosilicon compounds (47)–(51) have been obtained from the reaction of difluorosilylene with cyclopentadiene and cycloheptatriene in both the gas phase and by the cocondensation method [86].

Rice-Ramsperger-Kassel-Marcus calculations have been applied to experimental data for the fast reaction between silylene and hydrogen, and lead to a value of $85.3 \pm 1.5 \text{ kcal mol}^{-1}$ for $\Delta H^\circ_f(\text{SiH}_2)$ [87]. The mechanism of the thermal decomposition of silacyclobutane to silylene and propene has been determined by a detailed study of the pyrolysis of the 1,1-dideuterio derivative. The propene evolved is a mixture of d₀, d₁, and d₂ species with the deuterium being located on all the carbon atoms, and the reaction proceeds by an initial 1,2-migration of deuterium from silicon to carbon producing n-propylsilylene, which reversibly forms a silacyclopropane before ultimately decomposing to silylene and propene (Scheme 21) [88]. The ground state of disilylsilylene, (H₂Si)₂Si, is predicted to be the closed-shell (¹A in C_{2v} symmetry) state, about 6 Kcal mol⁻¹ below the lowest triplet (³B₁ in C_{2v} symmetry). The global minimum on the Si₃H₆ ground-state surface is predicted to be trisilacyclopropane [89]. An ion beam apparatus has been used to investigate the reactions of organosilanes with transition metal ions in the gas phase. Co⁺ and Ni⁺ react with silane to yield metal silylenes. Reaction with methylsilanes lead to the formation of metal silylenes as the major reaction channels, along with several other processes including hydride abstraction, dehydrogenation, and methane loss. Reaction with hexamethyldisilane proceeds mostly by Si-Si bond cleavage. The metal ion-silylene bond energies, $D^\circ(\text{M}^+-\text{SiH}_2)$ (M = Co, Ni), has

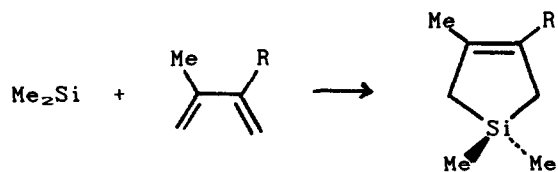
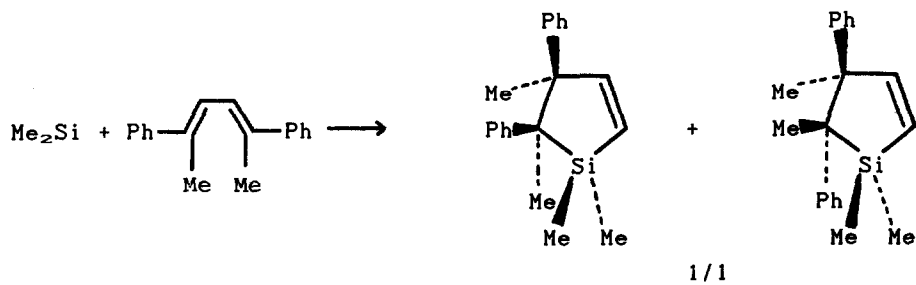
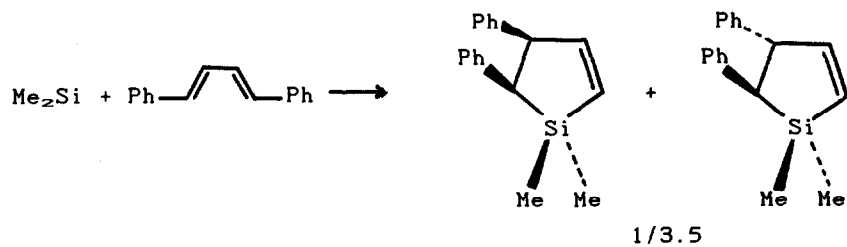
been estimated to be 67 ± 6 kcal mol⁻¹. In these complexes, back-donation of paired 3d electrons from the metal into the vacant 3p orbitals is suggested to supplement the donation of silicon lone pair electrons to a 4s orbital on the transition metal [90].

The ion-molecule chemistry of dimethylsilylene with fluoride and amide ions has been explored by the flowing afterglow technique. Fluoride adds to the silylene to give an adduct anion which was characterised by reaction with nitrous oxide. In contrast, amide ion abstracts a proton from dimethylsilylene giving an anion which was characterised by reaction with carbon disulphide and various acids. The gas phase acidity of this anion is near to that of methanol. The reaction with fluoride ion followed by nitrous oxide has been employed to study the isomerisation of dimethylsilylene to methylsilene. At the highest temperatures, the latter predominates slightly over the silylene [91]. The equilibrium geometries, vibrational frequencies, and infrared intensities of the three lowest lying states of dimethylsilylene have been predicted *bya priori* quantum mechanical methods [92]. Irradiation of matrix-isolated dimethyldiazidosilane affords dimethylsilylene as the major product. Further irradiation with polarized 488 nm light converts the silylene into 1-methylsilene, and the reverse process is accomplished by irradiation on 1-methylsilene with polarized 248 nm light. The resulting map of infrared transition moment directions together with other data allow little uncertainty as to the correctness of the vibrational assignments in both molecules [93]. Pyrolysis of dimethyl-*cis*-1-propenylvinylsilane leads to the extrusion of dimethylsilylene and the formation of a mixture of *cis*- and *trans*-piperlylenes via a sigmatropic hydrogen shift which gives rise to a *cis*-1,1,2-trimethyl-3-vinylsilirane intermediate [94]. Thermally generated dimethylsilylene reacts with phenylated alkynes to give 1,4-disilacyclohexadienes (52) (Scheme 22). However, bulky substituents prevent addition. The strained cycloalkyne (53) affords the silirene (54) (Scheme 23) whose transformation to the 1,4-disilacyclohexadiene is also prevented by steric effects. The products of the reaction with

thermally stable 1,3-dienes gives either 1-silacyclopent-2-enes or -3-enes depending on the substituents (Scheme 24) [95].

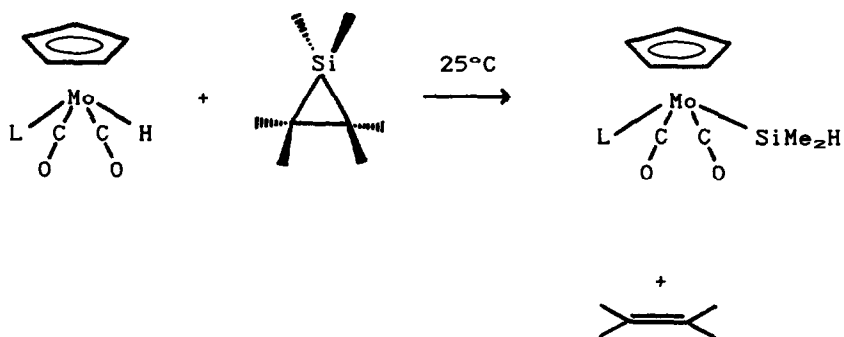
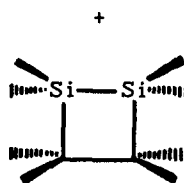
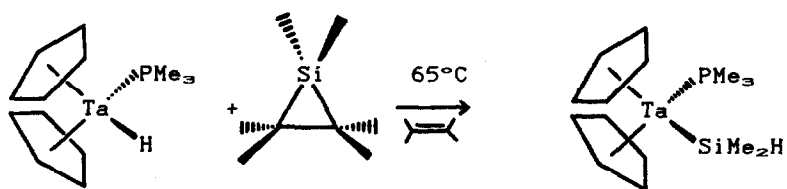
Several studies of interaction with transition metal complexes have been reported. Dimethylsilylene inserts into the Ta-H bond at 85° (no reaction occurs at room temperature) [96] and the Mo-H bond at 25° [97] (Scheme 25). The selectivity of the insertion reaction into the Ta-H bond is dramatically improved by the addition of trimethylphosphine. The acetonitrile-complexed silylene ruthenium complex (55) has been obtained by stirring $C_6Me_6(PMe_3)_2RuSiPh_2OTf$ (Tf = triflate) with $NaBPh_4$ in acetonitrile. The Ru-Si distance (2.328(2)Å) is the shortest such yet observed [98]. Similar complexes of donor molecule stabilised silylenes with $[Fe(CO)_4]$ residues (56) have also been characterised (Scheme 26). Both the complexes (56) are monomeric in the solid state and in solution, and can be sublimed in vacuo. For the complex (56, Do = HMPT), the silicon atom is in a distorted tetrahedral environment with a Si-Fe bond distance of 2.289(2)Å [99]. The intramolecularly base-stabilised complexes (57) have been prepared by substitution at tin in the corresponding $SnCl_2$ complex (Scheme 27). The coordination in each is similar with penta-coordinated tin [100]. The dihalogenogermylene complexes $X_2GeM(CO)_6 \cdot THF$ (X = F or Cl; M = Cr or W) react with 1,2 -dipoles such as aldehydes, imines and oximes by nucleophilic exchange at the germanium atom [101]. New germylene complexes have been obtained by dehydrochlorination of the products of these reactions, $Cl_2GeCr(CO)_6 \cdot B$ (B = $Ph_2C=NH$ or $PhCH=NOH$), using triethylamine or bis(triethylgermyl)mercury (Scheme 28), or by exchange reactions between $Cl_2GeCr(CO)_6 \cdot THF$ and triethylgermyl compounds (Scheme 29) [102].

The germylene, bis(2,4,6-tri-tert-butylphenyl)germanium(II), (58) (from the corresponding organolithium reagent and $GeCl_4$, dioxane at -10°) has been characterised by EXAFS. The data show that only the two aryl groups are located around the germanium atom and no Ge=Ge interaction is present [103]. At room temperature the germylene rearranges to the germaindane (59) by oxidative-addition of a C-H function from the ortho-tert-butyl

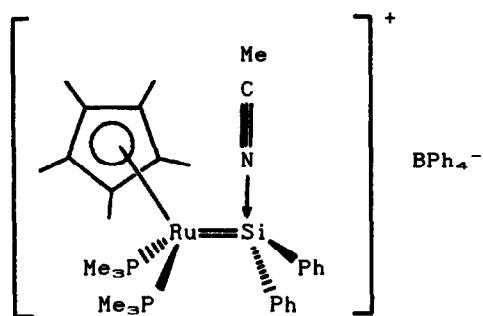


R = H or Me

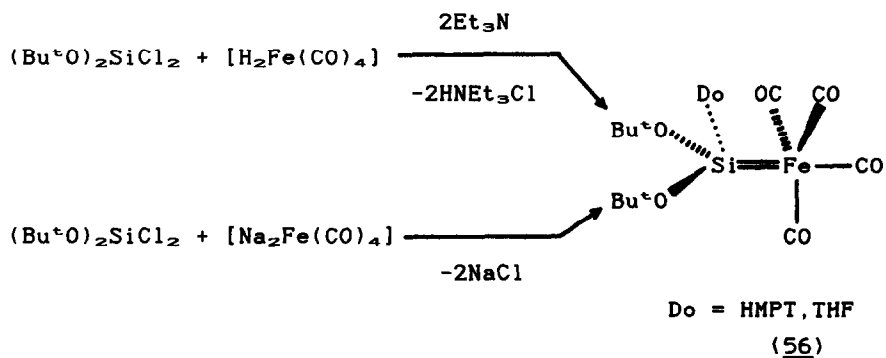
Scheme 24



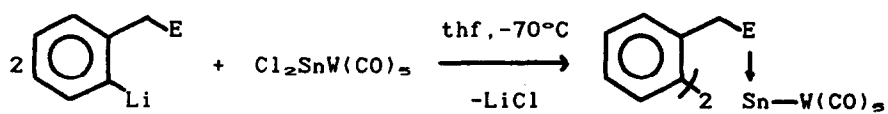
Scheme 25



(55)

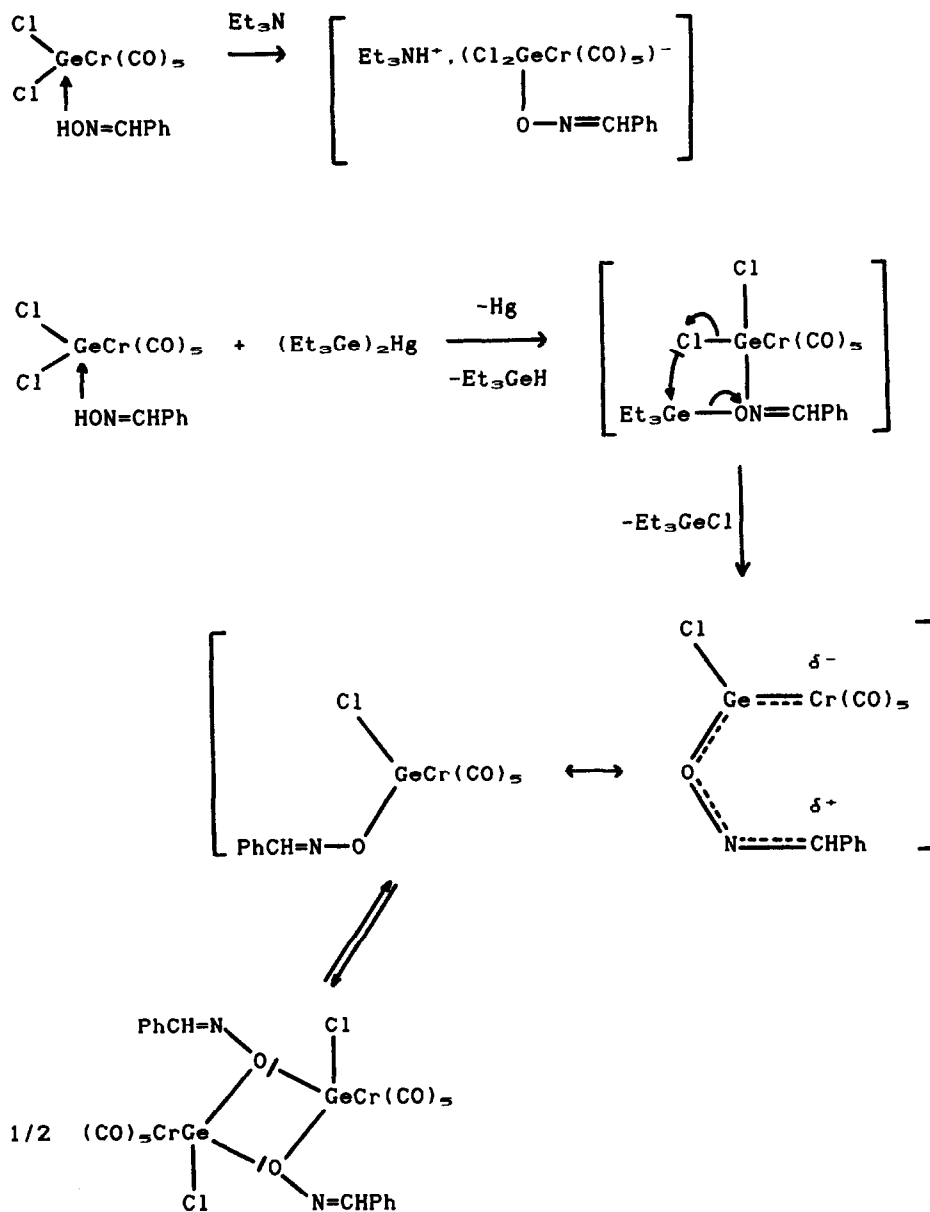


(56)

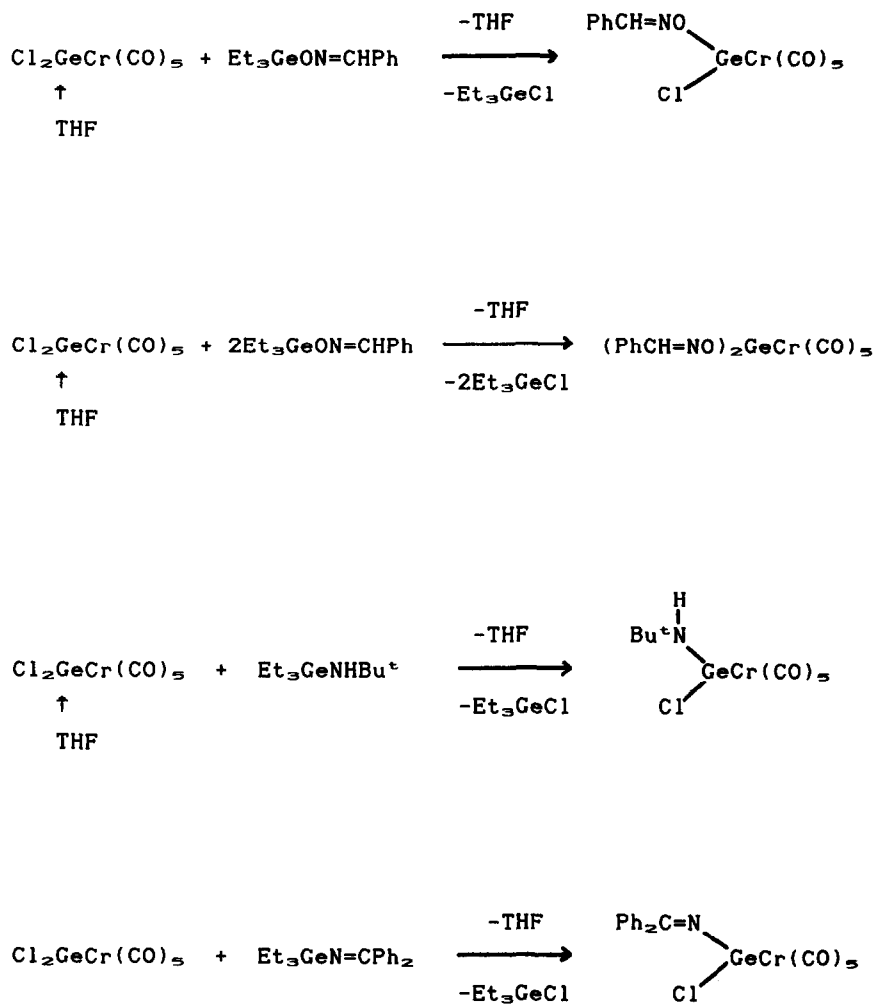
Scheme 26

(57)

Scheme 27



Scheme 28

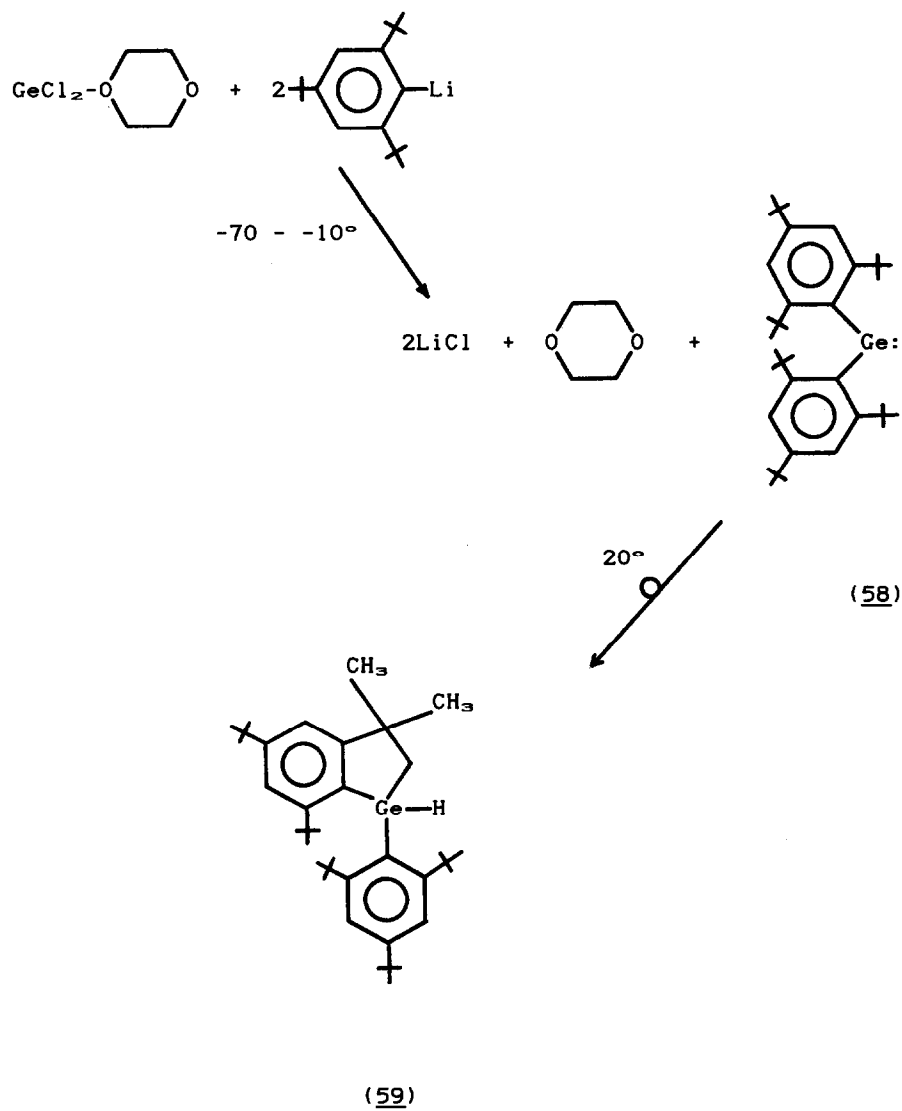
Scheme 29

groups of (58) to the low-valent germanium atom (Scheme 30). (58) is oxidised by elemental sulphur to give the germaindianethiol (60) derived similarly from the intermediate germathione (Scheme 31) [104]. The reaction of SnCl_2 with $\text{Li}[\text{Si}(\text{SiMe}_3)_3] \cdot 3\text{THF}$ in diethyl ether at -78° affords red crystals of the new stannylene (61) as $\text{LiCl} \cdot (3\text{THF})$ adduct. The geometry at tin(II) is pyramidal [105].

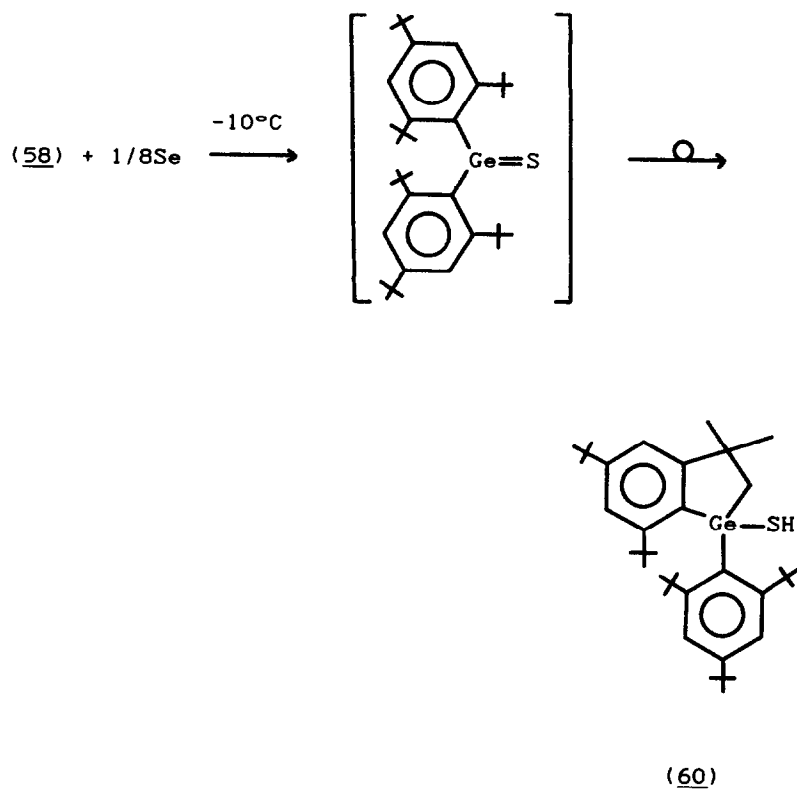
Reactions of the germylene, $\text{Ge}[\text{N}(\text{SiMe}_3)_2]_2$, and stannylene, $\text{Sn}[\text{N}(\text{SiMe}_3)_2]_2$, with diazo compounds have been investigated [106, 107]. Differences in behaviour are very apparent between the two. With $\text{MeCOOC}(\text{N}_2)\text{CO}(\text{OEt})$, the germylene affords a 1:1 adduct (the heterocycle (62)), whilst the stannylene gives a 1:2 adduct (the heterocycle (63)). The oxidative-addition of germanium(II), tin(II) and lead(II) amides, and $\text{Sn}[\text{CH}(\text{SiMe}_3)_2]_2$ with alkyl and phenyl halides and with chloromethanes, $\text{CH}_{4-n}\text{Cl}_n$ ($n = 2-4$), have been described [108]. Similar reactions also take place with pivoyl and benzoyl chlorides and also with trifluoroacetic anhydride to give novel acyl-metal products (Scheme 32). Heating the tin(II) amides $\text{Sn}[\text{N}(\text{SiMe}_3)\text{R}]_2$ ($\text{R} = t\text{-Bu}$, $t\text{-Oct}$) at $80-90^\circ$ for 1-4 hours leads to the aminosilanes $\text{H}[\text{N}(\text{SiMe}_3)\text{R}]$, tin and the cyclometallated spiro-compounds (64) [109]. Treatment of the iridium complex, $(\text{Ir}(\eta\text{-C}_6\text{H}_4)_2(\mu\text{-Cl}))_2$ with $\text{Ge}[\text{N}(\text{SiMe}_3)_2]_2$ in $n\text{-hexane}$ at 20° in the absence or presence leads to the formation of the complexes (65) and (66), respectively, whose structures were also determined [110]. The tin(II) amide, $\text{Sn}[\text{N}(\text{SiMe}_3)_2]_2$, reacts in different ways with the three trimetal dodecacarbonyls $\text{M}_3(\text{CO})_{12}$ ($\text{M} = \text{Fe}$, Ru , Os) and the acetonitrile derivatives (Scheme 33) [111]. The lead analogue $\text{Pb}[\text{N}(\text{SiMe}_3)_2]_2$ undergoes a variety of reactions with the molybdenum hydride complexes $[\text{Mo}(\text{R})(\text{CO})_5\text{H}]$ ($\text{R} = \text{C}_6\text{Me}_6$, $\text{C}_6\text{H}_5(\text{SiMe}_3)_2-1,3$, or C_6H_5) (Scheme 34) [112]. The structures of several of the products were confirmed by crystallography.

4.2.2 Multiple Bonds Involving Germanium, Tin and Lead

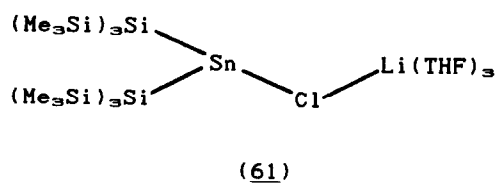
The chemistry of compounds containing multiple bonds involving the heavier Group IV elements continues to undergo rapid development and several new stable compounds have been described.

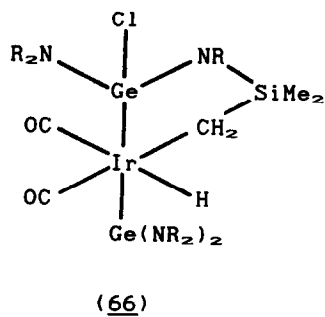
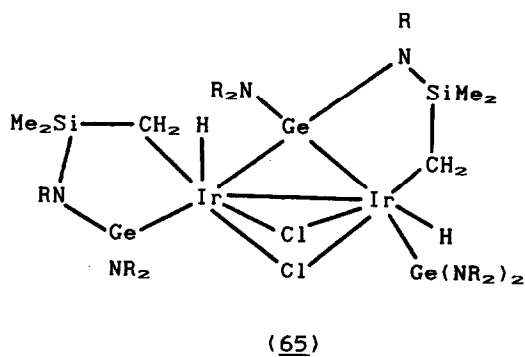
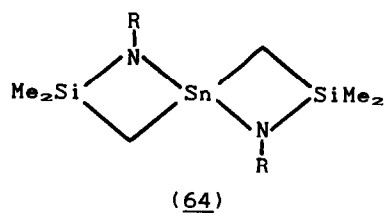
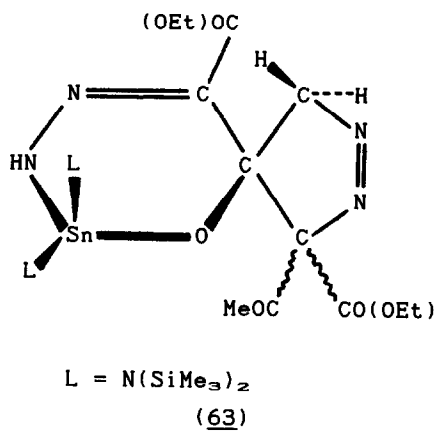
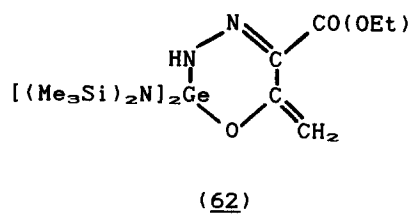


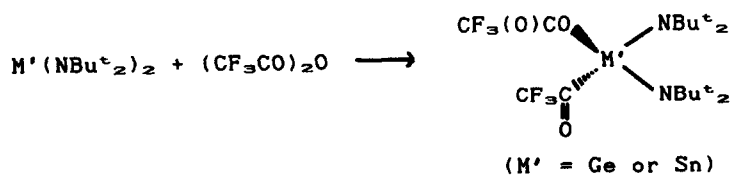
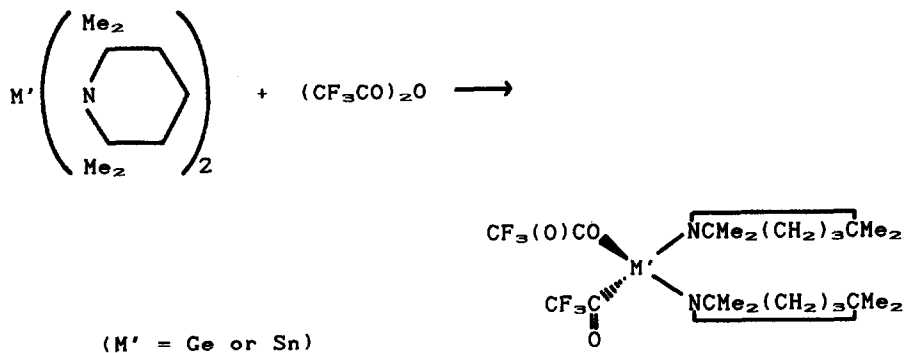
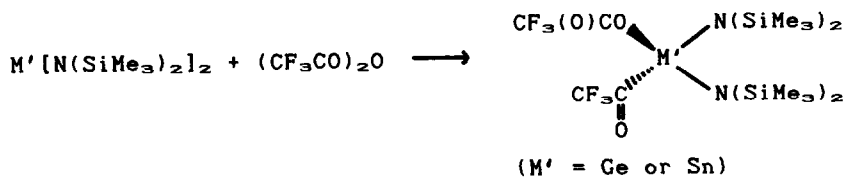
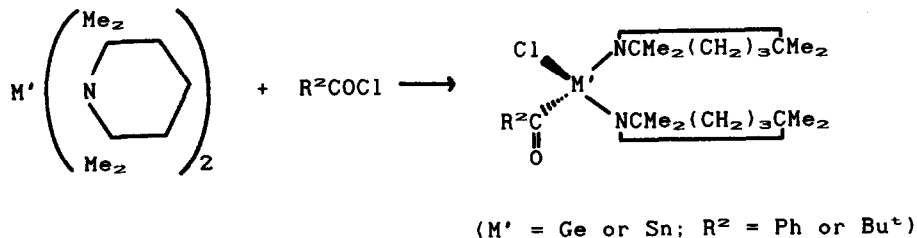
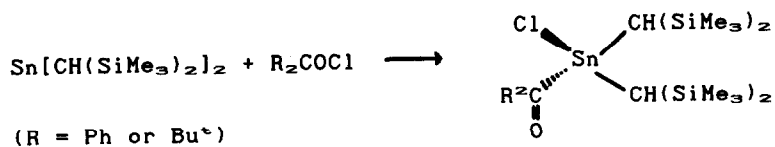
Scheme 30

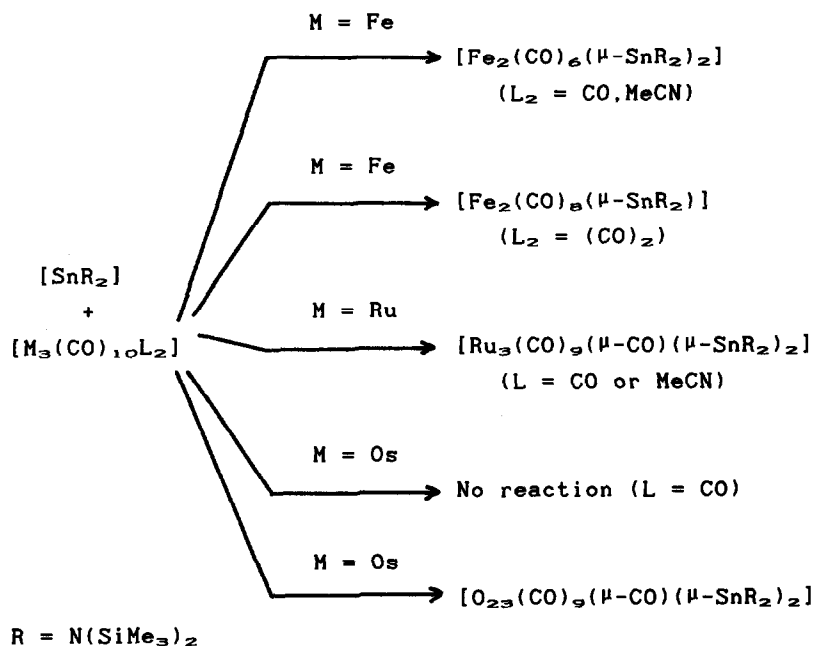


Scheme 31

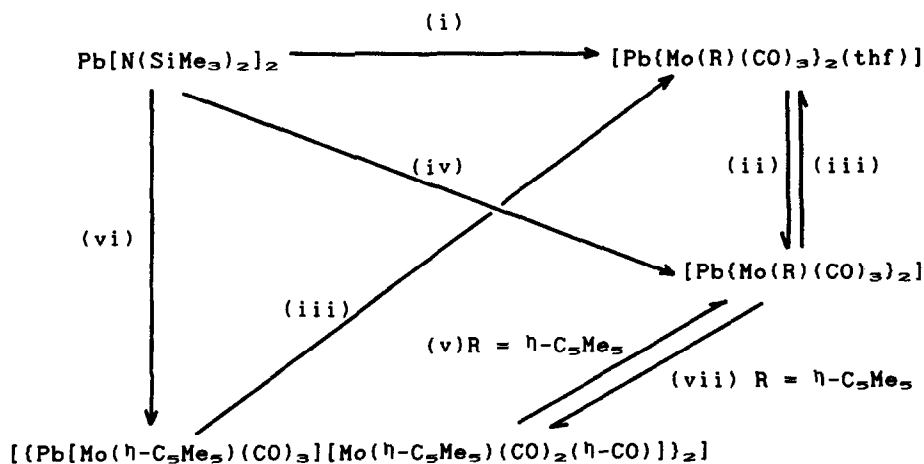




Scheme 32



Scheme 33

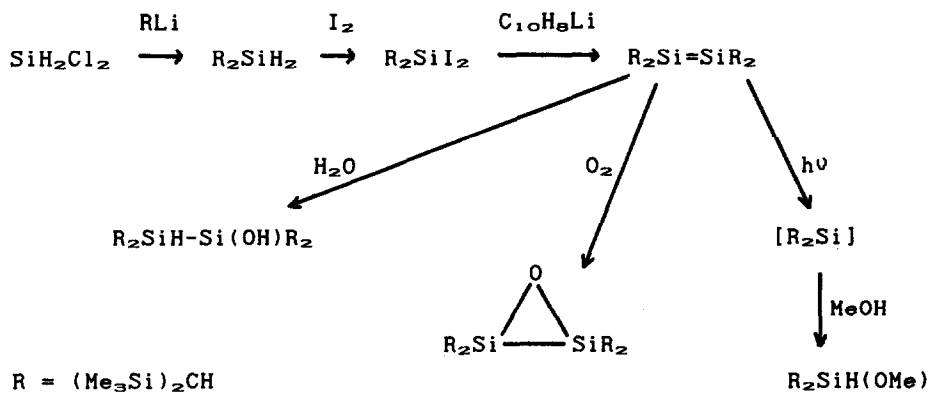
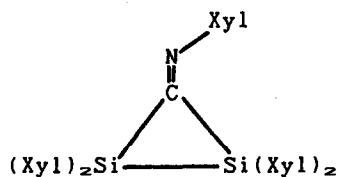


$\text{R} = \eta\text{-C}_5\text{Me}_5\text{(a), } \eta\text{-C}_5\text{H}_3(\text{SiMe}_3)_2\text{(b), } \eta\text{-C}_5\text{H}_5\text{(c)}$; (i) $2[\text{Mo(R)(CO)}_3\text{-H}], \text{thf}, 0^\circ\text{C}$; (ii) (b) $40^\circ\text{C}, 10^{-2}$ Torr, (a) and (c) $25^\circ\text{C}, 10^{-2}$ Torr; (iii) $\text{thf}, 25^\circ\text{C}$; (iv) $2[\text{Mo}(\eta\text{-C}_5\text{H}_3(\text{SiMe}_3)_2)(\text{CO})_3\text{H}], n\text{-C}_5\text{H}_{12}, 25^\circ\text{C}$; (vi) $[\text{Mo}(\eta\text{-C}_5\text{Me}_5)(\text{CO})_3\text{H}], n\text{-C}_5\text{H}_{12}\text{-}n\text{-C}_6\text{H}_{14}, 25^\circ\text{C}$; (vii) $\text{toluene } 40^\circ\text{C}, 10^{-2}$ Torr.

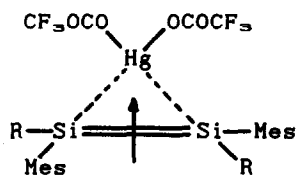
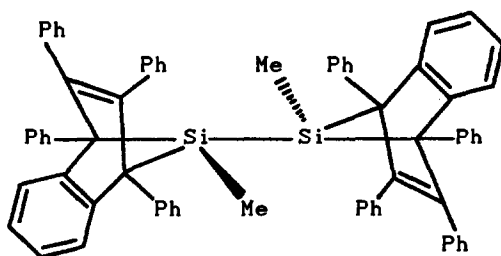
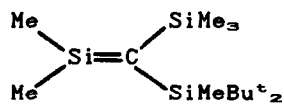
Scheme 34

The chemistry of the silicon-silicon double bond has been comprehensively reviewed [113]. *Ab initio* calculations show that π bonds in silenes are substantially less stable toward addition reactions than π bonds in phosphenes. Two factors contribute to this difference: π bonds in phosphenes are stronger than π bonds in silenes, whilst the converse is the case for the respective σ bonds, both of which can be traced to the preference of second row elements for orbitals containing unshared electrons to have large amounts of *s* character [114]. The electronic structure of disilene has been studied by unrestricted Hartree-Fock, generalized valence bond perfect pairing, and complete-active space self-consistent-field methods. The former undergoes a triplet instability and the electronic structure is a weak singlet diradical. The optimized geometry is shown to be a strongly trans-bent C_{2h} structure [115]. Evidence has been found for the rearrangement of $Me_2Si-Si-H$ to $Me_2HSi-Si-Me$ and for the intermediacy of the silene $Me_2Si=SiHMe$ [116]. The first tetraalkyldisilene, tetrakis(bis(trimethylsilyl)methyl)disilene, has been synthesised by the route in Scheme 35. Some reactions are also shown. Nmr data indicate that rapid inversion between two trans-bent conformers takes place in solution [117]. Silicon-29 nmr chemical shift data has been reported for five tetraaryldisilenes [118]. Shifts are in the range 63.14-65.19ppm. Tetra(2,6-dimethylphenyl)disilene reacts with (2,6-dimethylphenyl)isocyanide in benzene at room temperature to form disilacyclopropanimine (67) as a bright red crystalline solid whose structure was confirmed by X-ray crystallography [119]. Tetraaryldisilenes undergo a facile intramolecular rearrangement involving the exchange of two aryl substituents between the silicon atoms of the silicon=silicon double bond [120]. Intermediates of the type (68) are indicated from nmr data in the reaction of disilenes with mercury(II) trifluoroacetate [121]. (69) is a synthon for dimethyldisilyne, $MeSi\equiv SiMe$ [122].

The nature of the tin-tin bond in bis[bis(trimethylsilyl)methyl]tin has been probed by solid-state and solution nmr. The ^{119}Sn CP/MAS spectrum gives an isotropic

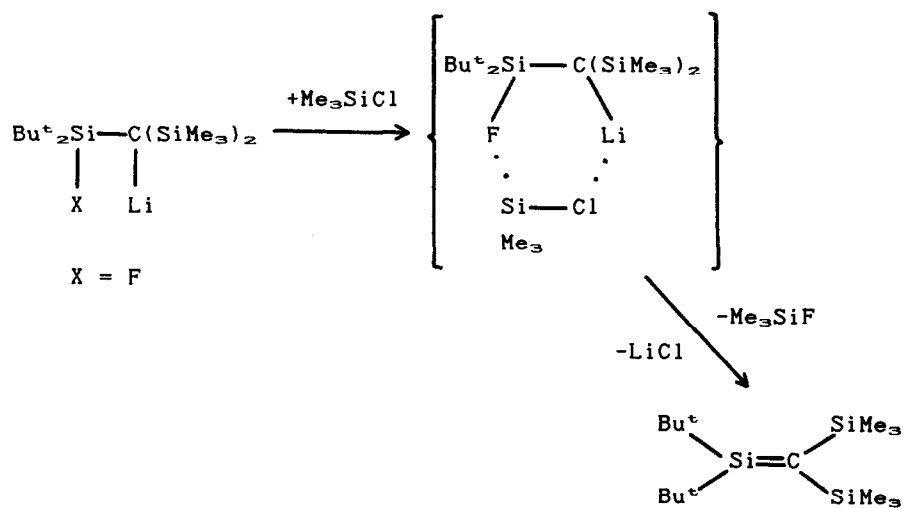
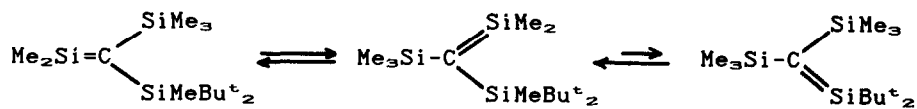
Scheme 35

Xyl = 2,6-dimethylphenyl

(67)(68)(69)(70)(71)

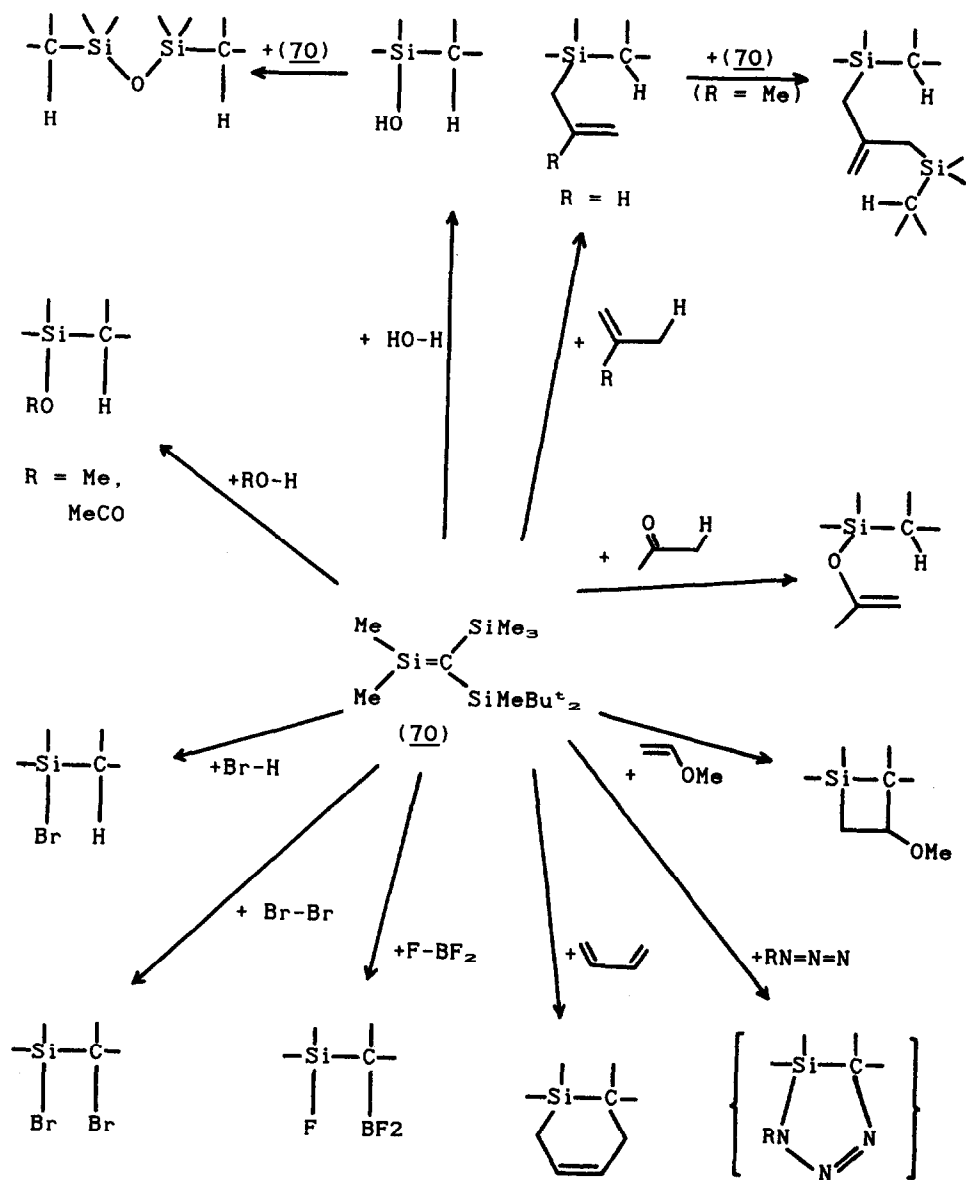
shift of 892ppm downfield from Me_4Sn , which moves upfield to 613ppm on cooling to 77K. Coupling to ^{117}Sn (1340 ± 10 Hz) is also observed. The ^{13}C CPMAS spectrum displays a single line for the methine carbon with coupling to both ^{119}Sn and ^{117}Sn , but on cooling this splits into three lines rationalised as a conformational equilibrium in the solid which is slowed by cooling. The low-temperature solution is consistent with a monomer=dimer equilibrium, and analysis of ^{13}C data gives $\Delta H = 12.8 \text{ kcal mol}^{-1}$ and $\Delta S = 33 \text{ eu}$. The low value of ΔH for dissociation and the small $J(^{119}\text{Sn}-^{117}\text{Sn})$ imply that the $\text{Sn}=\text{Sn}$ bond is exceptionally weak and not a covalent bond in the usual sense. In general, the data are consistent with the original proposal of Lappert of a double dative bond rather than a zwitterionic single-bond description [123].

π -Bond strengths in the alkene analogues $\text{H}_2\text{X}=\text{CH}_2$ ($\text{X} = \text{C}, \text{Si}, \text{Ge}, \text{Sn}$) have been calculated from the energy differences between planar (π -bonded) and perpendicular (diradical) structures and from the energies of disproportion of the products of hydrogen atom addition. Both methods yield nearly the same π -bond strengths: $\text{C}=\text{C}$, 64–68 kcal mol^{-1} ; $\text{C}=\text{Si}$, 35–38 kcal mol^{-1} ; $\text{C}=\text{Ge}$, 31 kcal mol^{-1} ; $\text{C}=\text{Sn}$, 19 kcal mol^{-1} [124]. In an interesting article, Brook [125] has related how his research lead to the synthesis of stable silaethylenes. Wiberg [126–129] has published more data on the synthesis and reactions of stable sila- and germaethenes. On gentle heating the sterically-crowded trisilylmethane, $^t\text{Bu}_2\text{SiF}-\text{CLi}(\text{SiMe}_3)_2$, rearranges into the compound $\text{Me}_2\text{SiF}-\text{CLi}(\text{SiMe}_3)(\text{SiMe}^*\text{Me}_2)$, which in turn decomposes at 100° into LiF and the silaethene $\text{Me}_2\text{Si}=\text{C}(\text{SiMe}_3)(\text{SiMe}^*\text{Me}_2)$ (70). In the absence of trapping reagents, (70) furnishes a mixture of secondary products, but with butadiene reacts to afford (71). The adduct $\text{Me}_2\text{SiF}-\text{CLi}(\text{SiMe}_3)(\text{SiMe}^*\text{Me}_2) \cdot 4\text{thf}$ decomposes in diethylether in the presence of Me_2SiCl at room temperature into the monotetrahydrofuran adduct of $\text{Me}_2\text{Si}=\text{C}(\text{SiMe}_3)(\text{SiMe}^*\text{Bu}_2)$ (Scheme 36). The unsolvated silaethene, which may be obtained by removal of the thf by azeotropic distillation, is kinetically stable at ambient temperatures but decomposes slowly at 80° . In solution

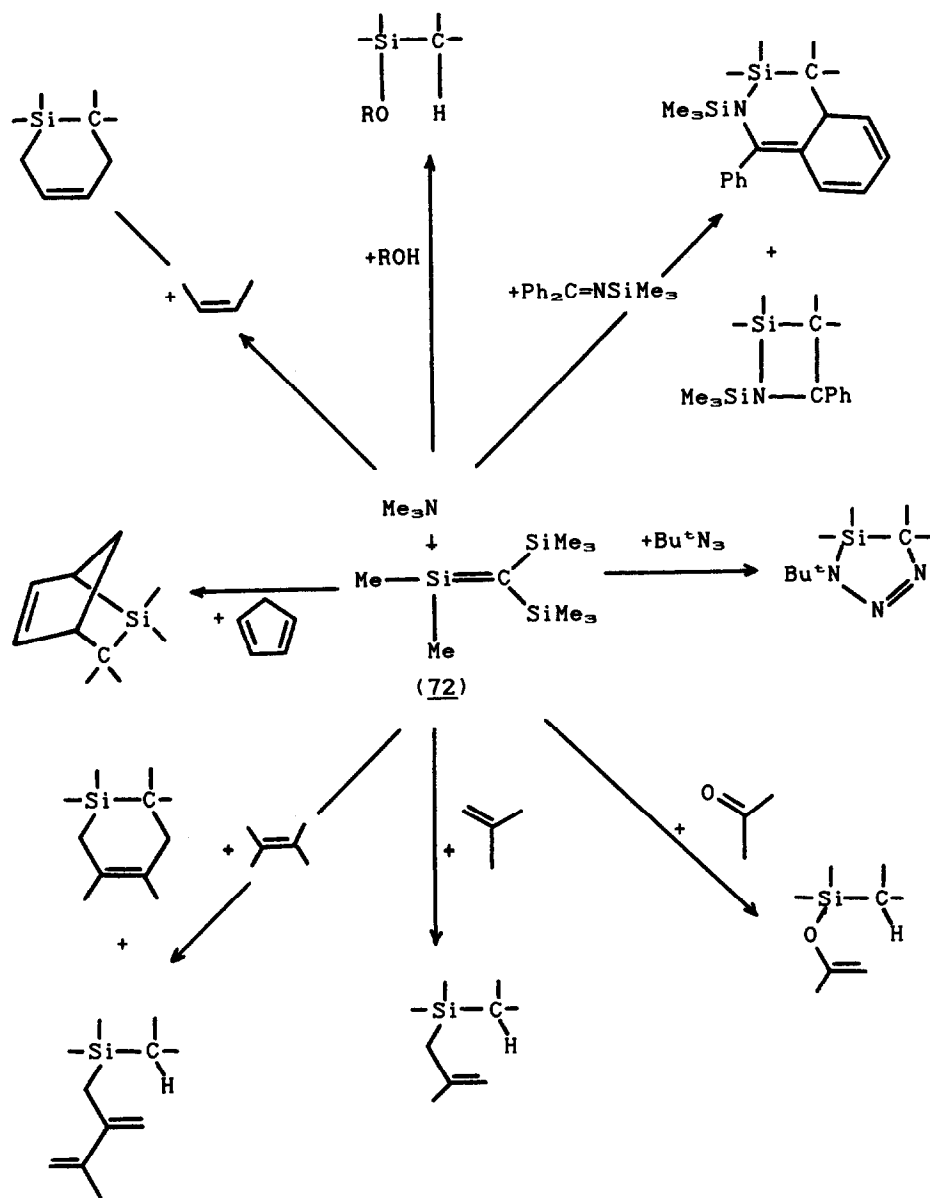
Scheme 36Scheme 37

the silaethene undergoes rapid intramolecular methyl group exchange (Scheme 37). Reactions are summarised in Scheme 38. $\text{Me}_2\text{Si}=\text{C}(\text{SiMe}_3)_2$ is unstable at -100° with respect to dimerization, but forms the adduct $\text{Me}_2\text{Si}=\text{C}(\text{SiMe}_3)_2 \cdot \text{NMe}_3$ (72) which is metastable at 0° . Further heating results in dissociation to its components, and hence the adduct is a useful source of the free silaethene. Typical reactions of (72) are shown in Scheme 39. $\text{Me}_2\text{Si}=\text{C}(\text{SiMe}_3)_2$ also forms 1:1 adducts with other donors (F^- , NMe_3 , NEt_3 , Br^- , thf), whose tendency towards thermal decomposition increases as the Lewis basicity of the donor increases. The analogous germaethene $\text{Me}_2\text{Ge}=\text{C}(\text{SiMe}_3)_2$ may be generated by similar methods, eg thermal elimination of LiX from $\text{Me}_2\text{XGe-Cl}(\text{SiMe}_3)_2$ or the thermal cycloreversion from Lewis base adducts, and undergoes similar types of reactions as the silaethene analogues. Wiberg has continued to investigate the chemistry of stable silaethenes [130-133]. The double-bond in (73) is essentially planar, with a twist about $\text{Si}=\text{C}$ of only 1.6° , and the $\text{Si}=\text{C}$ bond length ($1.702(5)\text{\AA}$) is substantially shorter than in the previously reported (74) ($1.764(3)\text{\AA}$), but in excellent agreement with theoretical predictions. (73) forms adducts with a variety of neutral and anionic donors such as THF, NMe_3 , pyridine and F^- , with the donor being coordinated in all cases to the unsaturated silicon atom. The structure of the fluoride adduct (as the $[\text{Li}(12\text{-crown-40})_2]^+$ salt) shows a distorted tetrahedral geometry at the fluorine-substituted silicon atom. Some reactions of the THF adduct are shown in Scheme 40. The methyl groups of $\text{Me}_2\text{Si}=\text{C}(\text{SiMe}_3)_2$ migrate with a rapid shift of the $\text{Si}=\text{C}$ double bond from silicon to silicon [132]. The same silaethene also reacts with trans-piperylene to yield exclusively the [4+2] adduct (75) in one step by a synchronous mechanism, but with cis-piperylene only to the [2+2] cyclic adduct (76), possibly by a two-step mechanism (Scheme 41) [133].

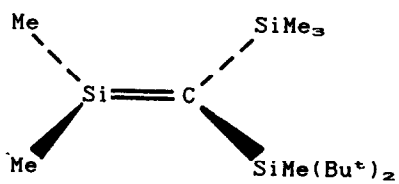
Stable germaethenes [134, 135] and a stable stannaethene [136] have been reported. (77), formed by dehydrofluorination of $\text{Me}_3\text{Ge}(\text{F})-(\text{Li})\text{CR}_2$, could not be isolated in pure form, but forms stable adducts with weak Lewis bases such as diethyl ether, THF,



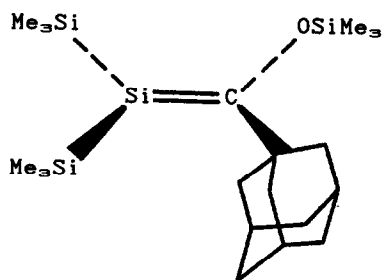
Scheme 38



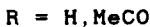
Scheme 39



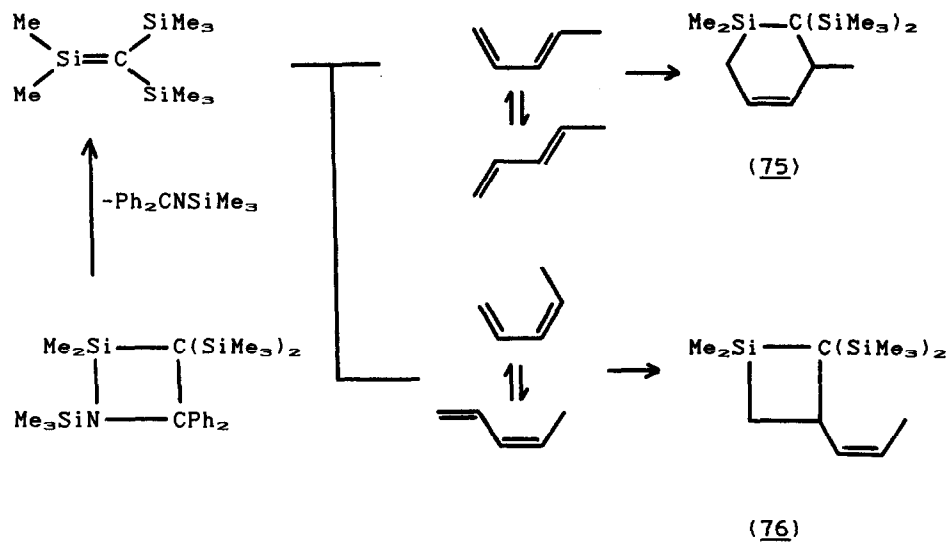
(73)



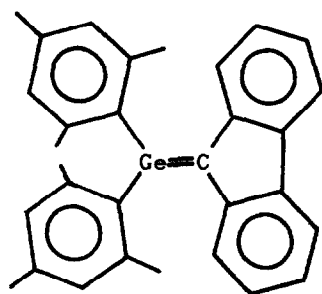
(74)



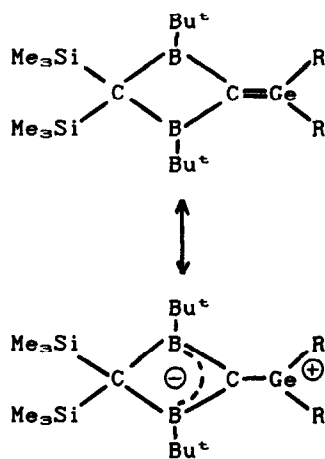
Scheme 40



Scheme 41



(77)

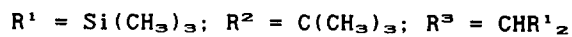
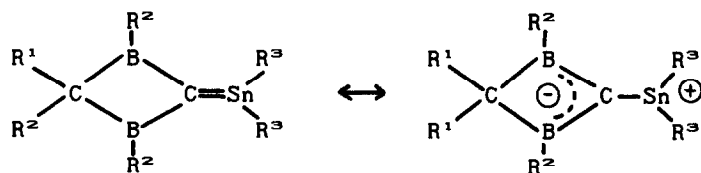


(78)

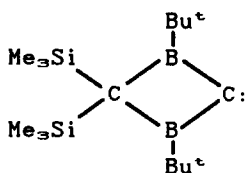
and NET_2 . The adducts are highly reactive (Scheme 42) [134]. The germæthenes (78) and the stannethene (79) have been obtained by reaction of the electrophilic cryptocarbene (80) with the appropriate germane- or stannanediyl. The structures of both have been determined which illustrate the significance of the ylide resonance forms in the bonding [135,136].

The thermal generation of (allyloxy)methylsilylene by flash vacuum pyrolysis of 1,1-bis(allyloxy)tetramethyldisilane affords unexpected products which indicate the formation of intermediate allylmethylsilanone, $\text{C}_3\text{H}_5\text{MeSi=O}$ (Scheme 43) [137]. Methylsilanone and dimethylsilanone have been generated in an argon matrix by the cocondensation of the appropriate silane and ozone and the positions of the $\nu(\text{Si=O})$ vibration identified [138]. Silathione, $\text{H}_2\text{Si=S}$, has been the subject of detailed *ab initio* calculations, and has been found to be kinetically stable with respect to unimolecular decomposition reactions eg to $\text{H}_2 + \text{SiS}$, $\text{H} + \text{HSiH}$, and HSiSH (cf. $\text{H}_2\text{Si=O}$ and $\text{H}_2\text{C=O}$), and is more thermodynamically stable than $\text{H}_2\text{Si=O}$ [139]. A reactive intermediate with a silicon-selenium double bond has been proposed in the photolysis of hexaethylcyclotrisilaselenane in the presence of hexamethylcyclotrisiloxane [140].

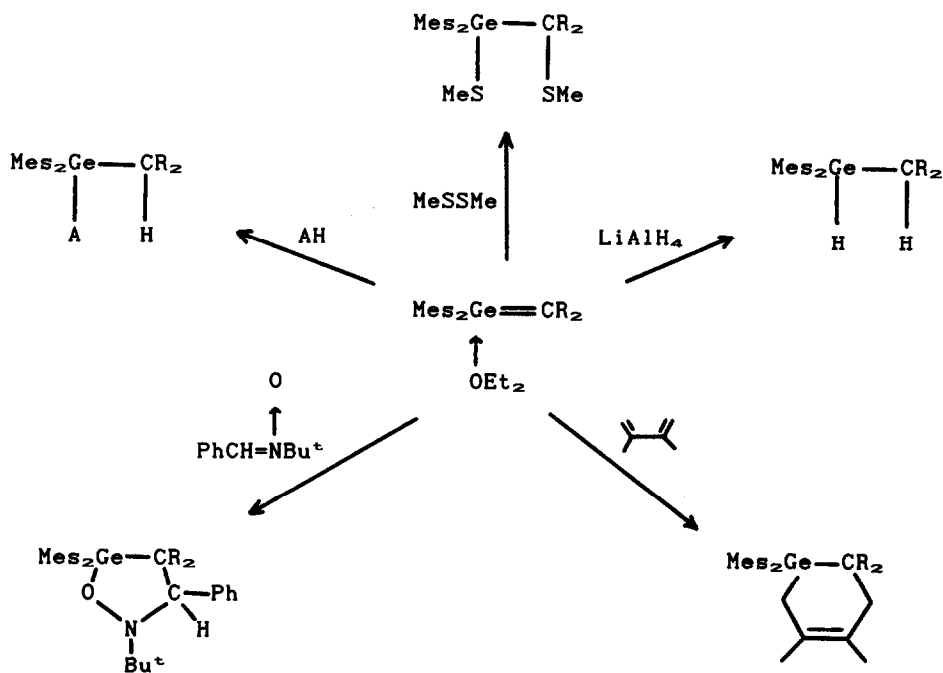
Ab initio calculations with a 6-31G* basis set indicate that silaimine, $\text{H}_2\text{Si=NH}$, is bent at nitrogen (126.6°), but has a low barrier to linearization ($6.0 \text{ kcal mol}^{-1}$). Hence, in accord with experimental results, substitution of an electropositive SiH_3 group produces a near linear skeleton (175.6°). The Si=N double bond is $54.1 \text{ kcal mol}^{-1}$ than two Si-N single bonds (cf carbon nitrogen bonds where the analogous difference is only $1.8 \text{ kcal mol}^{-1}$) [141]. Silan- and germanimines, $\text{Me}_2\text{E=NR}$ ($\text{E} = \text{Si, Ge}$; $\text{R} = \text{SiMe}_n\text{*Bu}_{3-n}$, SiPh_3 , $\text{EMe}_2\text{N}(\text{SiMe}_3)_2$), can be generated by the thermolysis of sila- and germa-dihydrotriazoles and react with azidoalkanes or -silanes $\text{R}'\text{N}_3$ by a [2+3] cycloaddition to form sila- or germa-tetrazoles [142]. In some cases, insertion products of the imine in the $\text{R}'\text{-N}$ bond of the azide is observed. As the cycloaddition reaction is reversible, the tetrazoles are convenient storable precursors for the imines [143,144]. The



(79)



(80)



AH = H_2O , MeOH , EtSH

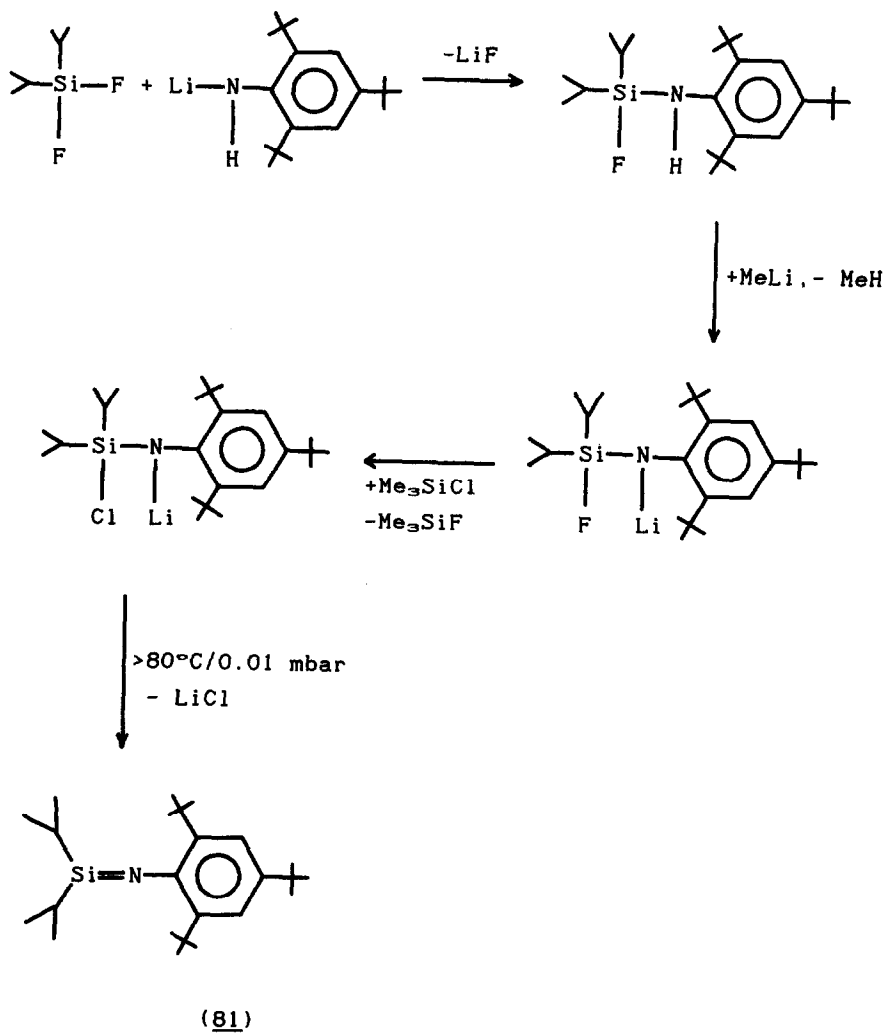
Scheme 42

syntheses of two stable silaimines have been reported. Diisopropyl (2,4,6-tri-*tert*-butylphenylimino)silane (**81**) has been obtained by the route in Scheme 44. (**81**) is a sublimable orange crystalline solid which melts without decomposition to a deep red liquid and is very oxygen and moisture sensitive [145]. The silaketimine (**82**), from the reaction between azido-di-*tert*-butylchlorosilane and tri-*tert*-butylsilyl sodium in dibutylether at -78° , forms pale yellow needles. The structure of (**82**) shows it to have an essentially linear skeleton (cf the *ab initio* calculations above) with a Si=N bond distance of 1.568(3)Å [146]. The first example of a silanediimine, $\text{Me}_3\text{SiN}=\text{Si}=\text{NSiMe}_3$, has been characterised in a glassy 3-methylpentane matrix at 77K [147]. Iminosilylene and its germanium analogue have been formed by gas-phase flash pyrolysis of trimethylsilyl and -germyl azides at 1100K at 10^{-4} mbar. *Ab initio* calculations predict the formation of several compounds in the pyrolysis of Me_3SiN_3 in the probability order $\text{Me}_2\text{HSiN}=\text{CH}_2 > \text{Si}=\text{NH} + \text{C}_2\text{H}_2 > \text{Me}_2\text{HSiCH}=\text{NH} > \text{Si}=\text{NMe} + \text{C}_2\text{H}_2$ [148].

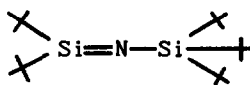
Several examples of phosphasilenes, $\text{ArP}=\text{SiR}'\text{R}''$, have been synthesised by the reaction of $\text{ArP}^+\text{H}^-\text{Li}$ and the appropriate dichlorosilane $\text{R}'\text{R}''\text{SiCl}_2$, followed by the elimination of HCl. However, because of side reactions and the low stability of the phosphasilenes, they were not isolated in a pure form but rather characterized by nmr. In particular, the ^{29}Si resonance is strongly deshielded (148–176ppm) and the $^1\text{J}(\text{PSi})$ coupling constant large (ca. 150 Hz) [149]. The stable germaphosphenes, $\text{Me}_2\text{Ge}=\text{PAR}$, are very reactive towards compounds with active hydrogens producing secondary phosphines (**83**) with a high regiospecificity and towards halogens to give (**84**) and (**85**) [150]. Thermolysis produces the germaphosphetene (**86**), the first four-membered heterocycle with a Ge-P-C linkage, nearly quantitatively [151].

4.2.3 Other Low-valent Compounds

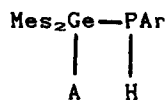
The most significant advance in this area has been the synthesis and characterisation by Jutzi of the first bivalent silicon compound which is stable under ordinary conditions.



Scheme 44

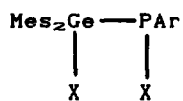


(82)

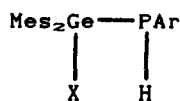


A = OH, OMe, Pr^tS, PhNH,
Cl, CH₃CO₂, Me₃P=CH,
PhC≡C

(83)

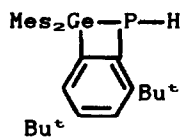


(84)



(85)

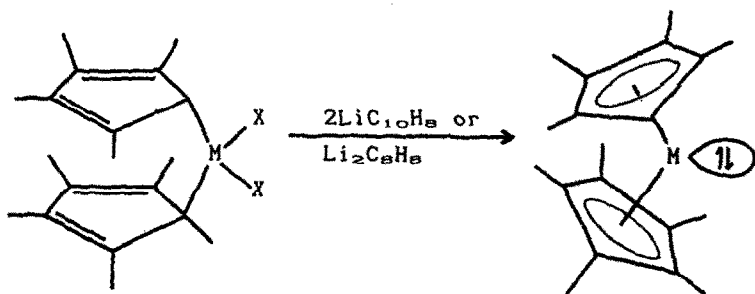
X = Br, I



(86)

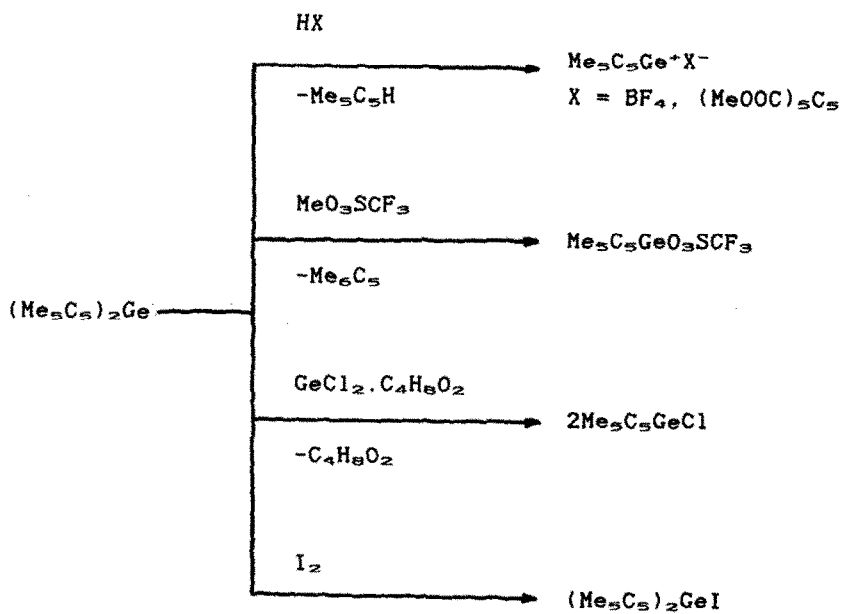
Decamethylsilicocene (bis(pentamethylcyclopentadienyl)silicon(II)) is obtained by reduction of dichloro(bis(pentamethylcyclopentadienyl)-silicon(IV) by naphthalenelithium, -sodium, or -potassium in thf (Scheme 45; $M = \text{Si}$, $X = \text{Cl}$). The compound is colourless (cf the yellow or orange colours of the heavier homologues), sublimes readily, and melts at 171° without decomposition, but is extremely air-sensitive. Surprisingly, two conformers are present in the crystal in the ratio 1:2. Both have sandwich structures, but whereas in one the two cyclopentadienyl rings are parallel and staggered, in the other the rings form an interplanar angle of 25.3° most probably due to intermolecular interactions and crystal packing effects [152]. Decamethylgermanocene and decamethylstannocene have also been prepared similarly (Scheme 45; $M = \text{Ge}$, Sn) [153]. These compounds undergo a wide variety of reactions. Typical reactions of decamethylgermanocene and $\text{Me}_5\text{C}_5\text{GeCH}(\text{SiMe}_3)_2$ with electrophiles are shown in Scheme 46) and Scheme 47, respectively, whereas reactions of $\text{Me}_5\text{C}_5\text{GeCl}$ are shown in Scheme 48 [154,155]. The unsymmetrically substituted germylenes exhibit no tendency to rearrange into the symmetrical compounds. X-ray analysis of $\text{Me}_5\text{C}_5\text{GeCH}(\text{SiMe}_3)_2$ shows it to be monomeric with the germanium atom bonded in a dihapto manner to the C_5 ring as in (87).

Alkylolithiums react with decamethylstannocene by nucleophilic substitution at the tin atom and the displacement of C_5Me_5 group. Thus reaction with $(\text{Me}_2\text{Si})_2\text{CHLi}$ yields $\text{Me}_5\text{C}_5\text{Li}$ and $[(\text{Me}_2\text{Si})_2\text{CH}]_2\text{Sn}$, but reaction with MeLi produces Me_5C_5 and a mixture of oligomeric stannylenes $(\text{Me}_2\text{Sn})_n$. However, trapping experiments demonstrated the initial formation of a short-lived $(\eta^1\text{-Me}_5\text{C}_5)_2\text{Sn}(\text{Me})\text{Li}$ intermediate [156]. Fenske-Hall m.o. calculations have been reported for stannocene and decaphenylstannocene and predict that the tin lone pair resides in the HOMO, a tin 5s-like orbital, in the latter compound, and is not delocalised onto the ring system of the ligands. Computer graphics show that the experimental structure (parallel rings) minimizes steric repulsion by placing the phenyl rings on the cyclopentadienyl ligands in a nearly perpendicular orientation

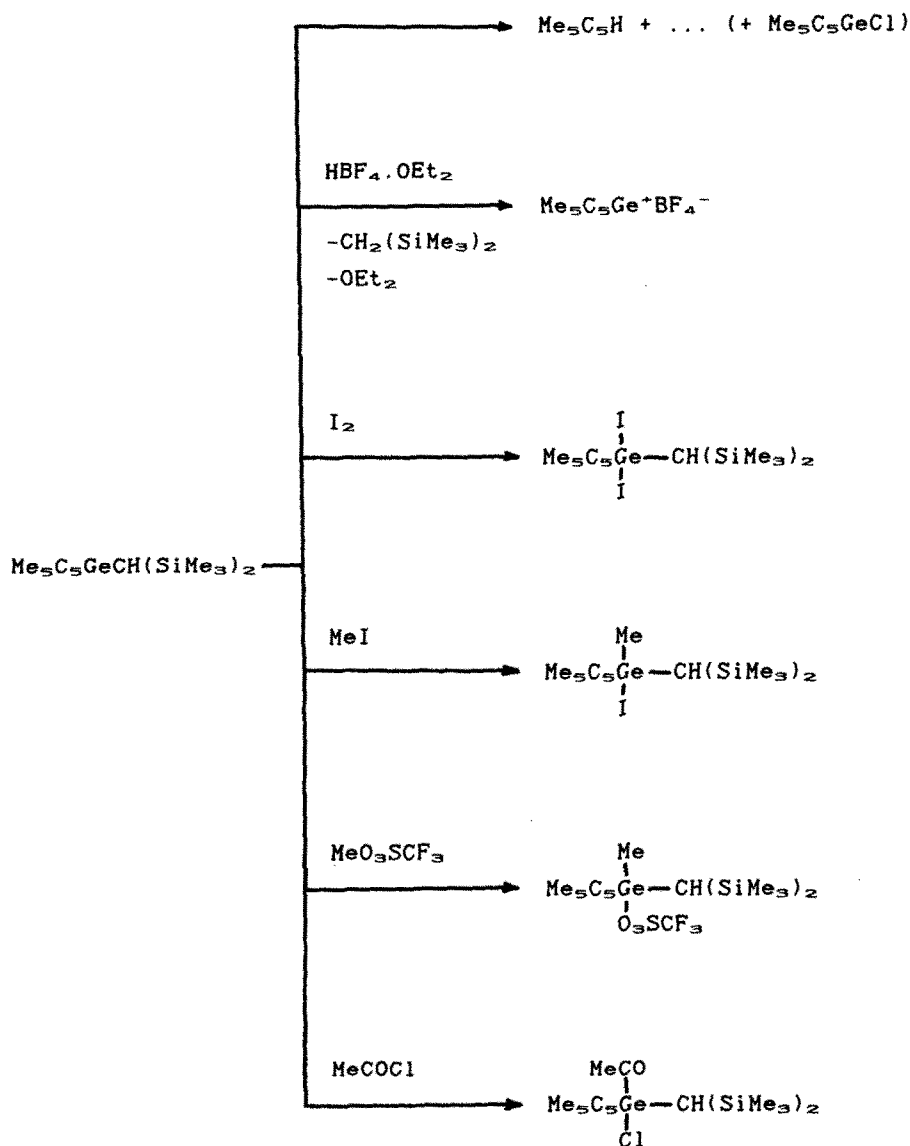


$\text{M} = \text{Si}, \text{Ge}, \text{Sn}.$

Scheme 45

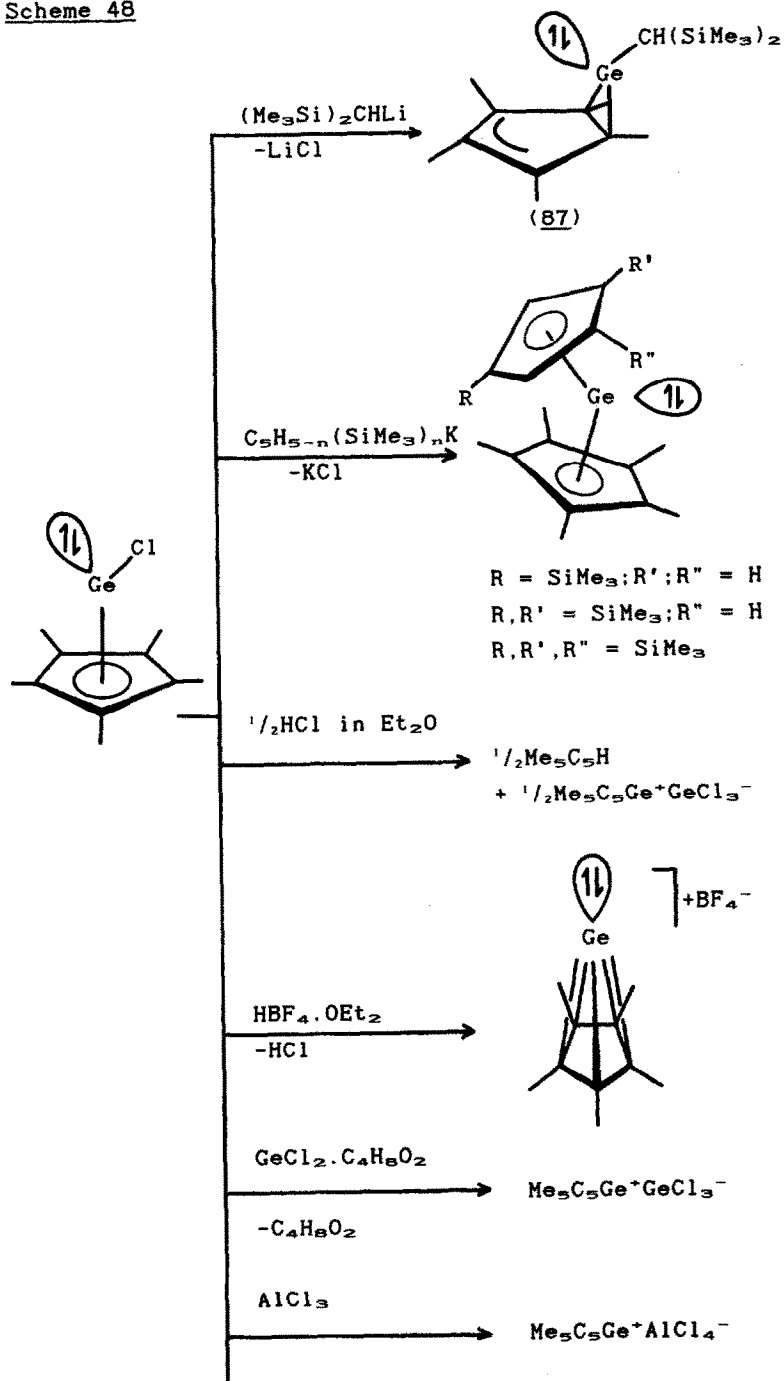


Scheme 46

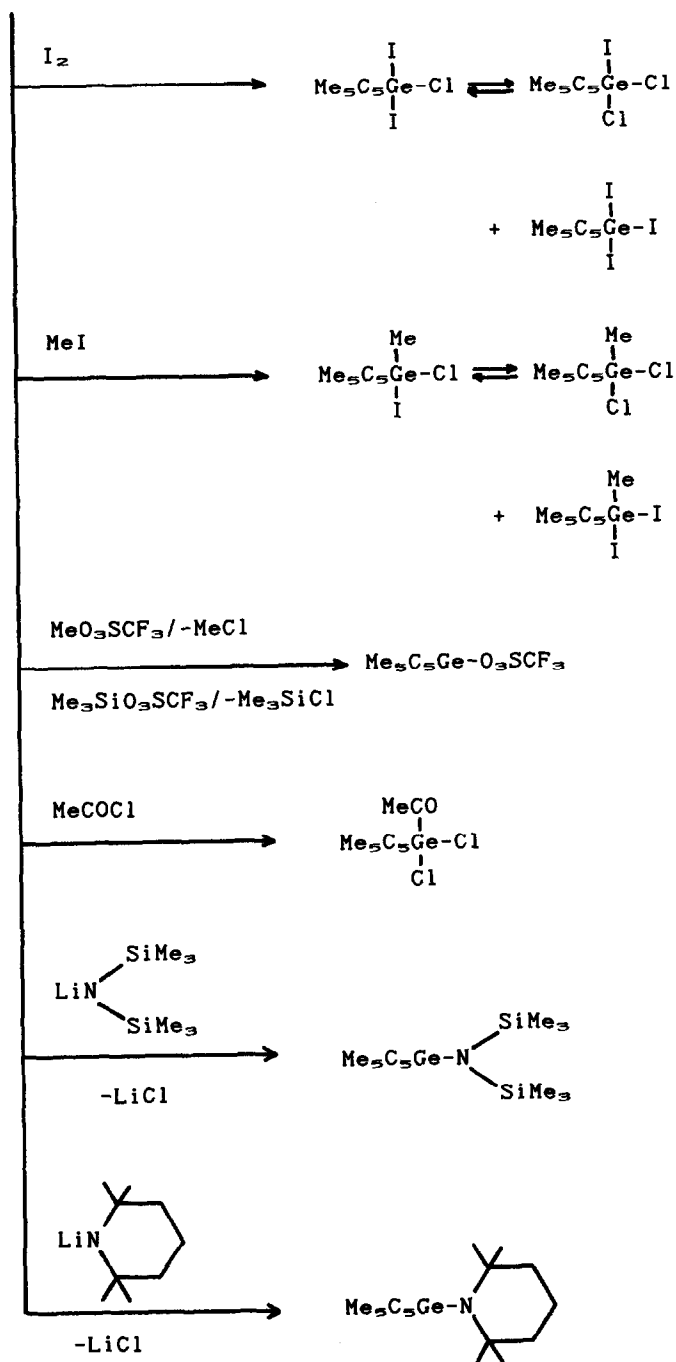


Scheme 47

Scheme 48



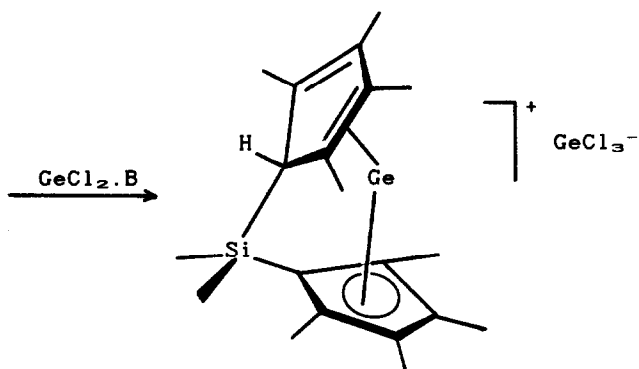
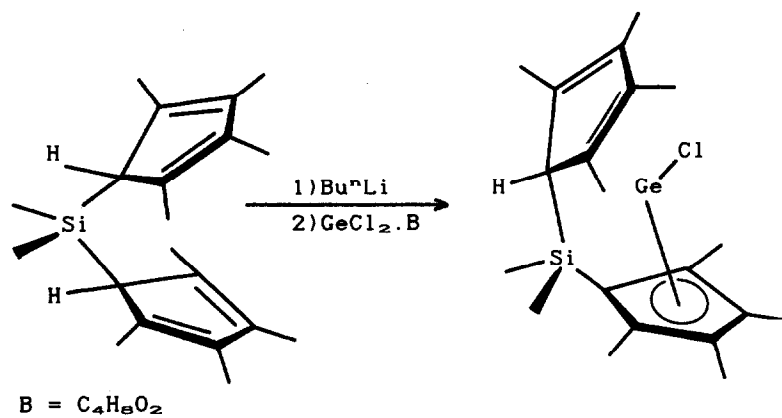
Scheme 48 - continued



[157]. Reaction of GeCl_4 , dioxane with mono-, bis-, and tris-(trimethylsilyl)cyclopentadienyllithium yields bis-, tetrakis-, and hexakis-(trimethylsilyl)germanocene, respectively. In the latter, the two C_5 rings are nearly parallel and have an eclipsed conformation [158]. Decabenzylgermanocene, -stannocene, and -plumbocene have been synthesized by substitution from GeI_4 , SnCl_4 or $\text{Pb}(\text{O}_2\text{CMe})_4$ and pentabenzyl lithium. All are air-stable and exhibit interplanar angles of between 31° and 36° [159].

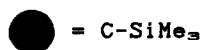
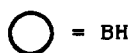
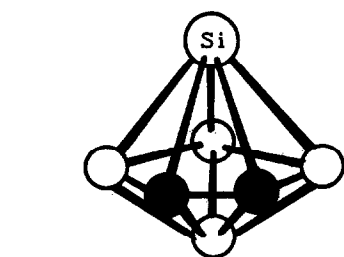
The compound $(\eta^5\text{-Me}_4\text{C}_5\text{H})\text{Me}_2\text{Si}(\eta^5\text{-Me}_4\text{C}_5)\text{Ge}^+\text{GeCl}_4^-$ (**88**) exhibits the extremely novel feature of an alkene-Main Group metal π -type interaction. Colourless crystals of (**88**) are obtained according to Scheme 49, and the coordination sphere of the germanium contains a pentahapto tetramethylcyclopentadienyl ring, the two carbon atoms of the second C_5 ring, and two chlorine atoms of the counterion. An additional contact from the third chlorine atom results in the formation of centrosymmetric dimers. Nmr data indicate that the alkene coordination is preserved in solution [160].

Several interesting analogous carborane compounds have also been described, and again the most intriguing is the bivalent silicon compound $[(\text{Me}_3\text{Si})_2\text{C}_2\text{B}_4\text{H}_4]\text{Si}$ (**89**) which is formed together with $[(\text{Me}_3\text{Si})_2\text{C}_2\text{B}_4\text{H}_4]_2\text{Si}$ in the reaction of SiCl_4 with $\text{Na}^+\text{Li}^+[(\text{Me}_3\text{Si})_2\text{C}_2\text{B}_4\text{H}_4]^{2-}$ in thf [161]. Similarly, the *closa*-germacarborane $[(\text{Me}_3\text{Si})_2\text{C}_2\text{B}_4\text{H}_4]\text{Ge}$ [162], and the stannacarboranes $[(\text{Me}_3\text{Si})_2\text{C}_2\text{B}_4\text{H}_4]\text{Sn}$, $[(\text{Me}_3\text{Si})\text{CH}_2\text{C}_2\text{B}_4\text{H}_4]\text{Sn}$, and $[(\text{Me}_3\text{Si})\text{C}_2\text{B}_4\text{H}_5]\text{Sn}$ (**90**) have been obtained. The three stannacarboranes form 1:1 donor-acceptor complexes with 2,2'-bipyridine, as well as weaker 1:2 complexes with thf. The crystal structures of (**90**) and the bipyridine complex $[(\text{Me}_3\text{Si})_2\text{C}_2\text{B}_4\text{H}_4]\text{Sn}.\text{bipy}$ have been determined, which confirm the *closa* structures, and show that the bipyridine group coordinates to the tin atom opposite to the carborane framework. Unusually, the coordination of bipyridine has only a small effect on the Mössbauer parameters, but all the spectroscopic data are consistent with a distorted pentagonal bipyramidal framework with the tin atom occupying an apical position and bonded exclusively to the three boron atoms of the

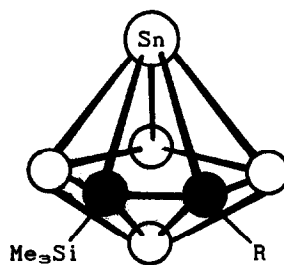


(88)

Scheme 49



(89)

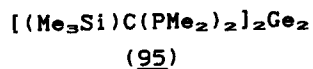
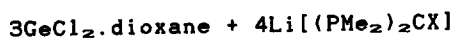
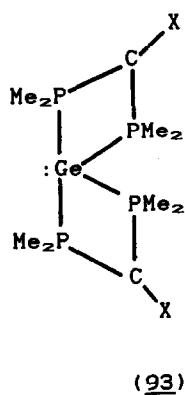
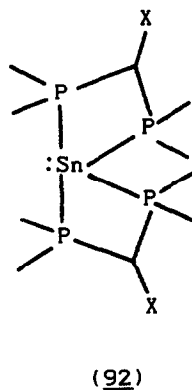
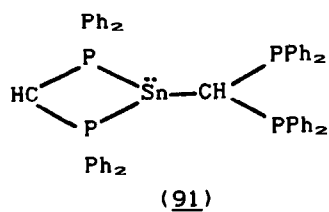


(90)

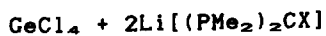
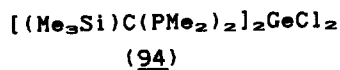
carborane ring [163].

Lappert [164,165] has published full details of the synthesis, structural determinations and m.o. calculations on the compounds $M[CH(SiMe_3)_2]_2$ ($M = Ge, Sn$). The germanium compound is conveniently prepared by the reaction of $GeCl_2 \cdot dioxane$ (from the improved synthesis from $GeCl_4$ and Bu_3SnH) and magnesium alkyls. The tin compound is obtained from $SnCl_4$ by successive reaction with two moles of the lithium alkyl and dilithium cyclooctatetraenide. Electron diffraction shows that both compounds are "V"-shaped monomers in the vapour with CMC angles of $107(2)^\circ$ (Ge) and $97(2)^\circ$ (Sn). In the solid both have the dimetallene centrosymmetric, *trans*-folded M_2R_2 framework, with fold angles of 32° (Ge) and 41° (Sn). The M-M distances in each are slightly shorter than those found in the tetrahedral elements. Double- ξ *ab initio* calculations predict somewhat shorter M-M distances, but show the *trans*-folded structure to be more stable than planar and M-M bond dissociation energies to be about half those found in H_2GeGeH_2 or Me_3MMe_3 .

The preparation and properties of the compounds $M[C(PR_2)_2X]_2$ ($M = Ge, Sn, Pb$; $X = H, PR_2$, or $SiMe_3$) have been reported [166-168]. $Li[CH(PPh_2)_2]$ reacts with $GeCl_2 \cdot l$ ($l = dioxane$ or PPh_3), $SnCl_2$ or $PbCl_2$ in thf to afford $M[CH(PPh_2)_2]_2$ ($M = Ge, Sn, Pb$) which are three coordinated in the solid with one group functioning as a chelating diphosphido ligand and the other as a unidentate carbon-bonded ligand as in (91). In contrast, the complex $Sn[C(PMe_2)_2]_2$ synthesised by similar methods has the four-coordinated pseudo-trigonal bipyramidal geometry (92) in which both groups function as diphosphido ligands. All the compounds are fluxional in solution. Several novel subvalent germanium structures have been determined [169-171]. $GeCl_2 \cdot dioxane$ reacts with $Li[(Me_2P)_2CX]$ ($X = PMe_2$ or $SiMe_3$) to give the phosphane (93) as indefinitely stable colourless crystals. However, when less than the required stoichiometric amount of lithium reagent is used, a redox process takes place and (94) and (95) are formed which (Scheme 50). The oxidation product (94), which can also be obtained from $GeCl_4$, is the first example of a *trans*-octahedral



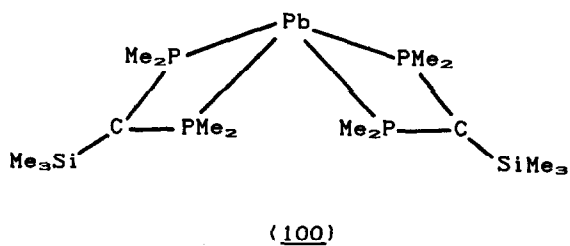
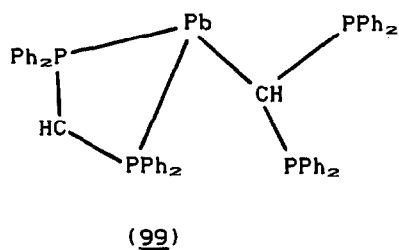
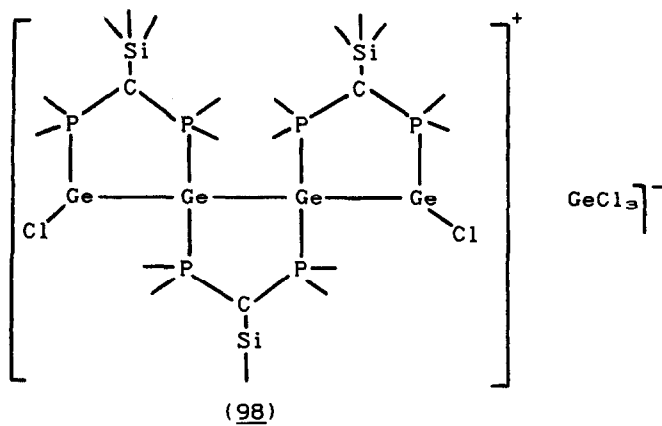
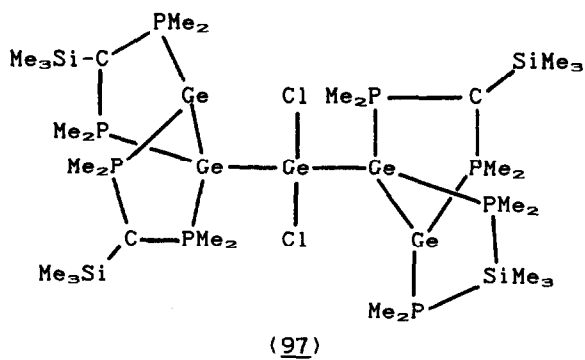
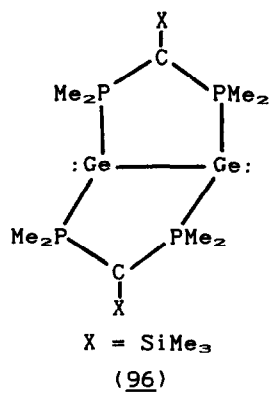
+

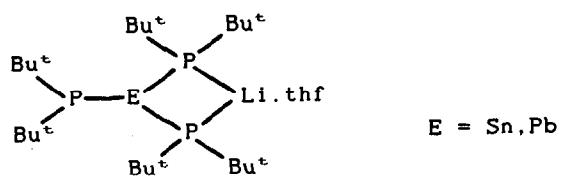


Scheme 50

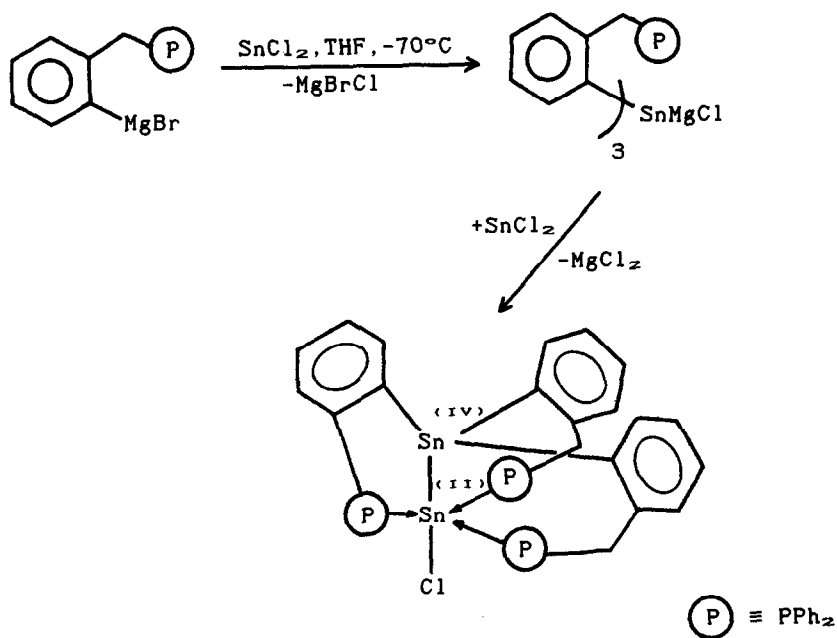
structure having four phosphorus and two chlorines at a germanium centre. The reduction product (95) is also obtained in near quantitative yield from GeCl_4 .dioxane and $\text{Li}[(\text{PMe}_2)_2\text{C}]$ in the presence of excess magnesium in THF, and is characterized by a double phosphinomethanide-bridged $[\text{Ge}^{\text{I}}-\text{Ge}^{\text{I}}]$ structural unit as in (96). The germanium(II) lone pairs in (96) are stereochemically active, and (96) reacts with further GeCl_4 .dioxane to form the 2:1 adduct (97). In solution, this adduct undergoes almost complete dissociation at room temperature, although undissociated at -100° . The structure of (97) is characterized by a bent $[\text{Ge}_2]$ chain of germanium atoms in both valence states. The complex (98) is formed in the reaction of GeCl_4 .dioxane with $\text{Li}[(\text{Me}_2\text{P})_2\text{C}(\text{SiMe}_3)]$ in the presence of magnesium, and contains discrete $[\text{GeCl}_3]$ anions and cationic chains of four germanium atoms with terminal chlorines and bridging diphosphinomethanide ligands. Reaction of $\text{LiCH}(\text{PPh}_2)_2$ with PbCl_2 in THF yields orange crystals of (99) as a THF adduct, in which the lead atom is pyramidally coordinated to the two phosphorus atoms of a chelating ligand and one carbon atom of a unidentate ligand. Similarly, reaction with $\text{Li}[(\text{Ph}_2\text{P})_2\text{C}(\text{SiMe}_3)]$ gives (100) in which lead is four-coordinated by two chelating ligands. Both compounds are fluxional in solution [172].

The tin(II) and lead(II) bis(tert-butyl)phosphido 'ate' complexes $\text{Li}(\text{thf})[\text{M}(\text{P}^t\text{Bu}_2)_2]$ ($\text{M} = \text{Sn}, \text{Pb}$) (101) have been obtained from $\text{Li}(\text{P}^t\text{Bu}_2)$ and the metal(II) chloride in thf. In the crystal both metals are pyramidal with two of the phosphorus atom coordinated to the lithium atom [173]. Reaction of σ -(diphenylphosphino)phenylmagnesium bromide with SnCl_4 lead to the formation of the mixed-valence compound (102) (Scheme 51). Treatment of the complex $\text{Cl}_2\text{Sn}-\text{W}(\text{CO})_6$ with the same grignard reagent produces (103) [174]. Several other complexes with transition metal carbonyl fragments have been described including the germylene complexes $\text{Me}_3\text{C}_2(\text{R})\text{Ge}-\text{W}(\text{CO})_6$ ($\text{R} = \text{Cl}, \text{Me}, (\text{Me}_2\text{Si})_2\text{N}, (\text{Me}_2\text{Si})_2\text{CH}$) [175, 176] and $\text{L}_2\text{X}_2\text{Ge}-\text{M}(\text{CO})_6$ ($\text{M} = \text{Cr}, \text{W}; \text{X} = \text{F}, \text{Cl}; \text{L} = \text{nitrene}$) [177], and the stannylene complexes $(\text{CO})_6\text{M}-\text{Sn}(\text{XCH}_2\text{CH}_2)_2\text{E}$ ($\text{M} = \text{Cr}, \text{Mo}, \text{W}; \text{X} = \text{O}, \text{S}; \text{E} = \text{NR}, \text{PPh}, \text{O}, \text{S}$)





(101)



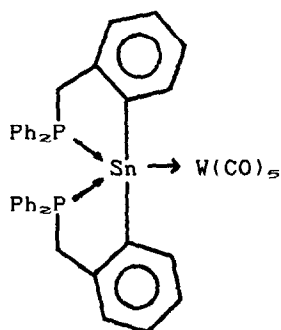
(102)

Scheme 51

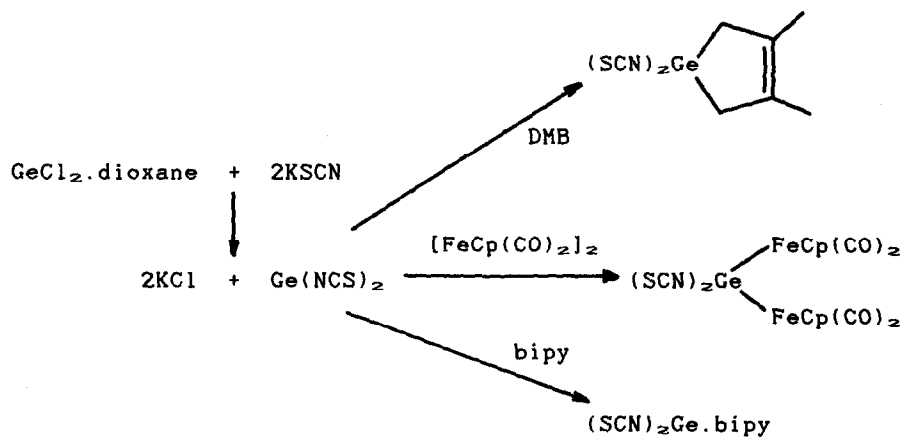
and $(\text{CO})_5\text{W-Sn}(\text{XCH}_2\text{CH}_2)_2\text{E.py}$ ($\text{E} = \text{NMe}, \text{O}, \text{S}$) [178, 179], and $[(\text{C}_6\text{H}_5)_3(\text{CO})_2\text{Sn}(\text{R}_2\text{P})_2\text{CX}]$ ($\text{M} = \text{W}, \text{R} = \text{Ph}, \text{X} = \text{PPh}; \text{M} = \text{Mo}, \text{R} = \text{Me}, \text{X} = \text{SiMe}_3$) [180], and the carbonyl-iron complexes $eq\text{-}[\text{Fe}(\text{CO})_4(\text{M}(\text{OAr})_2)]$ ($\text{M} = \text{Ge}, \text{Sn}; \text{Ar} = \text{C}_6\text{H}_4^t\text{Bu}-2,6\text{-Me-4}$) [181]. The crystal structures of several have been determined.

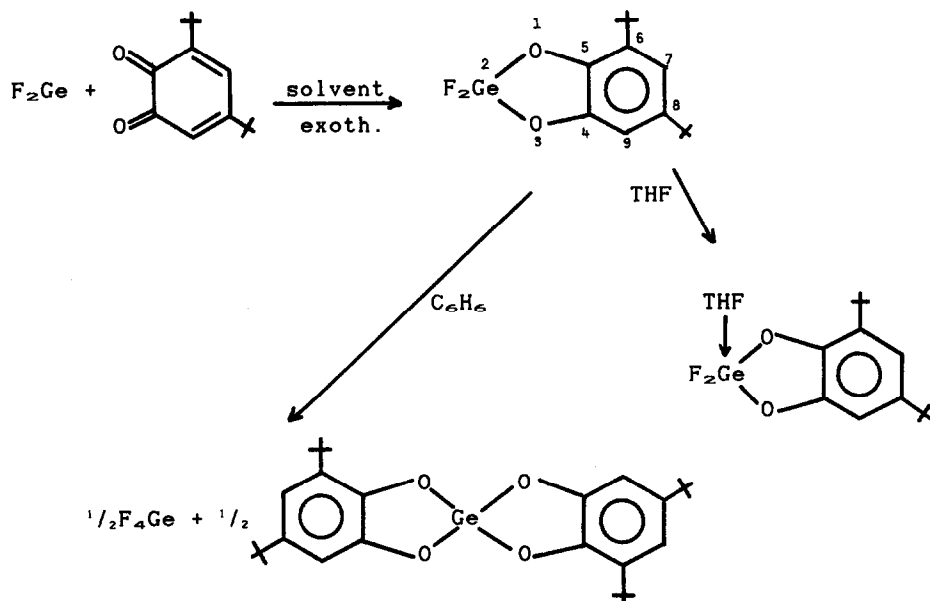
Surprisingly, the germanium(II) pseudohalides $\text{Ge}(\text{CN})_2$, $\text{Ge}(\text{NCO})_2$ and $\text{Ge}(\text{NCS})_2$ were unknown prior to their synthesis by the Toulouse group from the corresponding halides and either potassium or silver salts. They are stable in thf and acetone solution but such solutions are extremely sensitive to moisture, and undergo typical cycloaddition, insertion, and Lewis acid-base reactions characteristic of highly reactive germynes (Scheme 52) [182]. The germynes X_2Ge , RGeX , and R_2Ge ($\text{X} = \text{halogen}, \text{OR}; \text{R} = \text{alkyl or aryl}$) undergo regioselective cycloaddition to 3,5-di-*t*-butyl orthoquinone at room temperature to afford substituted 2-germa-1,3-dioxolanes in good yield (eg Scheme 53 [183]. ESR evidence has been presented for the existence of a radical species in the vapour of tin(II) fluoride [184].

Monomeric 1,4,2,3,5 λ^2 -diazadisilastannolidines and -plumbolidines (104) have been obtained according to Scheme 54 as thermochromic oily red liquids or orange solids [185]. Heating the acid-base adduct (105) to 120° in toluene leads to the formation of the pentacyclic compound (106), which has a centrosymmetric structure with a central $[(\text{CH})_2\text{Sn}_2]$ ring. The decomposition follows first-order kinetics, and proceeds via the intermediate (107), which, although possessing the same composition as (105), exhibits a completely different structure and is characterised by an intramolecular hydrogen-bond between an *o*-carbon atom of a phenyl group and a nitrogen atom of the four-membered $[\text{SiN}_2\text{Sn}]$ ring which may be considered responsible for a hydrogen atom transfer [186]. Strontium and barium bis(*tert*-butoxides) react with tin(II) *tert*-butoxide to afford the mixed alkoxides $[\text{Sn}(\text{O}^t\text{OBu})_2\text{M}(\text{O}^t\text{Bu})_2\text{Sn}]$ ($\text{M} = \text{Sr}, \text{Ba}$). The structure of the strontium derivative ($\text{M} = \text{Sr}$) is highly symmetrical with S_6 symmetry, and comprises a strontium atom sandwiched between two terdentate $[\text{Sn}(\text{O}^t\text{OBu})_2]$ units [187].

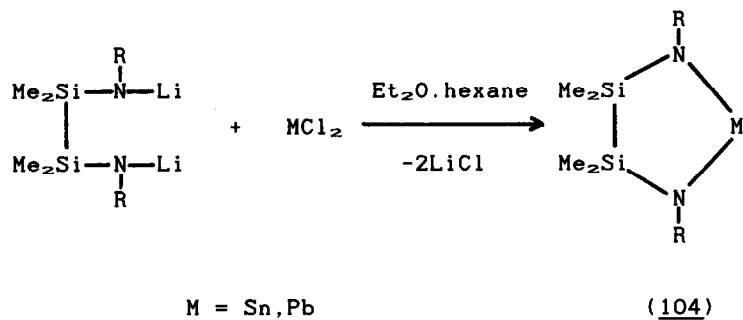


(103)

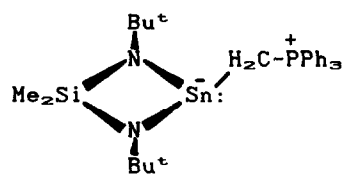
Scheme 52



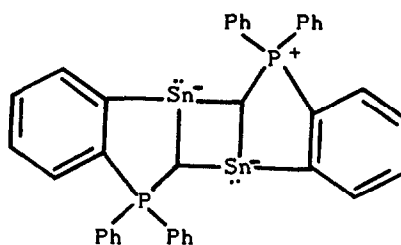
Scheme 53



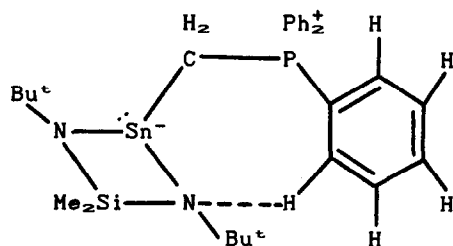
Scheme 54



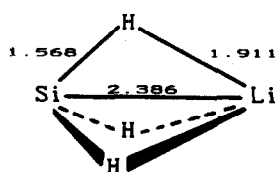
(105)



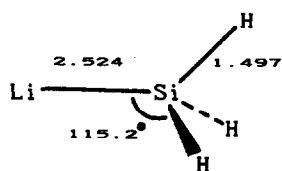
(106)



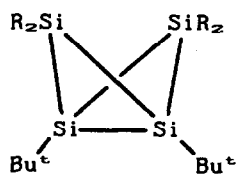
(107)



(108)



(109)



R = 2,6-Et₂C₆H₃

(110)

The germanium(II) and tin(II) porphyrin-tetracarbonyliron complexes $(P)MFe(CO)_4$ ($M = Ge, Sn$) have been synthesized by the reaction of $Na_2Fe(CO)_4$ and the corresponding $(P)M^IVCl_2$ complexes in thf. The complexes were extremely stable after electroreduction, and two reversible one-electron-transfer steps are observed without cleavage of the metal-metal bond. Whilst these reductions occur at the π ring system, irreversible oxidation takes place at the metal centre leading to $[(P)M^IV]^{2+}$ and $Fe_2(CO)_9$ as the main products [188]. Both the trichlorostannate(II) and perchlorate salts of chloro(1,4,7,10,13,16-hexaoxacyclo-octadecane)tin(II) contain the discrete $[Sn(18\text{-crown-6})Cl]^{+}$ cation in which the tin enjoys hexagonal pyramidal coordination by the hexadentate crown ether (equatorial sites) and the chlorine (axial site) [189]. A similar pyramidal coordination is exhibited by the lead complex $[PbCl(DAPSC)]^{+}NO_3^{-}$ (DAPSC = 2,6-diacetylpyridinedisemicarbazone) in which again a chlorine occupies the axial site and the five donor sites of the DAPSC ligand in the equatorial sites [190]. Lead is ten-coordinate in the complex $Pb(PHNSC)(NO_3)_2$ (PHNSC = 2,9-diformyl-1,10-phenanthrolinedisemicarbazone) [191], and has highly irregular coordination polyhedra in the 1,4,7-triazacyclononane (L) complexes $LPb(ClO_4)_2$ and $LPb(NO_3)_2$ [192]. Lead(II) tri-tert-butoxysilanethiolate is dimeric in the crystal with a central puckered four-membered $[Pb_2S_2]$ ring. The lead atoms are three-coordinated [193].

The "inert-pair" effect has a substantial effect on electronegativity. Thus, whereas the electronegativities of germanium(IV), tin(IV) and lead(IV) are 2.62, 2.30 and 2.29, respectively, those of germanium(II), tin(II) and lead(II) are only 0.56, 1.49 and 1.92, respectively [194].

4.2.4 Molecular Tetravalent Compounds of Silicon and Germanium

This area has presented its usual plethora of data and only a relatively small fraction can be reported here. Revised MNDO parameters have been described for silicon with results for a wide variety of silicon-containing compounds in much better agreement

with experiment [195]. MNDO methods have been used to estimate skeletal bending frequencies in linear and quasi-linear silyl compounds [196]. Semi-empirical methods have been employed to examine the ability of carbon, silicon and germanium to form square planar geometries. In all cases such planar geometries were found to be less stable than tetrahedral structures [197]. Theoretical calculations have been performed for silicon (AM1) [198] and germanium (MNDO) [199] compounds. Pathways for nucleophilic substitution at silicon have been investigated using a molecular orbital approach [200]. The attacking nucleophile and leaving group prefer axial entry and axial departure over equatorial entry and equatorial departure. In addition, a retention pathway via pseudorotation is of lower energy than retention occurring via equatorial attack and axial departure. In agreement with experimental observations, chlorine is predicted to be a better leaving group than fluorine, and prefers an inversion pathway rather than retention. In contrast, inversion and retention pathways are more equal in energy when fluorine is the leaving group.

The primary thermal decomposition processes for both silane and disilane have been calculated using extended basis sets [201,202]. The transition state for the molecular elimination from silane is predicted to be 56.9 kcal mol⁻¹ above silane, whereas for the reverse reaction it lies only 2 kcal mol⁻¹ over the two fragments, silylene and H₂. Of the four competing unimolecular decomposition pathways, the 1,1- and 1,2-eliminations of H₂ and the elimination of silylene to form silane all have high endothermicities, but the very high activation energy for the 1,2-elimination excludes this process as a significant contributor at low energies. The most likely source of disilane in the thermal decomposition is the rearrangement of its high energy isomer silylsilylene. The mechanisms of the pyrolyses of MeSiH₃ [203] and the methylchlorosilanes [204] have been studied in detail. For the former, under conditions of very low conversion and in carefully seasoned vessels the major products are H₂ and dimethylsilane. MeSiD₃ gives exclusively D₂. The pyrolysis of

this and the methylchlorosilanes proceeds by a radical chain mechanism.

Ab initio and MNDO calculations have been carried out to evaluate the gas-phase acidity of silane and the affinities of silane and the SiH_3^- anion. Only a marginally stable charge-dipole complex is predicted for SiH_3^- [205], however, this anion has been synthesized and characterised along with several of its simple alkyl derivatives in a flowing afterglow apparatus at 298K [206]. Both the SiH_3^- anion and the SiH_3 radical are pyramidal with inversion barriers of $9000 \pm 2000 \text{ cm}^{-1}$ and $1900 \pm 300 \text{ cm}^{-1}$, and HSiH bond angles of 94.5° and 112.5° , respectively. The Si-H bond dissociation energy in silane was estimated to be $90.3 \pm 2.4 \text{ kcal mol}^{-1}$ [207]. Because of the more favourable electrostatic interactions in the ion pair, $\text{SiH}_3^-\text{Li}^+$, the inverted C_{2v} geometry (108) is calculated to be $2.4 \text{ kcal mol}^{-1}$ more stable than the 'tetrahedral' isomer (109) [208]. All the silicon hydrides, SiH_n ($n = 1-4$), and the silyl compounds H_3SiX ($\text{X} = \text{Li}, \text{BeH}, \text{BH}_2, \text{CH}_3, \text{NH}_2, \text{OH}, \text{F}, \text{Na}, \text{MgH}, \text{AlH}_2, \text{SiH}_3, \text{PH}_2, \text{SH}$ and Cl), have been investigated by *ab initio* methods and compared with the corresponding methyl compounds. In most cases the equilibrium geometries of the methyl and silyl molecules are similar. The most notable exception is in silylamine, where a planar geometry is found at nitrogen. Addition of *d*-orbital functions to the second row atoms leads to a decrease in the bond lengths. The relative $\text{H}_3\text{Si-X}$ and $\text{H}_3\text{C-X}$ bond energies depend principally on the electronegativity of the group X. Since SiH_3 has a higher electron affinity and a lower ionization potential than CH_3 , groups which are very electronegative or very electropositive have stronger bonds to silicon than to carbon [209].

Hexa-*tert*-butyldisilane, formed by reaction of nitrosyl cations with tri-*tert*-butylsilylsodium or -potassium, shows an unusually long Si-Si distance of 289.7 pm [210]. Fluorination of chlorophenyldisilanes with zinc fluoride with silver powder as catalyst yields the corresponding fluorophenyldisilanes. 1,2-Difluorotetraphenyldisilane can be obtained by uv irradiation of bis-(fluorodiphenylsilyl)mercury [211]. The structures of several

other catenated silicon, germanium or tin compounds have also been determined including the α,ω -substituted permethylpolysilanes, $R(SiMe_2)_nR$ ($R = (t-BuO)_3Si$; $n = 2, 3, 6$) [212] and hexa-tert-butyl-1,3-diodotrisilane [213], the tetrasilabicyclo[1.1.0]butane (110) [214], the alkali metal silicides, K_9LiSi_4 and $K_7Li(Si_4)_2$, which contain tetrahedral $[Si_4]$ structural units [215], the large ring cyclopolysilanes $(Me_2Si)_n$ ($n = 13$ and 16) [216], the linear phenylpolygermanes, Ge_3Ph_6 , Ge_4Ph_{10} (as a bis-benzene solvate), Ge_5Ph_{12} , and $Cl(GePh_2)_nCl$ ($n = 2, 3$ and 4) [217-219].

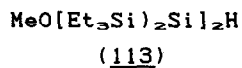
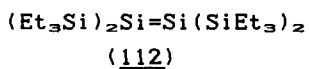
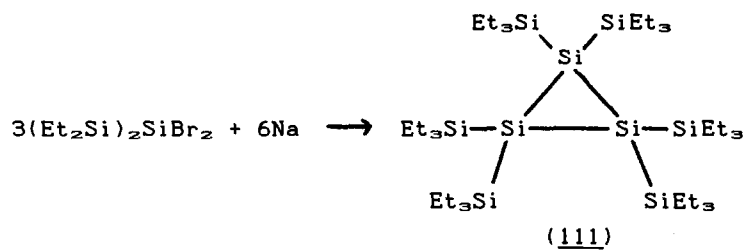
The electronic structure of polysilane molecules has been investigated both theoretically and experimentally [220-222]. In poly(di-n-hexyl)silane the polysilane chain is effectively separated into a series of chromophores, which appear to be all-trans segments separated by gauche links, communicating by rapid energy transfer. Energy band structures have been calculated for polysilane models, $-(SiXY)_n-$, with X and $Y = H, Me, Et, Pr$ and Ph . Polysilane has a directly allowed type band structure, and a $\sigma-\sigma^*$ interband optical transition is allowed. Band-edge states are formed mainly of skeleton Si atomic orbitals, which results in a skeleton band gap. This skeleton band gap tends to be reduced when larger alkyl groups are substituted for side chains. The σ and σ^* band-edge states are well delocalized on the skeleton axis. Poly(phenylsilane) exhibits a characteristic band-edge structure due to $\sigma-n$ mixing between the Si skeleton and the phenyl side chains. Variable temperature ^{29}Si and ^{13}C CP/MAS NMR spectra confirm that poly(di-n-hexyl)silane is in a rigid form at temperatures below 310 K. The observed thermochromism of the UV spectrum is due to backbone disordering above the transition temperature resulting from increasing contributions from gauche conformations at elevated temperatures [223]. Poly(di-n-pentylsilane) exists in the solid-state at room temperature in a regular 7/3 helical conformation, in contrast to poly(di-n-hexylsilane) which prefers a planar zig-zag conformation below 41° , implying that the trans planar backbone conformation adopted by higher polysilanes is due to side-chain crystallization [224].

Ab initio calculations at the SCF level show that the

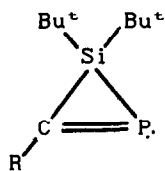
silicon-silicon bonds in cyclosilanes are weaker than the carbon-carbon bonds in alkanes, since the s valence orbitals can contribute less to the formation of strong hybrid orbitals. Stabilization of the cyclosilane rings is due to intramolecular perturbational orbital interaction [225]. Hyperconjugative interactions are much stronger in polysilylene chains than in polyethylene chains due to the presence of energetically low-lying orbitals in silicon systems and the electropositive character of silicon. As a consequence of orbital non-hybridization, tetrasilabicyclo[1.1.0]butane and pentasil[1.1.1]propellane suffer from an extremely facile bond-stretching isomerisation. The lability of the central bond in these systems is also enforced by the relatively high ring strain in cyclotrisilane as compared with that in cyclotetrasilane. For tetrasilabicyclo[1.1.0]butane, the preference for a closed or open structure depends on the substituents on the silicon atoms [226].

The novel persilylcyclotrisilane (111) has been obtained by the reaction of 2,2-dibromohexaethyltrisilane with sodium. UV irradiation of (111) in the presence of methanol affords (113) presumably via the disilene (112) (Scheme 34) [227]. Irradiation of hexa-tert-butylcyclotrisilane with phosphalkynes $RC\equiv P$ (R = adamantyl, tBu) gives the phosphasilirenes (114) which reacts (R = adamantyl) with $W(CO)_6 \cdot THF$ to produce the complex (115) [228]. Permethylcyclosilanes rearrange in the presence of an $Al(Fe)Cl_3$ catalyst to form isomeric branched cyclopentasilanes or cyclohexasilanes [229]. Calculations show that thermodynamically the preferred isomer is that with the lower steric energy [230]. The reaction of $Ph_4Ge_2Cl_2$ with $t-Bu_2Ge(OH)_2$ leads to the germanium-oxygen heterocycle (116), which has an almost planar $[Ge_2O_2]$ ring [231].

Irradiation of hexaneopentyltrisilaioxetane (117) gives tetraopentylidisilaoxirane (118) with the extrusion of dineopentylsilanediyl [232]. Empirical, MNDO and ab initio molecular orbital methods applied to the four-membered ring molecules $(H_nSiX)_2$ ($X = O, NH, CH_3, S$) show that the electronic structures of all are similar and the short non-bonded 1,3-Si-Si

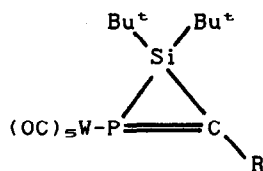


Scheme 55

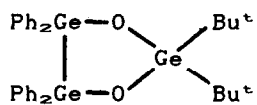


(114)

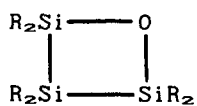
R = adamantyl



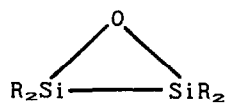
(115)



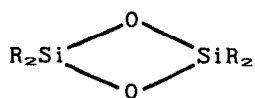
(116)



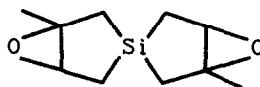
(117)

R = Bu^tCH₂

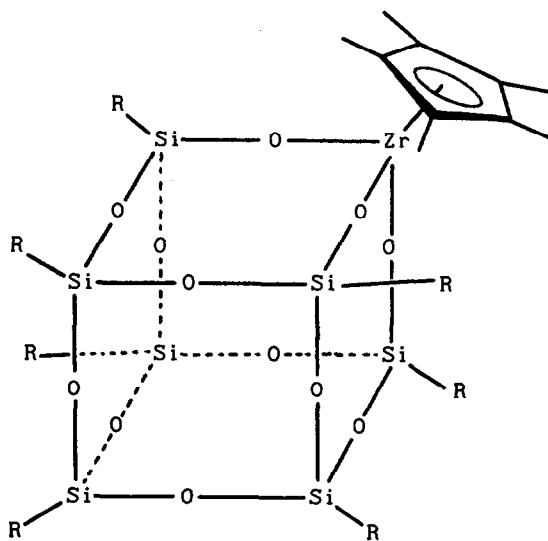
(118)



(119)



(120)



(121)

distances are predominantly determined by the Si-X distance. The small antibonding Si-Si interactions increase with increasing Si-Si distance [233]. The ^{29}Si chemical shifts for several cyclodisiloxanes fall in the range $3.85\text{--}4.02 \pm 0.1$ Hz are consistent with the non-Si-Si bonded structure (119). However, the nmr data, which indicate little or no s orbital contribution to the bonding between the silicon atoms, are also consistent with an "unsupported n bond" model [118].

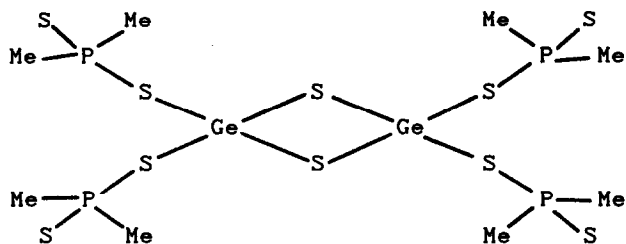
Flash vacuum pyrolysis of (120) with cyclotetra- or cyclopentasiloxanes leads to products resulting from the insertion of $\text{O}=\text{Si}=\text{O}$ (or equivalent synthon) into the Si-O bonds of the siloxanes [234, 235]. The synthesis and crystal structures of the cyclodisiloxanes, tetramesitylcyclodisiloxane, trans-1,3-dimesityl-1,3-di-tert-butylcyclodisiloxane, and cis-1,3-bis[bis(trimethylsilyl)amino]-1,3-dimesitylcyclodisiloxane have been reported. Whilst the $[\text{Si}_2\text{O}_2]$ in the former and latter compounds are slightly puckered, that in trans-1,3-dimesityl-1,3-di-tert-butylcyclodisiloxane is planar. The Si-Si non-bonding distances in all three compounds are short and of the order of normal Si-Si bond distances, and were considered to arise from antibonding interactions between the oxygen atoms [236]. Tetraphenyldisiloxane crystallizes at 298K in the monoclinic $\text{P2}_1/\text{n}$ space group but undergoes a second order phase transition at 200K to a triclinic phase with an almost unchanged structure. At 298K the Si-O-Si bridge is bent with an angle of 180° with static or dynamic disorder of the bridging oxygen atom [237]. The Si-O-Si fragment in the R,S diastereoisomer of $[(\text{C}_6\text{H}_5)(\text{CO})_2\text{FeSi}(\text{CH}_2\text{F})_2\text{O}]_n$ is linear even at 120K, but the data indicate severe disorder [238]. Hexa(tri-tert-butoxy)disiloxane also has a linear Si-O-Si skeleton, but the corresponding disilthiane is bent [239]. The product of the reaction of Me_2SiCl_2 with 1,2-dihydroxybenzene, bis(o-phenylenedioxy)dimethylsilane, is dimeric with a ten-membered $[\text{Si}_2\text{C}_4\text{O}_4]$ ring [240]. Siloxy cage compounds such as (121) have been synthesised and characterised as models for silica-supported transition metal catalysts [241].

Molecules of $(\text{MeC}_6\text{H}_4)_2\text{TlSiMe}_2$ contain a

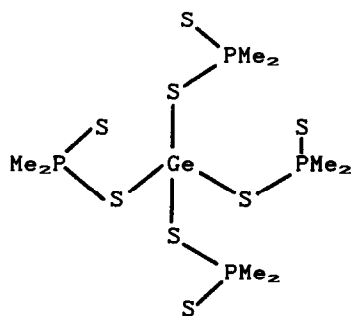
(crystallographically-imposed) planar four-membered $[\text{TiS}_2\text{Si}]$ ring in which the Ti-S bonds are substantially more labile than the Si-S bonds [242]. The unexpected compound, $[(\mu\text{-S})\text{Ge}[\text{S}_2\text{P}(\text{OMe})_2]_2]_2$ (122), was also isolated from the synthesis of the tetrakis compound, $\text{Ge}[\text{S}_2\text{P}(\text{OMe})_2]_4$ (123). The dithiophosphate ligands are unidentate in both compounds [243]. The monogermanium sulphide and selenide, $(\text{RM})_4\text{E}_2$ ($\text{R} = \text{CF}_3$, $\text{M} = \text{Ge}$, $\text{E} = \text{S}$, Se) have the adamantane structure (124) [244].

The question as to why cyclodisilazane rings are more stable than cyclodisiloxanes has been examined by simple m.o. theory. In the latter, high silicon $3p_z$ orbital contribution to the siloxane HOMO prevents any strengthening of the Si-O bond by silicon $3d$ orbitals. In contrast, considerable $\text{Si}(3d_{\pi}, -\text{N}(2p_{\pi}))$ bonding may occur in the disilazanes which is responsible for their relative stability [245]. The structure of chlorosilyl-N,N-dimethylamine has been determined in both the gaseous and solid phases. In the gas phase the molecule is monomeric with four-coordinated silicon, but crystals comprise well separated dimers [246]. Disilazanes have been obtained by deprotonation of dimethylhydroaminosilanes by a mechanism thought to involve an intermediate silaimine species [247]. The $[\text{Si}_2\text{N}_2]$ ring in $(\text{Ph}_2\text{SiNC}_6\text{F}_5)_2$ is planar but not square. The pentafluorophenyl groups are twisted by ca. 160° from the plane of the four-membered ring [248]. Cyclosilazane cations have been obtained by treatment of the disilazane with aluminium(III) chloride (Scheme 56) [249]. A variety of homogeneous and heterogeneous catalysts promote the ring-opening oligomerization of octamethylcyclotetrasilazane. Low pressures of hydrogen (1 atmosphere) also enhance transition metal catalysed ring opening by up to two orders of magnitude. The metal hydrides which are thus formed are also active catalysts in the absence of hydrogen [250].

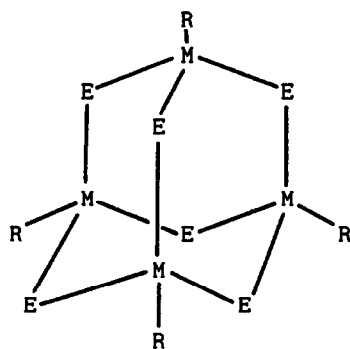
The triphenylsilyl cation has been obtained by hydride transfer from the silane to the trityl cation [251]. The structures of two silylmethyl lithium derivatives have been determined. That of trimethylsilylmethyl lithium comprises hexameric $(\text{LiCH}_2\text{SiMe}_3)_6$ units with two distinct Li-Li distances



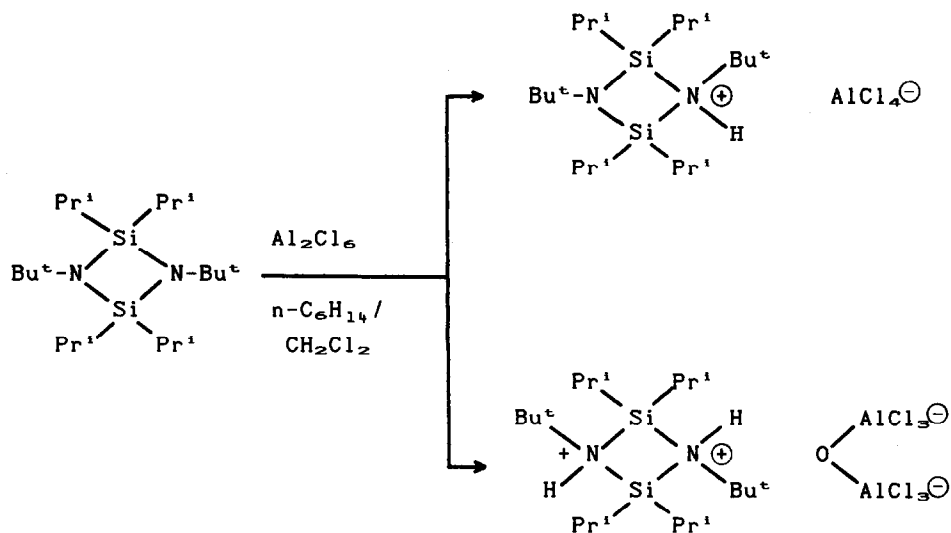
(122)



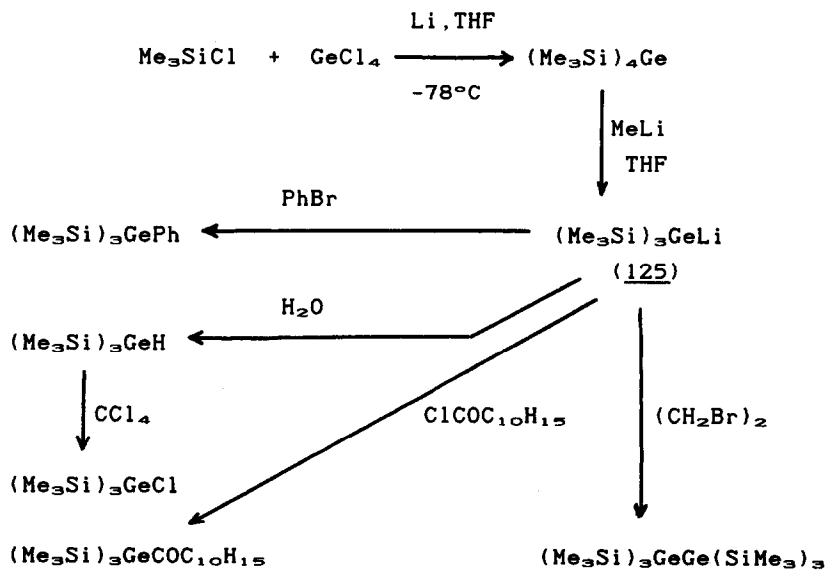
(123)



(124)



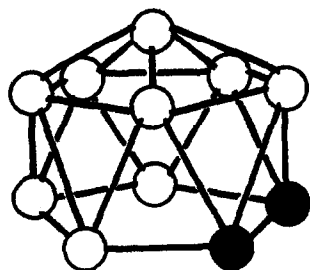
Scheme 56



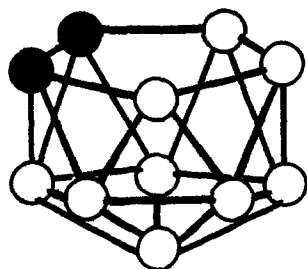
Scheme 57

[252]. The organolithium reagent derived from $(\text{MeOMe}_2\text{Si})_2\text{CCl}$ crystallises as a dimer $[\{\text{LiC}(\text{SiMe}_2\text{OMe})_2\}_2]$, in which the Li-C bonds are unusually long and the C-SiMe₂ bonds unusually short [253]. Metal vapours of cadmium and zinc react with trifluorosilyl radicals to give bis(trifluorosilyl)cadmium and -zinc, which were isolated at low temperatures. Both compounds are unstable at room temperature [254]. Treatment of gallium(III) and indium(III) chloride with three equivalents of $\text{Li}[(\text{Si}(\text{SiMe}_3)_2)_2\text{.3thf}]$ affords the compounds $[\{(\text{Me}_3\text{Si})_2\text{Si}\}_2\text{M}(\mu\text{-Cl})_2\text{Li}(\text{thf})_2]$ (M = Ga or In). The structures of the compounds can be regarded as a double-bridged complex of $[\{(\text{Me}_3\text{Si})_2\text{Si}\}_2\text{MCl}]$ and solvated LiCl [255]. The germyl lithium compound (125) has been prepared from $(\text{Me}_3\text{Si})_4\text{Ge}$, and its reactions are summarised in Scheme 57 [256]. The novel bis(η^5 -dicarbollide) (126) has been obtained by substitution from SiCl_4 and the lithium salt of the carbollide. It is stable in dry air and soluble in most organic solvents. The silicon atom resides on a crystallographic centre of symmetry, being equidistant from the planar parallel faces of the two ligands [257].

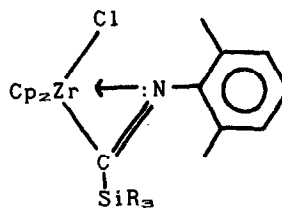
Trifluorosilyl radicals generated in a radio frequency discharge of hexafluorodisilane react with metal atoms to give the first homoleptic trifluorosilyl metal compounds, $(\text{CF}_3)_2\text{Te}$, $(\text{CF}_3)_2\text{Bi}$, $(\text{CF}_3)_2\text{Sb}$ and $(\text{CF}_3)_2\text{Hg}$. In addition, the same method can be adapted to afford complexes including $(\text{CF}_3)(\text{PMe}_3)\text{Ni}$, $(\eta\text{-C}_6\text{H}_5\text{Me})(\text{CF}_3)_2\text{Ni}$, $(\text{CF}_3)_2((\text{PMe}_3)_2\text{Pd})$, $(\text{CF}_3)_2\text{Cd}(\text{glyme})$, and $(\text{CF}_3)_2\text{Zn}(\text{pyridine})_2$ [258]. The reaction of $(\text{Me}_3\text{Si})_2\text{Al.Et}_2\text{O}$ and NH_3 in a 1:1 ratio yields $[(\text{Me}_3\text{Si})_2\text{AlNH}_2]_2$ which has a planar central four-membered $[\text{Al}_2\text{N}_2]$ ring. Thermolysis gives solid solutions of AlN and SiC [259]. Several complexes of coordinatively unsaturated transition metals have been synthesised using the very bulky tris(trimethylsilyl)silyl ligand (Scheme 58) [260, 261]. The chromium(III) complex is unstable at room temperature, but may be stored indefinitely at -20° . The iron and manganese complexes are stable at room temperature under nitrogen. Reaction of $(\text{C}_6\text{H}_5)_2\text{Zr}(\text{SiMe}_3)_2\text{Cl}$ with CO gives the silyl-acyl complex $(\text{C}_6\text{H}_5)_2\text{Zr}(\eta^2\text{-COOSiMe}_3)\text{Cl}$, the first observation of insertion of CO



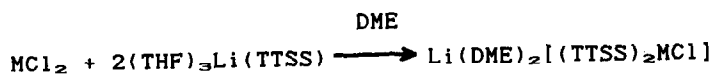
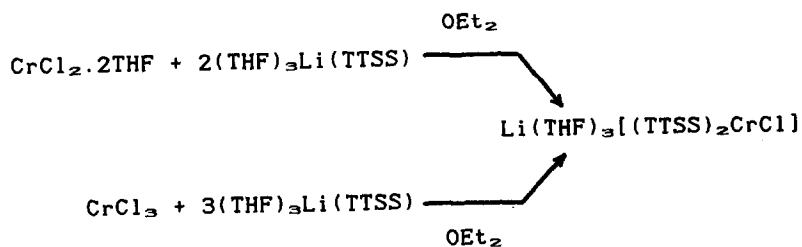
Si



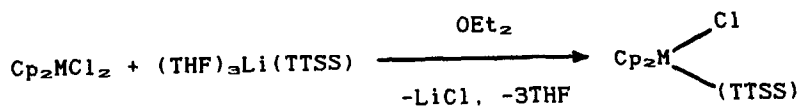
(126)



(127)



TTSS = $\text{Si}(\text{SiMe}_3)_3$; M = Mn, Fe

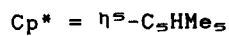
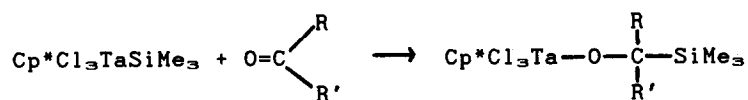
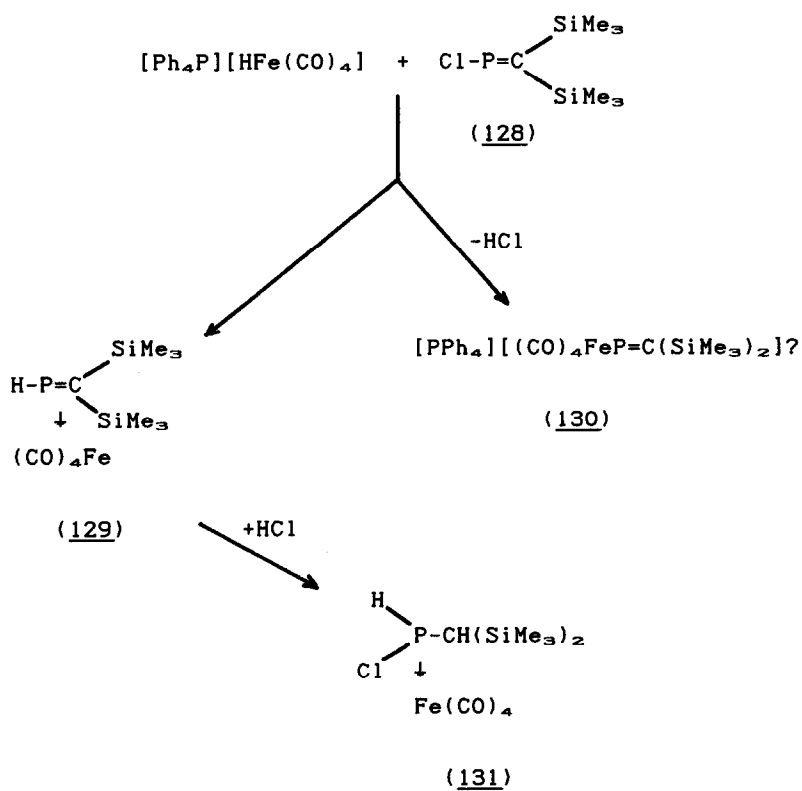


TTSS = $\text{Si}(\text{SiMe}_3)_3$; M = Zr, Hf

into a transition metal-silicon bond. The complexes $(C_6H_5)_2Zr[Si(SiMe_3)_3]SiMe_3$ and $(C_6H_5)_2Zr[Si(SiMe_3)_3]Me$ react similarly, but the titanium complex $(C_6H_5)_2Ti(SiMe_3)_2Cl$ undergoes an apparent ligand-induced reductive elimination to produce $(C_6H_5)_2Ti(CO)_2$ and Me_3SiCl . Insertion of the isocyanide 2,6- $Me_2C_6H_3NC$ into the Zr-Si bonds of $(C_6H_5)_2Zr(SiMe_3)_2Cl$ and $(C_6H_5)_2Zr(SiMe_3)_2Me$ occurs readily to the complexes [127]. The Zr-Si bonds are cleaved by molecular hydrogen [261]. Organic carbonyl compounds have been shown to insert into the Ta-Si bond (Scheme 59). Kinetic data are consistent with a second-order rate law. Hydrolysis of the insertion products affords the corresponding asilyl alcohols [262]. Similarly, 2,6-dimethylphenyl isocyanide inserts into the U-Ge bond of $(C_6H_5)_3GePh$ [263]. The silyl-chromium complex $(C_6H_5)(CO)_2Cr(H)SiHPh_2$ contains a Cr-H-Si two-electron three-centre bond in its ground state [264]. The reactions of dihalogenogermanes with magnesium and magnesium bromide in THF produces the corresponding cyclotrigermanes and cyclotetragermanes, the ring size depending on the steric bulk of the substituents on germanium [265].

The vibrational spectra of the three (amino)monohalogenosilanes $SiH_3X(NMe_2)_2$ ($X = Cl, Br, I$) exhibit dramatic changes on solidification, but those of $SiHCl_2(NMe_2)_2$ are very similar in all three phases, indicating the formation of dimers in the solid for the former compounds, confirmed by a crystallographic study at 118K. In the gas phase the three (amino)monohalogenosilanes have monomeric structures with the three bonds at nitrogen close to planarity, but not exactly so [266, 267]. $SiHCl_2(NMe_2)_2$ is also monomeric in the gas phase, but with planar nitrogen. Both nitrogens in $SiH(NMe_2)_2$ are non-planar in the gas phase [268]; $SiMe(NMe_2)_2$ has a planar $[NCSi_2]$ skeleton [269].

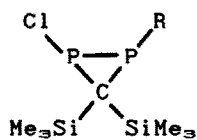
Treatment of $(Me_3Si)_3P$ with *n*-butyllithium in THF affords $[Li(\mu-PPe_2)(THF)_2]_2$, which slowly loses THF in vacuo to give $Li_4(\mu_2-PPe_2)_2(\mu_3-PPe_2)_2(THF)_2$ and reacts with *N,N,N',N',N'*-pentamethyl-diethylenetriamine (PMDETA) in toluene to give $Li(PPe_2)(PMDETA)$. The structures of the first two have been

Scheme 59Scheme 60

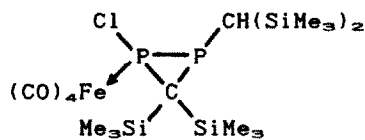
determined. $[\text{Li}(\mu\text{-PR}_2)(\text{THF})_2]_2$ is centrosymmetric with a $(\text{LiP})_2$ core, whilst $\text{Li}_4(\mu_2\text{-PR}_2)_2(\mu_3\text{-PR}_2)_2(\text{THF})_2$ has a fused tricyclic $(\text{LiP})_4$ ladder skeleton [270].

Two competitive reactions occur when an equimolecular amount of $[\text{HFe}(\text{CO})_4]^-$ is added to the phosphaaalkene (128): elimination of Ph_4PBr and the formation of (129), and HCl evolution with the formation of a minor product which could be (130). (131) is also formed as a by-product (Scheme 80). Complex (131) is obtained directly when $(\text{Me}_3\text{Si})_2\text{CHPCl}_2$ is treated with one mole equivalent of the hydride. Three products (129), and the phosphirane compounds (132) and (133) (or (134)) are formed when a dichloromethane solution of the hydride is added slowly to the pure phosphaaalkene (128) at room temperature [271]. The reaction of $\text{ClP}[\text{C}(\text{SiMe}_3)_2]_2$ with $^i\text{PrMgCl}$ affords the phosphaaallene $\text{HP}[\text{C}(\text{SiMe}_3)_2]_2$, which isomerises to the phosphaaalkene (135) by a reductive hydride shift [272]. With $[(\text{C}_6\text{H}_5)_3\text{Fe}(\text{CO})_2]\text{K}$, $\text{ClP}[\text{C}(\text{SiMe}_3)_2]_2$ affords the complex (136), the first example of a three-coordinate metallo-bis(methylene)phosphorane (metallophosphaaallene) [273]. The reaction of $\text{MeP}(\text{SiMe}_3)_2$ with PCl_3 at -78° in pentane yields $\text{P}[\text{P}(\text{SiMe}_3)_2]_3$, which has approximately C_3 symmetry in the crystal [274]. Linear silylated triphosphanes have been obtained by first reacting PCl_3 with the trimethylsilylated phosphine $\text{P}(\text{SiMe}_3)\text{R}$ to afford $\text{R}(\text{Me}_3\text{Si})\text{P}-\text{PCl}_2$, which is then treated with the lithiated phosphine $\text{LiP}(\text{SiMe}_3)_2\text{R}'$ [275]. Reaction of the fully silylated triphosphane, $(\text{Me}_3\text{Si})_2\text{-P}(\text{SiMe}_3)\text{-P}(\text{SiMe}_3)_2$, with $^t\text{BuPBI}_2$ affords *cis*- $\text{P}_4(\text{SiMe}_3)_4^t\text{Bu}$ [276]. The cyclotetraphosphanes $\text{P}_4^t\text{Bu}_2(\text{SiMe}_3)_2$ and *trans*- $\text{P}_4^t\text{Bu}_2(\text{SiMe}_3)_2$ react with MeLi and $^n\text{BuLi}$ in *thf* via cleavage of a trimethylsilyl group leaving the $[\text{P}_4]$ ring intact. *cis*- $\text{P}_4^t\text{Bu}_2(\text{SiMe}_3)_2$ and P_4 rings with a higher degree of silylation, however, react differently, undergoing P-P bond cleavage to produce primary *n*-tetraphosphides which rearrange even at low temperature in *thf* to form the corresponding secondary *n*-tetraphosphides [277].

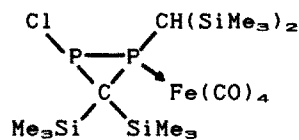
Several complexes of transition metals have already been mentioned, but several others are worthy of note. (137) and (138)



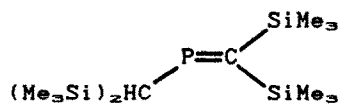
(132)



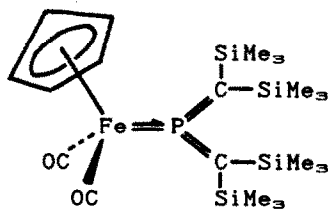
(133)



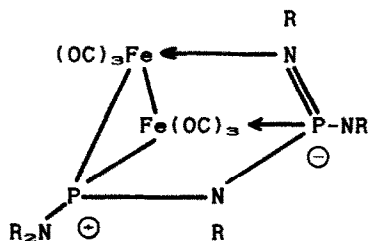
(134)



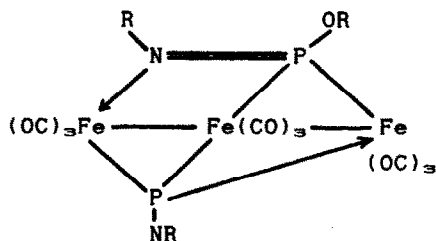
(135)



(136)



(137)

R = SiMe₃

(138)

are formed from $\text{Fe}_3(\text{CO})_{12}$ and $(\text{Me}_3\text{Si})_2\text{N-P=NSiMe}_3$ in toluene at 90° [278]. (139) is obtained by the route shown in Scheme 81 [279].

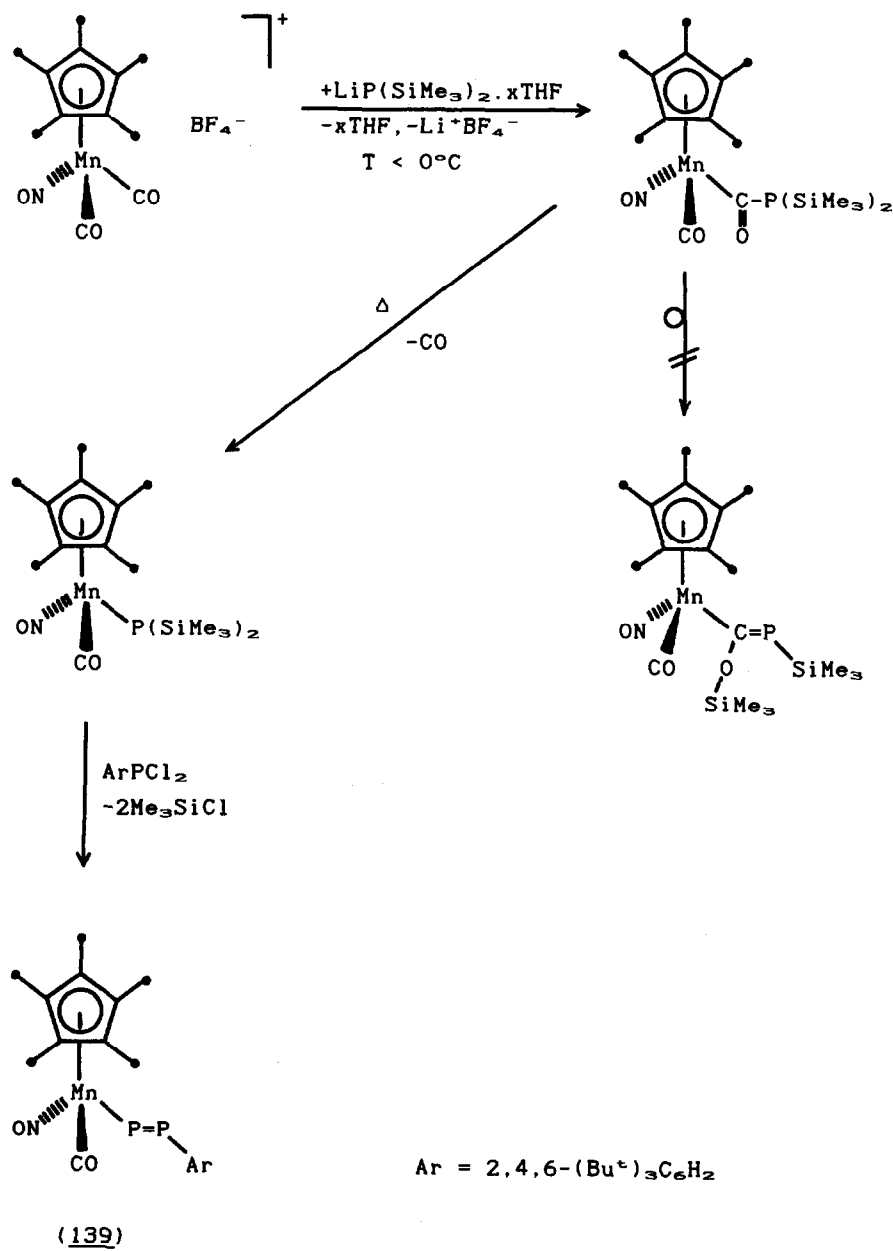
4.2.5 Structures and Spectroscopy of Tin and Lead Compounds

Crystallography continues to play a very important role in the elucidation of the more subtle structural features of tin compounds. The large number reported in the past year or so precludes more than a brief mention of most. In some cases crystallographic data is used to aid interpretation of spectroscopic data.

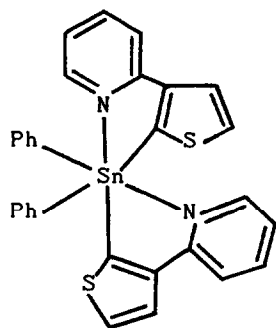
Several structures are quite unusual, and form the first examples of new structural types. In this category fall those of bis(3-(2-pyridyl)-2-thienyl-C,N)diphenyltin (140) [280], the first example of a six-coordinated tin compound containing four tin-carbon bonds, {C,N-[3-(2-pyridyl)-2-thienyl]}tri(p-tolyl)tin (141) [281], a compound also with four tin-carbon bonds which is highly distorted from tetrahedral towards trigonal bipyramidal geometry, tribenzyl (2-pyridinethiolato-n-oxide)tin (142) [282, 283], a rare example of square pyramidal geometry at tin(IV), and the sterically-crowded tin(IV) monohalides, $(\text{Me}_3\text{Si})_3\text{CSnMe}_2\text{F}$ [284], $(\text{Me}_3\text{Si})_3\text{CSnPh}_2\text{F}$ [284], $(\text{PhMe}_2\text{Si})_3\text{CSnMe}_2\text{F}$ [284], $[\eta\text{-C}_6\text{H}_5\text{Fe}(\text{CO})_2]_2(\text{p-tolyl})\text{SnBr}$ [285], and $[(\text{Me}_3\text{Si})_2\text{N}]_2\text{SnBr}$ [108], all of which have (distorted) tetrahedral geometries with intermolecular tin...halogen interactions.

Five coordination at tin has been confirmed in $\text{Cl}_3\text{SnCH}_2\text{CH}_2\text{CO}_2^i\text{Pr}$ [286], $(\text{NCS})\text{Ph}_3\text{Sn}(\text{O}_2\text{CC}_6\text{H}_4\text{N-2})\cdot\text{H}_2\text{O}$ [287], $2\text{-Me}_2\text{NC}_6\text{H}_4\text{CH}(\text{SiMe}_3)\text{SnMePhBr}$ [288], $(\text{p-tolyl})_3\text{SnBr}\cdot(\text{quinoline-N-oxide})$ [289], {3-[t-butyl(phenyl)phosphino]propyl}dimethyltin chloride [290], and $\text{Me}_2\text{ClSn}[(1\text{-pyrazolyl})_2\text{BH}_2]$ [291], whilst six-coordinated Sn^{IV} atoms are present in the mixed-valence compound $\text{Sn}^{\text{II}}_2\text{Sn}^{\text{IV}}_2\text{F}_4(\text{O}_2\text{CCF}_3)_2\cdot 2\text{CF}_3\text{COOH}$ (the Sn^{II} sites have square pyramidal geometries) [292].

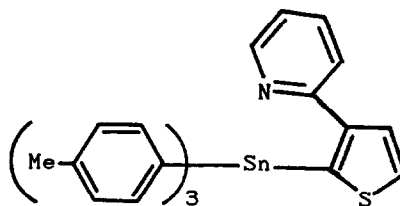
The tin-tin bonded heterocycles (143) ($\text{Y} = \text{S}, \text{Se}, \text{Te}$) have planar ring skeletons [293]. Reaction of Ph_3SnLi with Ph_2MCl_2 ($\text{M} = \text{Si}, \text{Ge}$) gives $(\text{Ph}_3\text{Sn})\text{MPh}_2$. The $[\text{C}_3\text{-SiC}_2\text{-SnC}_3]$ skeleton has symmetry close to C_2 [294]. Similarly, reaction with the



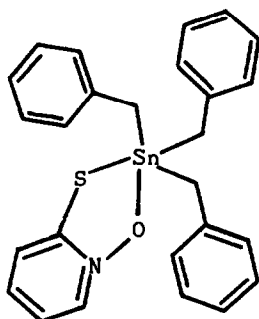
Scheme 61



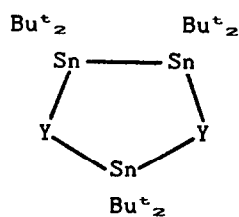
(140)



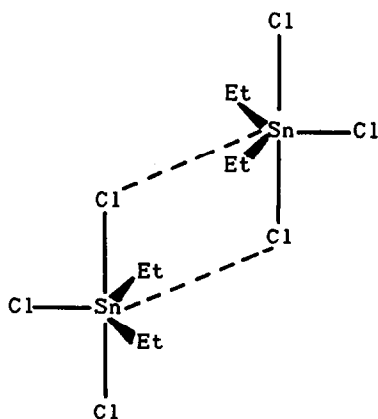
(141)



(142)



(143)



(144)

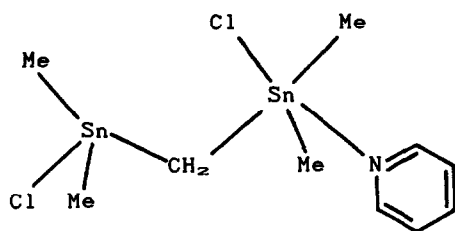
α, ω -diiodopolystannanes, $I(t\text{-Bu}_2\text{Sn})_nI$, affords the linear stannanes, $\text{Ph}_2\text{Sn}-((t\text{-Bu}_2\text{Sn})_n-\text{SnPh}_2)$ ($n = 1-4$), the structures of which have been determined. Electron-rich substituents on the tin atoms generally effect an increase of the Sn-Sn bond length. Thus, the central bond when $n = 5$ is the longest yet observed (2.986(3)Å) [295]. The structures of the cyclotetrestannanes, $(t\text{-Bu}_2\text{Sn})_4$ (planar) and $(t\text{-amyl}_2\text{Sn})_4$ (Puckered) have also been determined [296].

1,2-Dichlorotetramethyldistannane, $\text{ClMe}_2\text{SnSnMe}_2\text{Cl}$, forms a tin-tin connected double helical structure [297]. The structure of methylphenyltin dichloride in the crystal comprises essentially isolated $[\text{MePhSnCl}_2]$ units, although the intermolecular Sn-Cl contacts are moderately short (3.4-3.8Å), suggesting a situation intermediate between a true monomer and a one-dimensional polymeric structure [298]. Crystals of dicyclohexyltin dichloride and dibromide (isomorphous) [299] and methyltin triiodide [300] comprise discrete tetradral molecules. Theoretical m.o. calculations indicate a small back-donation from the iodine atoms to tin. Lewis acidities of triorganotin halides, R_3SnX ($\text{R} = \text{Me, Et, Pr, Bu, and Ph; X} = \text{Cl, Br, and I}$), [301] and organotin iodides, SnI_4 , R_2SnI_2 ($\text{R} = \text{Me, Ph, PhCH}_2$) and R_2SnI ($\text{R} = \text{Ph, PhCH}_2$), and di- and tribenzyltin chlorides [302] have been estimated by calorimetric and nmr methods. Acidities decrease slightly as the size of the alkyl group increases and increase as the size of the halogen increases. ^1H T₁ measurements have been made with dimethyltin dichloride and its complex with bipyridyl in mixed solvents of dichloromethane and weak bases to elucidate the role of the solvent in the dynamic behaviour of organotin compounds. In the line shape analysis of the exchange reaction between Me_2SnCl_2 and its bipyridyl complex, the dissociation rate constant of the complex supports an exchange mechanism of dissociation followed by a recombination step. Data indicate more extensive solvation in the activated state than in the ground state of the complex [303].

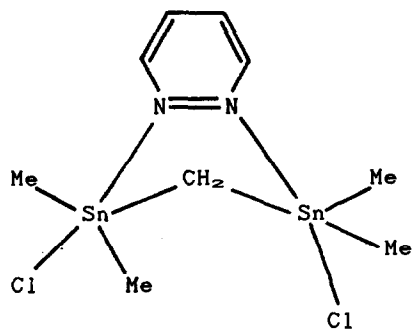
The structures of several complexes of organotin halides with high coordination numbers have been described. The $[\text{SnEt}_2\text{Cl}_3]^-$

anions in the dibenzotetrathiafulvalenium salt exist as dimers (144) [304]. Unique is the trinuclear methylchlorotin anion, $[\text{Sn}_3\text{Me}_6\text{Cl}_6]^{2-}$, present in crystals of the salt $[\text{DBTTF}]_2[\text{Sn}_3\text{Me}_6\text{Cl}_6]^{2-} \cdot \text{PhCN}$ (DBTTF = dibenzotetrathiafulvalene), in which each tin atom is six-coordinated and chlorine-bridged [305]. The structures of no less than seven complexes of bis(chlorodimethylstannyl)methane and bis(dichloromethylstannyl)methane with aromatic nitrogen heterocycles have been determined, and these are illustrated in (145)–(151) [306]. Notable is the ability of the two nitrogen donors in pyridazine to span the Sn–C–Sn linkage in (146) and (147), whereas both pyrazine and bipyridyl cannot and form the complexes (148) and (151), respectively. Pyrazine forms a 1:2 adduct with bis(chlorodimethylstannyl)methane (149) leaving one tin atom uncomplexed. In contrast, the pyrazine nitrogens coordinate both tin atoms in bis(dichloromethylstannyl)methane giving rise to a one-dimensional polymeric structure (150). Six-coordination is present in $\text{SnCl}_2\text{Br}_2(\text{DMSO})_2$ [307] and *cis*-(*p*-tolyl) $\text{SnCl}_2 \cdot 2,2'$ -bipyridyl [308],

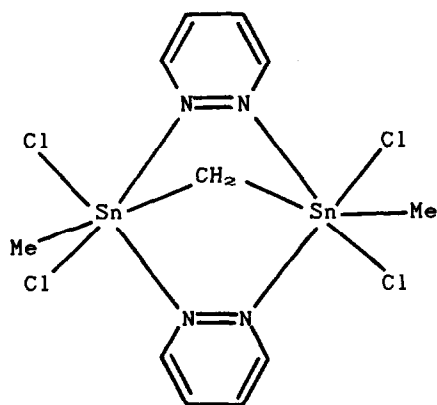
A common method of determining the stereochemistry of the $[\text{PR}'\text{Sn}]$ moiety in six-coordinated compounds or complexes is by the magnitude of the Mössbauer quadrupole splitting (ca. 2 mm s⁻¹ for *cis* geometries and ca 4 mm s⁻¹ for *trans* geometries). Substituents in the carbon- and hetero-atom donor ligands attached to tin can have a strong influence on the stereochemistry in such situations [309]. Only in one case to date, that of the 4,4'-dimethyl-2,2'-bipyridyl adducts of bis(4-chlorophenyl)tin dichloride, have both *cis* and *trans* geometries been characterised by crystallography. The *cis* isomer is obtained exclusively when the components are mixed in ethanol, but on recrystallization from dimethylformamide the *trans* isomer is obtained. Reconversion to the *cis* form occurs in toluene [310]. The complex of Me_2SnCl_2 with 2(1H)-pyridinethione has the all-*trans* octahedral geometry (152) [311], but the 2:1 complex of Me_2SnBr_2 with 1,4-dithiane has the dinuclear structure (153) with adjacent molecules connected by intermolecular Sn...Br interactions into a chain structure [312].



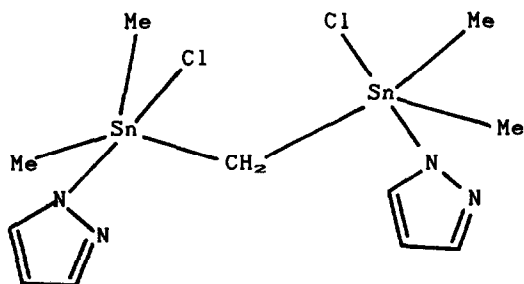
(145)



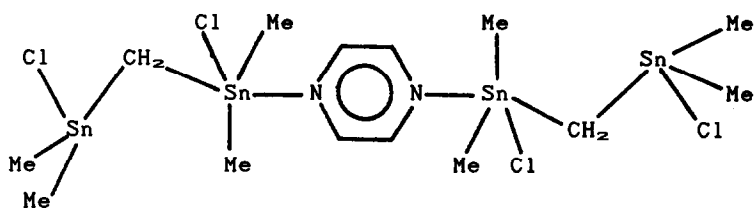
(146)



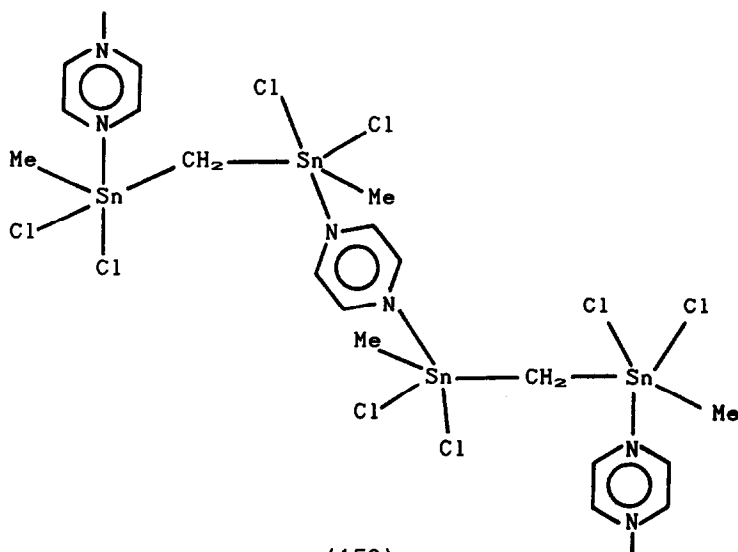
(147)



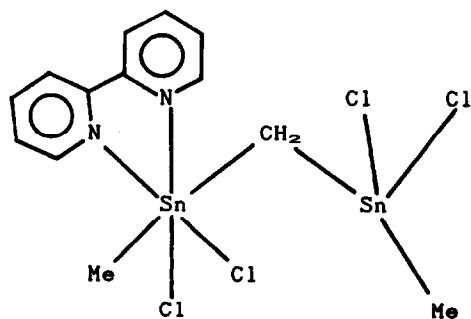
(148)



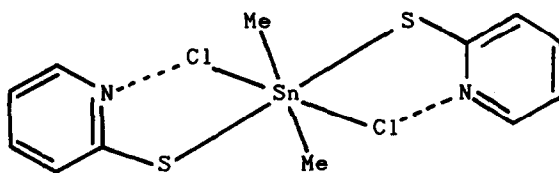
(149)



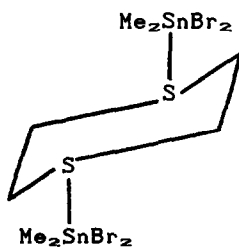
(150)



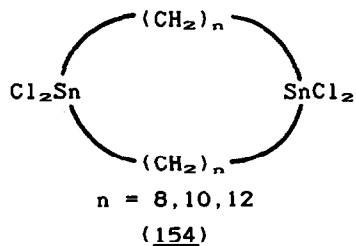
(151)



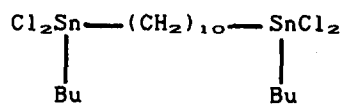
(152)



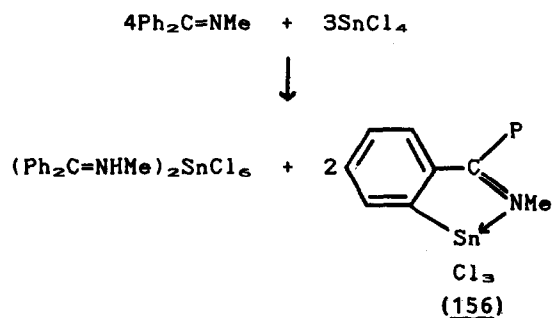
(153)



(154)



(155)



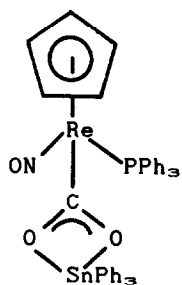
Scheme 62

Solution equilibria occurring in solutions of diorganotin dihalides and bases such as PPh_3O , DMSO, DMA, diphenyl sulphoxide, dibenzyl sulphoxide, pyridine N-oxide and acetonitrile have been investigated by nmr. Experimental data are attributed to predominant formation of the 1:1 adduct along with the associated adduct. The formation of the 1:2 adduct also occurs in solution as demonstrated by the isolation of 1:2 adducts and the curvature obtained in the chemical shift plots for weak acids and bases. The size of the substituents on the acid were shown to have a significant effect on the equilibrium constants. Thus the constants for di-*tert*-butyltin dichloride are a factor of 100 lower than those for Me_2SnCl_2 [313]. Similar methods have been employed to study the complexation of the distanna heterocycles (154), the acyclic analogue (155) and Bu_2SnCl_2 with chloride anion in acetonitrile. Rapid exchange of chloride occurred with all the organotin chlorides. Binding constants for chloride were evaluated. The macrocycles exhibited small cooperative effects in binding chloride in comparison to the acyclic organotin chlorides leading to an increased binding energy [314]. Treatment of tin(IV) halides with Schiff's bases in boiling toluene leads to the formation of immonium hexahalogenostannate salts and orthometallated compounds such as (156) which has a trigonal bipyramidal geometry at tin (axial nitrogen and chlorine) (Scheme 62) [315]. The complex $\text{SnCl}_4 \cdot 2(4\text{-t-BuC}_6\text{H}_4\text{CHO})$ has the *cis* octahedral geometry [316].

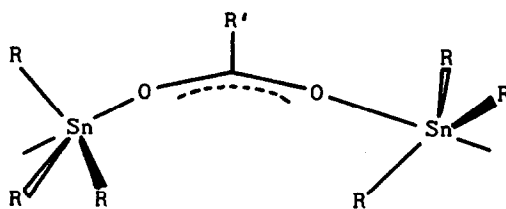
The synthesis and structures of several organotin carboxylates have been reported. Di-*t*-butyltin bis(carboxylates) have been synthesised from di-*t*-butyltin oxide trimer and the appropriate acid, and are monomeric and pentacoordinated except for the picolinate which is hexacoordinated [317]. Tin is tetrahedrally coordinated in tricyclohexylstannyl 3-indolyacetate, but an 'S'-shaped polymer is present in the crystal, propagated by intermolecular $\text{NH}\cdots\text{OC}$ hydrogen bonds [318]. Of the two chlorobenzoates, $\text{Ph}_2\text{Sn}(\text{O}_2\text{CC}_6\text{H}_4\text{Cl-o})$ is a five-coordinated monomer in the crystal whereas $\text{Ph}_2\text{Sn}(\text{O}_2\text{CC}_6\text{H}_4\text{Cl-p})$ is a one dimensional polymer [319], as are $\text{Me}_2\text{SnO}_2\text{CC}_6\text{H}_4\text{OMe-2}$ and

$\text{Me}_2\text{SnO}_2\text{CC}_6\text{H}_4\text{OH} \cdot 2$ [320]. The sophisticated carboxylate (157) is one of the few unassociated triorganotin carboxylates, and is the only one with equal C-O bond lengths [321]. It undergoes decarboxylation at 180° . The majority of triorganotin carboxylates, exemplified by triphenyltin formate and acetate [322], are associated into polymeric chains with trigonal bipyramidal geometry at tin as in (158). Triphenyltin 8-quinolylacetate hydrate associates differently in the solid, and forms one-dimensional helical chains by intermolecular hydrogen-bonding between adjacent $[\text{Ph}_3\text{SnO}_2\text{CCH}_2(8\text{-C}_9\text{H}_6\text{NO})\cdot\text{H}_2\text{O}]$ units [323]. Triorganotin derivatives of other oxyacids behave similarly, and both $\text{Me}_2\text{SnO}_2\text{FMe}_2$ and $\text{Me}_2\text{SnO}_2\text{PCl}_2$ form helical chain structures in which $[\text{Me}_2\text{Sn}]$ units are bridged by $[\text{O}_2\text{PX}_2]$ groups [324]. In the three ditin dicarboxylates, $\text{Ph}_4\text{Sn}_2(\text{O}_2\text{CX}_3)_2$ ($\text{X} = \text{H}, \text{F}, \text{Cl}$), the two carboxylate groups span the two tin atoms as in (159). Different conformations involving different orientations of the phenyl groups are observed [325].

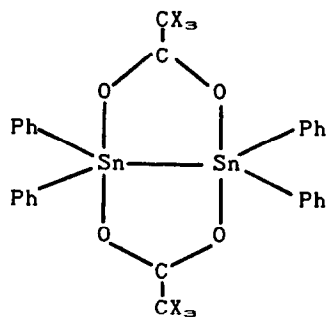
The first structures of diorganotin dicarboxylates, dimethyltin diacetate [326] and dipicolinate [327], have been determined. The former is monomeric with distorted octahedral coordination (160) and a Me-Sn-Me angle of $135.9(2)^\circ$, close to that predicted from solid-state and solution nmr studies. The dipicolinate, however, has the polymeric structure (161) in which both picolinate ligands chelate the tin atom via one oxygen and the nitrogen, with seven coordination at tin being completed by a bridging oxygen. The Me-Sn-Me angle is $174.5(3)^\circ$ as expected from the solid-state nmr data. The tin in the $[\text{Me}_2\text{Sn}(\text{OAc})_3]^-$ anion is also seven-coordinated with a Me-Sn-Me angle of 165.8° . Two acetate groups are anisobidentate whilst the third is unidentate. Molecules of dimethyltin bis(tropolonate) adopt a distorted cis-octahedral structure with a Me-Sn-Me angle of $107.9(6)^\circ$ [327]. Both dimethyltin bis(kojate) (as a bis(methanol) solvate) [327] and dimethyltin bis(2-pyridinethiolato-N-oxide) [328] both adopt the skew trapezoidal structure with Me-Sn-Me angles of $147.9(3)/148.5(3)^\circ$ and $138.9(2)^\circ$, respectively. A similar situation pertains for dimethyltin bis(monothio- β -diketonates)



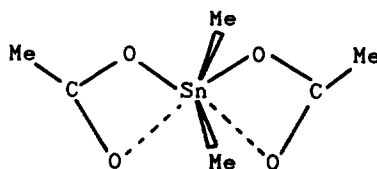
(157)



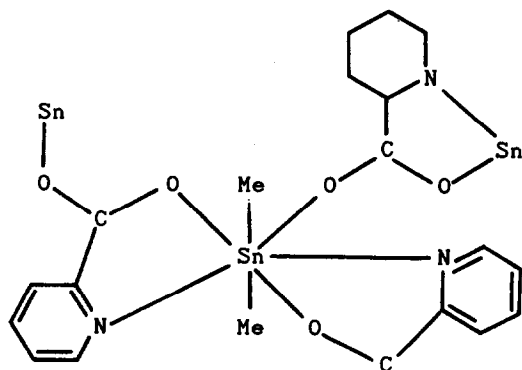
(158)



(159)



(160)

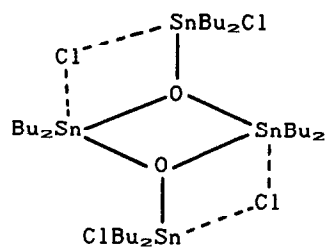


(161)

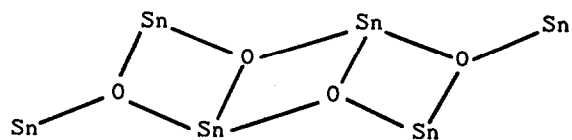
(Me-Sn-Me angles of 134.2 and 139.4°, respectively, for the benzoyl (thiobenzoyl)methane and monothioacetylacetone derivatives). However, the corresponding dichlorotin compounds have the cis-octahedral geometry [329].

Bis(trimethyltin)carbonate has a polymeric structure resulting from the terdentate mode of coordination of the carbonate dianion [330]. Other structures which have been described include 2,2-dibutyl-1,3,2-dioxastannolane (associated into an infinite ribbon structure) [331], $[\text{SnBu}_3(\text{OH})_2]_2[\text{C}_6(\text{CO}_2\text{Me})_6]$ [332], $\text{Bu}_2\text{Sn}[\text{O}_2\text{C}_6\text{HPh}]_2$ [333], $(\text{SnPh}_3\text{NO}_2)_2 \cdot \text{dpaoe}$ (dpaoe = 1,2-bis(diphenylarsoryl)ethane) and $\text{SnPh}_3(\text{NO}_2)_2 \cdot \text{dppom}$ (dppom = bis(diphenylphosphoryl)methane) [334], $\text{Ph}_3\text{PbO}_2\text{CCO}_2\text{Me}$ [335], $\text{Ph}_3\text{Sn}(\text{S}_2\text{CO}^i\text{Pr})$ [336], $[(t\text{-Bu})_2\text{Sn}(\text{ebdtc})]_2 \cdot 4\text{THF}$ (ebdtc = ethylenebis(dithiocarbamate) [337], $[\text{Me}_2\text{SnS}_2\text{P}(\text{Ph})\text{CH}_2\text{CH}_2]_2 \cdot \text{HMPT}$ [338], Dimethyltin bis(diethyl dithiophosphinate), $\text{Me}_2\text{Sn}(\text{S}_2\text{PET}_2)_2$, has a distorted tetrahedral structure, with additional long Sn...S contacts at 3.336(2) Å [339]. $(\text{C}_6\text{F}_5\text{Sn})_4\text{S}_6$ has the adamantane structure [340].

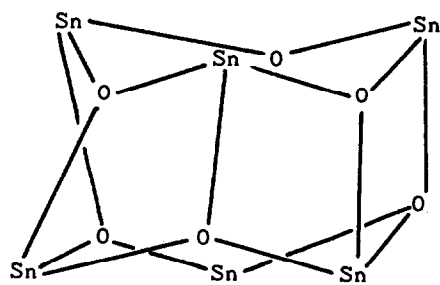
The distannoxane, $\text{Bu}_4\text{Sn}_2\text{Cl}_2\text{O}$, has a very similar dimeric tetranuclear structure (162) to that determined previously for the methyl analogue [341]. Examples of higher "ladder" and "drum" structures have been characterized for organotin oxide carboxylates [342, 343]. The compounds $[(n\text{-BuSn}(\text{O})\text{O}_2\text{CPh})_2(n\text{-BuSn}(\text{Cl})(\text{O}_2\text{CPh})_2)]_2$, $[(n\text{-BuSn}(\text{O})\text{O}_2\text{CR})_2(n\text{-BuSn}(\text{O}_2\text{CR})_2)]_2$, (R = Me, Ph, C_6H_{11}) and $[(\text{MeSn}(\text{O})\text{O}_2\text{CC}_6\text{H}_{11})_2(\text{MeSn}(\text{O}_2\text{CC}_6\text{H}_{11})_2)]_2$ all have the "ladder" structure (skeleton (163), whereas $[n\text{-BuSn}(\text{O})\text{O}_2\text{CR}]_n \cdot \text{C}_6\text{H}_6$ (R = C_6H_5 , C_6H_{11}) and $[n\text{-BuSn}(\text{O})\text{O}_2\text{CC}_6\text{H}_4\text{NO}_2 \cdot 2]_n \cdot 3\text{C}_6\text{H}_6$ have the "drum" structure skeleton (164). In solution the "drum" and "ladder" structures interconvert reversibly. Two similar organotin oxide phosphate clusters, $[(n\text{-BuSn}(\text{OH})\text{O}_2\text{PPh}_2)_3\text{O}][\text{Ph}_2\text{PO}_2]$ (165) [344] and $[n\text{-BuSn}(\text{O})\text{O}_2\text{P}(\text{C}_6\text{H}_{11})_2]_4$ (166) [345] have also been characterized. Partial oxidation of $\text{Sn}(\text{O}_2\text{CCF}_3)_2$ affords the mixed-valence tin carboxylate (167), which is not centrosymmetric and has a central $[\text{Sn}^{\text{IV}}_4\text{Sn}^{\text{II}}\text{O}_6]$ unit containing two μ_3 -oxygen atoms each of which bridge between a tin(IV) and two symmetry-



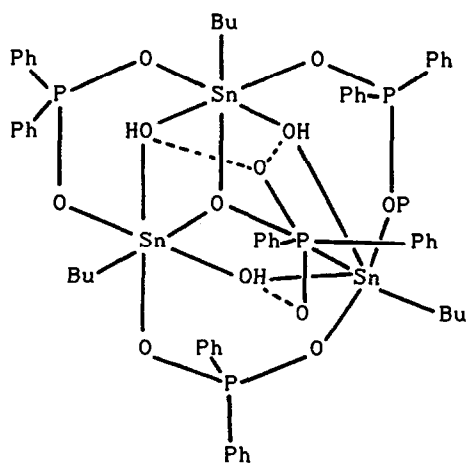
(162)



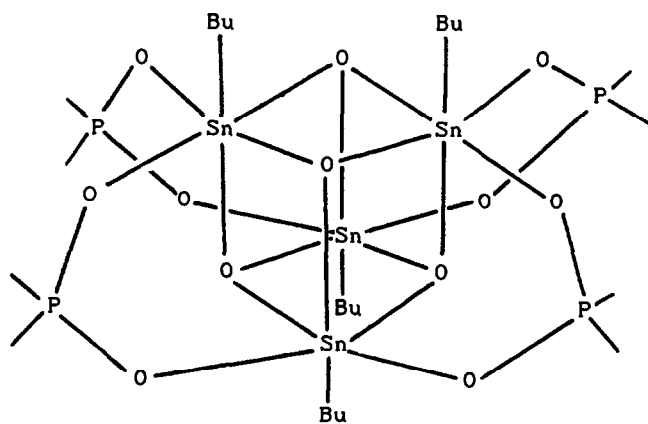
(163)



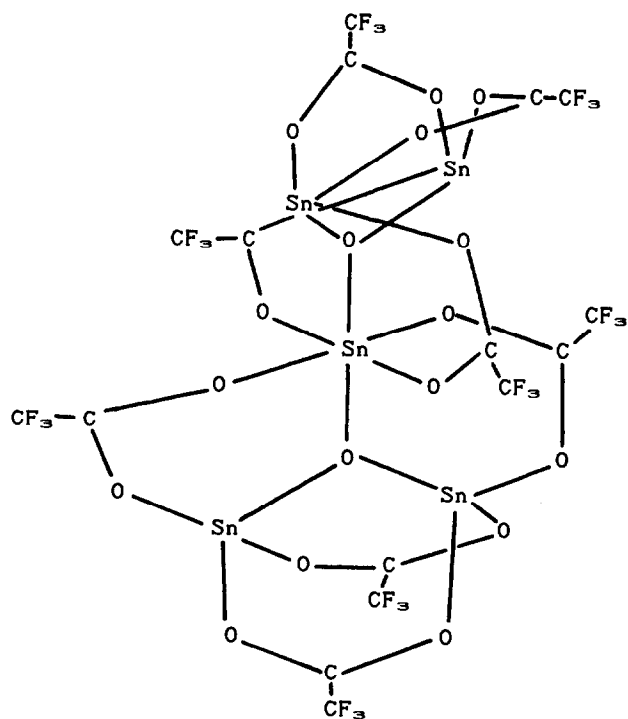
(164)



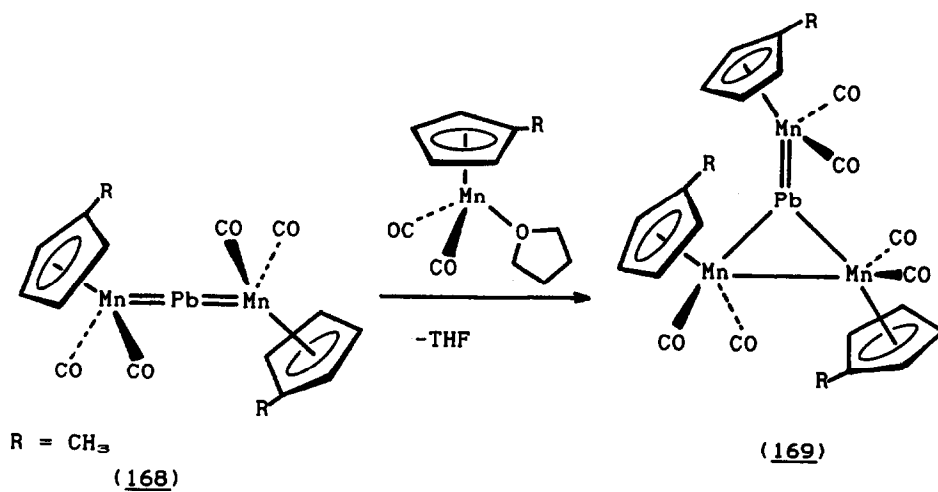
(165)



(166)



(167)



(168)

(169)

Scheme 63

related tin(II) atoms [346].

The structures of $(C_5H_5)_2USnPh_2$ (the first example of a uranium-tin bond) [347], $(C_5H_5)_2TaH_2MeCl_2$ [348], the osmium-tin clusters, $Os_3(\mu-H)_2(CO)_{10}(SnMe_3)_2$ [349] and $Os_3SnCl_2(CO)_{11}(\mu-CH_3)$ [350], and $[Et_4N][Pb(Fe(CO)_4)_2(Fe_2(CO)_9)]$ [351] have all been determined. Treatment of the heterocumulene $MnPbMn$ species (168) with an excess of the solvent-stabilized fragment $(MeC_5H_4)Mn(CO)_2(THF)$ yields a reaction mixture from which the novel complex (169), which has a planar $[Mn_3Pb]$ core, was isolated (Scheme 63) [352].

Many of the reports already mentioned contain substantial amounts of nmr (particularly ^{119}Sn) and Mössbauer data. Solid-state ^{13}C nmr data for methyltin compounds show that the ^{13}C chemical shifts for the methyl groups bound to tin generally increase (more deshielded) in the series tetra- < penta- < hepta-coordination at tin and tri- < di- < monomethyltin compounds, although there is considerable overlap between the groups, and that there is a good correlation between the $^1J(^{119}Sn-^{13}C)$ coupling constant and the $Me-Sn-Me$ bond angle [353]. ^{119}Sn CP-MAS high resolution nmr spectra have been obtained for the two polymeric dialkyltin oxides, $(R_2SnO)_n$ ($R = Me, Bu$), and are consistent with previously proposed structures [354]. The largest recorded primary (10.7%) and secondary (3.0%) deuterium isotope effects on spin-spin coupling constants have been observed for $^1J(^{119}Sn-H)$ in the ^{119}Sn nmr spectrum of the stannyl ion $[SnH_{3-n}D_n]^-$ ($n \leq 3$) [355]. The mixed species $R_3Sn-X-SnR'_3$ ($R, R' = Bu, Ph, C_6H_{11}$; $X = O, S$), which exist in solution along with the symmetrical species, have been identified by ^{119}Sn nmr [356]. The ^{119}Sn chemical shifts and $^1J(^{119}Sn-^{13}C)$ coupling constants in solutions of tribenzyltin compounds depend on the coordination number of the central atom and the geometry of the coordination polyhedra [357]. ^{119}Sn nmr has been employed to identify thiocyanato-, and cyano-derivatives of the $[SnX_6]^{2-}$ anions of the types $[SnX_5Y_n]^{2-}$ ($X = Cl, Br$; $Y = NCS, CN$) [358]. Exchange reactions occurring in solutions of trichlorostannate-platinum(II) species have been studied by two-dimensional ^{31}P nmr [359]. ^{119}Sn

Mössbauer spectroscopy shows that dialkyltin derivatives of adenosine 5'-monophosphate contain a distorted octahedral tin environment with a bent SnC_2 unit embedded in a two-dimensional polymeric lattice [360].

Nmr continues to prove an exceptionally useful tool for structural investigations, especially with the advent of solid-state techniques. The combined techniques of high-power decoupling, cross-polarisation and magic-angle rotation have been applied to lead-207 nmr of solid organolead compounds [361]. Carbon-13 MAS-nmr has been used to study organotin compounds, and is extremely useful for structural elucidation of powders [362] and the study of polymorphism [363]. The structures of dimethyltin diacetate and its hydrolysis product $(\text{Me}_2[\text{Sn}(\text{OAc})]_2\text{O})_n$ have been studied by both solid-state and solution nmr. Coupling constant data suggest a value of ca. 135° for the C-Sn-C bond angle in $\text{Me}_2\text{Sn}(\text{OAc})_2$, and carbon-13 spectra indicate the occurrence of a second crystalline modification. The distannoxane forms dimeric units with a central $[\text{Sn}_2\text{O}_2]$ ring, with an overall polymeric structure formed by an additional bonding interaction between an exocyclic tin atom and an oxygen atom of a carboxylate group of adjacent dimers. Unlike others similar molecules, no centre of symmetry is present. Solution nmr data indicate the presence of two types of tin atom, both of which are hexacoordinated and adopt distorted *trans*-dimethyloctahedral conformations (C-Sn-C angles ca. 141° and 145°) [364]. The two bond $^2J(^{119}\text{Sn}-^1\text{H})$ coupling constant in methyltin compounds has been shown to be related (by a smooth curve) to the C-Sn-C bond angle [365]; similarly the dependence of the one-bond $^1J(^{119}\text{Sn}-^{13}\text{C})$ coupling constant to the C-Sn-C bond angle in butyltin compounds has been demonstrated [366]. Several other solution nmr studies are worthy of mention. A one-bond $^{117,119}\text{Sn}-^{14}\text{N}$ coupling has been observed for the first time (in tricyclohexyltin isothiocyanate) [367]. Tetraalkoxygermanes have been investigated by ^{13}C , ^{17}O and ^{73}Ge nmr. The ^{73}Ge signals are more sensitive to structure variations than those of ^{29}Si in isostructural alkoxysilanes [368]. The ^{119}Sn chemical shift and

one-bond $^1J(^{119}\text{Sn}-^{13}\text{C})$ coupling constant can be used semi-quantitatively to describe the shape of the coordination polyhedra about tin in dibutyltin compounds and their complexes. Values of the chemical shift define regions with different coordination numbers, so that four-coordinate compounds have $\delta(^{119}\text{Sn})$ ranging from +200 to -60 ppm, five-coordinate compounds -90 to -190 ppm, and six-coordinate compounds -210 to -400 ppm. Magnitudes of the coupling constants can be used to estimate the C-Sn-C angle [369]. Similar conclusions have also been arrived at by French workers in studies of bisalkoxytin derivatives of the type, $\text{R}_2\text{SnO}-\text{A}-\text{OSnR}_2$ [370]. The combination of ^{119}Sn nmr and ^{119}Sn Mössbauer spectroscopies can also be powerful [371,372], whilst the application of multinuclear (^{119}Sn , ^{208}Tl , and ^{207}Pb) has enabled the characterisation of the anionic clusters formed by dissolving alkali metal alloys of Ge, Sn, Sb, Tl, Pb and Bi in liquid ethylenediamine [373]. Mass spectroscopy has been employed to characterise neutral analogues of these anionic clusters in the gas phase such as Pb_3Sb_2 , Pb_5Sb_4 and Sn_5Bi_4 [374].

REFERENCES

1. G.E. Scuseria, M. Durán, R.G.A.R. MacLagan and H.F. Schaeffer, *J. Am. Chem. Soc.*, 1986, **108**, 3248.
2. G.A. Ganzer, R.S. Sheridan and M.T.H. Liu, *J. Am. Chem. Soc.*, 1986, **108**, 1517.
3. M.A. Kesselmayr and R.S. Sheridan, *J. Am. Chem. Soc.*, 1986, **108**, 99.
4. M.A. Kesselmayr and R.S. Sheridan, *J. Am. Chem. Soc.*, 1986, **108**, 844.
5. E. Leyva, R.L. Barcus and M.S. Platz, *J. Am. Chem. Soc.*, 1986, **108**, 7786.
6. H. Boch, G. Tschmutowa and H.P. Wolf, *J. Chem. Soc., Chem. Commun.*, 1986, 1068.
7. D.R. Myers, V.P. Senthilnathan, M.S. Platz and M. Jones, *J. Am. Chem. Soc.*, 1986, **108**, 4232.
8. H. Barcus, L.M. Hadel, L.J. Johnston, M.S. Platz, T.G. Savino and J.C. Scaiano, *J. Am. Chem. Soc.*, 1986, **108**, 3928.
9. M.T. Nguyen and A.F. Hegarty, *J. Chem. Soc., Chem. Commun.*, 1986, 773.
10. M. Rahmann, M.L. McKee and P.B. Shevlin, *J. Am. Chem. Soc.*, 1986, **108**, 6296.
11. R. Lesclaux, P. Roussel, B. Veyret and C. Pouchan, *J. Am. Chem. Soc.*, 1986, **108**, 3872.
12. B. van Baar, P.C. Burgers, J.K. Terlouw and H. Schwarz, *J. Chem. Soc., Chem. Commun.*, 1986, 1607.

13. D.A. Dixon, J.C. Calabrese and J.S. Miller, *J. Am. Chem. Soc.*, 1986, 108, 2582.
14. S. Okada, Y. Abe, A. Taniguchi and S. Yamabe, *J. Am. Chem. Soc.*, 109, 1987, 295.
15. J.D. Evanseck, J.F. Blake and W.L. Jorgesen, *J. Am. Chem. Soc.*, 109, 1987, 2349.
16. D.J. Clothier and D.C. Moule, *J. Am. Chem. Soc.*, 109, 1987, 6259.
17. M. L. McKee, *J. Am. Chem. Soc.*, 1986, 108, 5059.
18. P. Luger, C. Zaki, J. Buschmann and R. Ruders, *Angew. Chem., Int. Ed. Engl.*, 1986, 25, 276.
19. D.A. Dixon, T. Fukumaga and B.E. Smart, *J. Am. Chem. Soc.*, 1986, 108, 1585.
20. S.K. Sengupta, H. Justnes, C.W. Gillies and N.C. Craig, *J. Am. Chem. Soc.*, 1986, 108, 876.
21. H. Justnes, J. Zozom, C.W. Gillies, and S.K. Sengupta and B.C. Craig, *J. Am. Chem. Soc.*, 1986, 108, 881.
22. R.N. Beauchamp, J.W. Agopovich and C.W. Gillies, *J. Am. Chem. Soc.*, 1986, 108, 2552.
23. T.D. Norden, S.W. Staley, W.H. Taylor and M.D. Harmony, *J. Am. Chem. Soc.*, 1986, 108, 7912.
24. E. Vajda, J. Tremmel, B. Rozsondai, L. Hargittai, A.K. Maltsev, N.D. Kagramanov and O.M. Nefedov, *J. Am. Chem. Soc.*, 1986, 108, 4352.
25. S.W. Froelicher, B.S. Freiser and R.R. Squires, *J. Am. Chem. Soc.*, 1986, 108, 2853.
26. K. Lammertsma, J.A. Pople and P. von R. Schleyer, *J. Am. Chem. Soc.*, 1986, 108, 7.
27. P. Dowd and Y.H. Paik, *J. Am. Chem. Soc.*, 1986, 108, 2788.
28. B. van Baar, T. Weiske, J.K. Terlouw and H. Schwarz, *Angew. Chem., Int. Ed. Engl.*, 1986, 25, 282.
29. B. van Baar, W. Koch, C. Lebrilla, J.K. Terlouw, T. Weiske and H. Schwarz, *Angew. Chem., Int. Ed. Engl.*, 1986, 25, 827.
30. J. Wessel, H. Hard and K. Seppelt, *Chem. Ber.*, 1986, 119, 453.
31. R. Weiss, G.E. Miess, A. Haller and W. Reinhardt, *Angew. Chem., Int. Ed. Engl.*, 1986, 25, 103.
32. O. Ayed, A. Loutellier, L. Manceron and J.P. Perchard, *J. Am. Chem. Soc.*, 1986, 108, 8138.
33. B. Silvi, O. Ayed and W.B. Person, *J. Am. Chem. Soc.*, 1986, 108, 8148.
34. J.-Y. Liang and W.N. Lipscomb, *J. Am. Chem. Soc.*, 1986, 108, 5051.
35. J.K. Terlouw, C.B. Lebrilla and H. Schwarz, *Angew. Chem., Int. Ed. Engl.*, 26, 1987, 354.
36. H. Eckert and B. Forster, *Angew. Chem., Int. Ed. Engl.*, 26, 1987, 894.
37. D. Semmingsen and P. Gorth, *J. Am. Chem. Soc.*, 109, 1987, 7238.
38. O. Ermer and J. Les, *Angew. Chem., Int. Ed. Engl.*, 26, 1987, 447.
39. Y.-T. Chang, Y. Yamaguchi, W.H. Miller and H.F. Schaeffer, *J. Am. Chem. Soc.*, 109, 1987, 7245.
40. W. Sander and A. Patyk, *Angew. Chem., Int. Ed. Engl.*, 26,

- 1987, 475.
41. G. Baum, F.-J. Kaiser, W. Massa and G. Seitz, *Angew. Chem., Int. Ed. Engl.*, 26, 1987, 1163.
42. R. Okazaki, A. Ishii and N. Inamoto, *J. Am. Chem. Soc.*, 109, 1987, 279.
43. R.D. Brown, P.D. Godfrey, P.S. Elmes and D. McNaughton, *J. Chem. Soc., Chem. Commun*, 1987, 573.
44. A. Haas and W. Wanzke, *Chem. Ber.*, 120, 1987, 429.
45. W. Eul, G. Kiel and G. Gattow, *Z. anorg. allg. Chem.*, 544, 1987, 149.
46. W. Eul and G. Gattow, *Z. anorg. allg. Chem.*, 545, 1987, 125.
47. R. Gleiter, G. Krennrich and M. Langer, *Angew. Chem., Int. Ed. Engl.*, 1986, 25, 999.
48. W. Sander, *Angew. Chem., Int. Ed. Engl.*, 1986, 25, 255.
49. R.D. Brown, P.D. Godfrey and M. Rodler, *J. Am. Chem. Soc.*, 1986, 108, 1296.
50. R. Diercks, J.C. Armstrong, R. Boese and K.P.C. Vollhardt, *Angew. Chem., Int. Ed. Engl.*, 1986, 25, 268.
51. S. Chowdhury, E.P. Grimsrud, T. Heinis and P. Kebarle, *J. Am. Chem. Soc.*, 1986, 108, 3630.
52. B.S. Ault, *Inorg. Chem.*, 1986, 25, 1013.
53. W.A. Kamil, F. Haspel-Hentrich and J.M. Shreeve, *Inorg. Chem.*, 1986, 25, 376.
54. T. Huang and J.M. Shreeve, *Inorg. Chem.*, 1986, 25, 496.
55. A. Waterfeld and R. Mews, *Chem. Ber.*, 1986, 118, 4997.
56. J. Antel, K. Harms, P.G. Jones, R. Mews, G.M. Sheldrick and A. Waterfeld, *Chem. Ber.*, 1986, 118, 5006.
57. K.D. Gupta, R. Mews, A. Waterfeld, J.M. Shreeve and H. Oberhammer, *Inorg. Chem.*, 1986, 25, 275.
58. M. Schwab and W. Sundermeyer, *Chem. Ber.*, 1986, 118, 2458.
59. S. Singh, D.D. DesMarteau, S.S. Zuberi, M. Witz and H.-N. Huang, *J. Am. Chem. Soc.*, 109, 1987, 7194.
60. D. Lentz, I. Brüdgen and H. Hartl, *Angew. Chem., Int. Ed. Engl.*, 26, 1987, 921.
61. D. Christen, H.-G. Mack, C.J. Marsden, H. Oberhammer, G. Schatte, K. Seppelt and H. Willner, *J. Am. Chem. Soc.*, 109, 1987, 4009.
62. R.N. Beauchamp, C.W. Gillies and N.C. Craig, *J. Am. Chem. Soc.*, 109, 1987, 1696.
63. E.G. Awere, N. Burford, C. Mailer, J. Passmore, M.J. Schriver, P.S. White, A.J. Bannister, H. Oberhammer and L.H. Surcliffe, *J. Chem. Soc., Chem. Commun*, 1987, 66.
64. D.A. Dixon and B.E. Smart, *J. Am. Chem. Soc.*, 1986, 108, 2688.
65. H. Bock, R. Dammel and D. Jaculi, *J. Am. Chem. Soc.*, 1986, 108, 7844.
66. R.D. Brown, P.D. Godfrey, M.J. Ball, S. Godfrey, D. McNaughton, M. Rodler, B. Kleibömer and R. Champion, *J. Am. Chem. Soc.*, 1986, 108, 8534.
67. W. Eul and G. Gattow, *Z. anorg. allg. Chem.*, 1986, 537, 189.
68. W. Eul and G. Gattow, *Z. anorg. allg. Chem.*, 1986, 538, 151.
69. W. Eul, G. Kiel and G. Gattow, *Z. anorg. allg. Chem.*, 1986, 542, 182.
70. W. Eul and G. Gattow, *Z. anorg. allg. Chem.*, 1986, 543, 81.

71. W. Eul and G. Gattow, *Z. anorg. allg. Chem.*, 1986, 535, 159.
72. W. Eul, G. Kiel and G. Gattow, *Z. anorg. allg. Chem.*, 1986, 535, 167.
73. W. Eul and G. Gattow, *Z. anorg. allg. Chem.*, 1986, 536, 119.
74. G. Gattow and S. Lotz, *Z. anorg. allg. Chem.*, 1986, 533, 99.
75. G. Gattow and S. Lotz, *Z. anorg. allg. Chem.*, 1986, 533, 109.
76. B. Gerner and G. Kiel, *Z. anorg. allg. Chem.*, 1986, 532, 99.
77. D.R. Armstrong, A.J. Bannister, W. Clegg and W.R. Gibb, *J. Chem. Soc., Chem. Commun.*, 1986, 1672.
78. J.P. LaFemina and J.P. Lowe, *J. Am. Chem. Soc.*, 1986, 108, 2527.
79. S. Koyama, T. Maeda and K. Okamura, *Z. anorg. allg. Chem.*, 1986, 540/541, 117.
80. J. Kouvetakis, R.B. Kaner, M.L. Sattler and N. Bartlett, *J. Chem. Soc., Chem. Commun.*, 1986, 1758.
81. H. Preiss, M. Goerlich and H. Sprenger, *Z. anorg. allg. Chem.*, 1986, 533, 37.
82. H. Preiss, U. Nissel and H. Sprenger, *Z. anorg. allg. Chem.*, 1986, 543, 133.
83. H. Preiss, A. Lehmann and H. Sprenger, *Z. anorg. allg. Chem.*, 1986, 543, 143.
84. B.S. Suresh and J.C. Thompson, *J. Chem. Soc., Dalton Trans.*, 1987, 1123.
85. S. Konieczny, P.P. Gaspar and J. Wormhoudt, *J. Organomet. Chem.*, 1986, 307, 151.
86. W.L. Lee, C.F. Shieh and C.S. Liu, *J. Organomet. Chem.*, 1986, 302, 23.
87. H.M. Frey, R. Walsh and I.M. Watts, *J. Chem. Soc., Chem. Commun.*, 1986, 1189.
88. T.J. Barton and N. Tillman, *J. Am. Chem. Soc.*, 109, 1987, 6711.
89. M.S. Gordon and D. Bartol, *J. Am. Chem. Soc.*, 109, 1987, 5948.
90. H. Kang, D.B. Jacobson, S.K. Shin, J.L. Beauchamp and M.T. Bowers, *J. Am. Chem. Soc.*, 1986, 108, 5668.
91. R. Damrauer, C.H. DePuy, I.M.T. Davidson and K. Hughes, *Organometallics*, 1986, 5, 2054.
92. R.S. Grev and H.F. Schaeffer, *J. Am. Chem. Soc.*, 1986, 108, 5804.
93. G. Raabe, H. Vancik, R. West and J. Michl, *J. Am. Chem. Soc.*, 1986, 108, 671.
94. P.P. Gaspar and D. Lei, *Organometallics*, 1986, 5, 1276.
95. H. Appler and W.P. Neumann, *J. Organomet. Chem.*, 1986, 314, 261.
96. D.H. Berry and Q. Jiang, *J. Am. Chem. Soc.*, 109, 1987, 6210.
97. D.H. Berry and J.H. Mitsifer, *J. Am. Chem. Soc.*, 109, 1987, 3777.
98. D.A. Strauss, T.D. Tilley, A.L. Rheingold and S.J. Geib, *J. Am. Chem. Soc.*, 109, 1987, 5872.
99. C. Zybili and G. Müller, *Angew. Chem., Int. Ed. Engl.*, 26, 1987, 669.
100. H.-P. Abicht, K. Jurkschat, A. Tzschach, K. Peters, E.M. Peters and H.G. von Schnering, *J. Organomet. Chem.*, 326, 1987, 357.

101. A. Castel, P. Riviere, J. Satge and M. Abbala, *J. Organomet. Chem.*, **328**, 1987, 123.
102. A. Castel, P. Riviere, J. Satge and M. Abbala, *J. Organomet. Chem.*, **331**, 1987, 11.
103. K. Mochida, A. Fujii, N. Tsuchiya, K. Tohji and Y. Udagawa, *Organometallics*, **6**, 1987, 1811.
104. L. Lange, B. Meyer and W.W. duMont, *J. Organomet. Chem.*, **329**, 1987, C17.
105. A.M. Arif, A.H. Cowley and T.M. Elkins, *J. Organomet. Chem.*, **325**, 1987, C11.
106. C. Glidewell, D. Lloyd and K.W. Lumbard, *J. Chem. Soc., Dalton Trans.*, 1987, 501.
107. C. Glidewell, D. Lloyd and K.W. Lumbard, *J. Chem. Soc., Dalton Trans.*, 1987, 509.
108. M.F. Lappert, M.C. Misra, M. Onyszchuk, R.S. Rowe, P.P. Power and M.J. Slade, *J. Organomet. Chem.*, **330**, 1987, 31.
109. C. Stader and B. Wrackmeyer, *J. Organomet. Chem.*, **321**, 1987, C1.
110. S.M. Hawkins, P.B. Hitchcock, M.F. Lappert and A.K. Rai, *J. Chem. Soc., Chem. Commun.*, 1986, 1689.
111. C.J. Cardin, D.J. Cardin, G.A. Lawless, J.M. Power and M.B. Power, *J. Organomet. Chem.*, **325**, 1987, 203.
112. P.B. Hitchcock, M.F. Lappert and M.J. Michalczyk, *J. Chem. Soc., Dalton Trans.*, 1987, 2635.
113. R. West, *Angew. Chem., Int. Ed. Engl.*, **26**, 1987, 1201.
114. H. Sun, D.A. Hrovat and W.T. Borden, *J. Am. Chem. Soc.*, **109**, 1987, 5275.
115. H. Teramae, *J. Am. Chem. Soc.*, **109**, 1987, 4140.
116. B.H. Boo and P.P. Gaspar, *Organometallics*, 1986, **5**, 696.
117. S. Masamune, Y. Eriyama and T. Kawase, *Angew. Chem., Int. Ed. Engl.*, **26**, 1987, 584.
118. H.B. Yokelson, A.J. Millevolte, B.R. Adams and R. West, *J. Am. Chem. Soc.*, **109**, 1987, 4118.
119. H.B. Yokelson, A.J. Millevolte, K.J. Haller and R. West, *J. Chem. Soc., Chem. Commun.*, 1987, 1605.
120. H.B. Yokelson, J. Maxka, D.A. Siegel and R. West, *J. Am. Chem. Soc.*, 1986, **108**, 4239.
121. C. Zybail and R. West, *J. Chem. Soc., Chem. Commun.*, 1986, 857.
122. A. Sekiguchi, S.S. Zigler and R. West, *J. Am. Chem. Soc.*, 1986, **108**, 4241.
123. K.W. Zilm, G.A. Lawless, R.M. Merrill, J.M. Millar and G.G. Webb, *J. Am. Chem. Soc.*, **109**, 1987, 7236.
124. K.D. Dobbs and W.J. Hehre, *Organometallics*, 1986, **5**, 2057.
125. A.G. Brook, *J. Organomet. Chem.*, 1986, **300**, 21.
126. N. Wiberg and G. Wagner, *Chem. Ber.*, 1986, **119**, 1455.
127. N. Wiberg and G. Wagner, *Chem. Ber.*, 1986, **119**, 1467.
128. N. Wiberg and H. Köpf, *J. Organometal. Chem.*, 1986, **315**, 9.
129. N. Wiberg and C.-K. Kim, *Chem. Ber.*, 1986, **119**, 2966.
130. N. Wiberg and C.-K. Kim, *Chem. Ber.*, 1986, **119**, 2980.
131. N. Wiberg, G. Wagner, J. Riede and G. Müller, *Organometallics*, **6**, 1987, 32.
132. N. Wiberg, G. Wagner, G. Reber, J. Riede and G. Müller, *Organometallics*, **6**, 1987, 35.

133. N. Wiberg and H. Köpf, *Chem. Ber.*, 120, 1987, 653.
132. N. Wiberg, G. Hischer and K. Schurz, *Chem. Ber.*, 120, 1987, 1605.
134. C. Couret, J. Escudie, J. Satge and M. Lazraq, *J. Am. Chem. Soc.*, 109, 1987, 4411.
135. H. Meyer, G. Baum, W. Massa and A. Bernt, *Angew. Chem., Int. Ed. Engl.*, 26, 1987, 798.
136. H. Meyer, G. Baum, W. Massa, S. Berger and A. Bernt, *Angew. Chem., Int. Ed. Engl.*, 26, 1987, 548.
137. L. Linder, A. Revis and T.J. Barton, *J. Am. Chem. Soc.*, 1986, 108, 2742.
138. R. Withnall and L. Andrews, *J. Am. Chem. Soc.*, 1986, 108, 8118.
139. T. Kudo and S. Nagase, *Organometallics*, 1986, 5, 1207.
140. D.P. Thompson and P. Boudjouk, *J. Chem. Soc., Chem. Commun.*, 1987, 1468.
141. P von R. Schleyer and P.D. Stout, *J. Chem. Soc., Chem. Commun.*, 1986, 1373.
142. N. Wiberg, P. Karampatses and C.-K. Kim, *Chem. Ber.*, 120, 1987, 1203.
143. N. Wiberg, P. Karampatses and C.-K. Kim, *Chem. Ber.*, 120, 1987, 1213.
144. N. Wiberg, G. Preiner, P. Karampatses, C.-K. Kim and K. Schurz, *Chem. Ber.*, 120, 1987, 1357.
145. M. Hesse and U. Klingebiel, *Angew. Chem., Int. Ed. Engl.*, 1986, 25, 649.
146. N. Wiberg, K. Schurz, G. Reber and G. Müller, *J. Chem. Soc., Chem. Commun.*, 1986, 591.
147. S.S. Ziegler, K.M. Welsh and R. West, *J. Am. Chem. Soc.*, 109, 1987, 4392.
148. C. Gulmon and G. Pfister-Guillouzo, *Organometallics*, 6, 1987, 1387.
149. C.N. Smit and F. Bickelhaupt, *Organometallics*, 6, 1987, 1158.
150. J. Escudie, C. Couret, M. Andrianarison and J. Satge, *J. Am. Chem. Soc.*, 109, 1987, 386.
151. M. Andrianarison, C. Couret, J.-P. Declercq, A. Dubourg, J. Escudie and J. Satge, *J. Chem. Soc., Chem. Commun.*, 1987, 921.
152. P. Jutzi, D. Kanne and C. Krüger, *Angew. Chem., Int. Ed. Engl.*, 1986, 25, 164.
153. P. Jutzi and B. Hielscher, *Organometallics*, 1986, 5, 1201.
154. P. Jutzi and B. Hampel, *Organometallics*, 1986, 5, 730.
155. P. Jutzi, B. Hampel, M.B. Hursthouse and A.J. Howes, *Organometallics*, 1986, 5, 1944.
156. P. Jutzi and B. Hielscher, *Organometallics*, 1986, 5, 2511.
157. R.L. Williamson and M.B. Hall, *Organometallics*, 1986, 5, 2142.
158. P. Jutzi, E. Schlöter, M.B. Hursthouse, A.M. Arif and R.L. Short, *J. Organometal. Chem.*, 1986, 299, 285.
159. H. Schumann, C. Janiak, E. Hahn, C. Kolax, J. Loebel, M.D. Rausch, J.J. Zuckerman and M.J. Heeg, *Chem. Ber.*, 1986, 119, 2658.
160. F. Kohl, R. Dickbreder, P. Jutzi, G. Müller and B. Huber, *J. Organometal. Chem.*, 1986, 309, C43.

161. N.S. Hosmane, P. de Meester, U. Siriwardane, M.S. Islam and S.S.C. Chu, *J. Chem. Soc., Chem. Commun.*, 1986, 1421.
162. N.S. Hosmane, P. de Meester, U. Siriwardane, M.S. Islam and S.S.C. Chu, *J. Am. Chem. Soc.*, 1986, 108, 6050.
163. N.S. Hosmane, P. de Meester, N.N. Maldar, S.B. Potts, S.S.C. Chu and R.H. Herber, *Organometallics*, 1986, 5, 772.
164. T. Fjeldberg, A. Haaland, B.E.R. Schilling, M.F. Lappert and A.J. Thorne, *J. Chem. Soc., Dalton Trans.*, 1986, 1551.
165. D.E. Goldberg, P.B. Hitchcock, M.F. Lappert, K.M. Thomas, A.J. Thorne, T. Fjeldberg, A. Haaland and B.E.R. Schilling, *J. Chem. Soc., Dalton Trans.*, 1986, 2387.
166. A.L. Balch and D.E. Oram, *Organometallics*, 1986, 5, 2159.
167. H.H. Karsch, A. Appelt and G. Hanika, *J. Organometal. Chem.*, 1986, 312, C1.
168. H.H. Karsch, A. Appelt and G. Müller, *Organometallics*, 1986, 5, 1664.
169. H.H. Karsch, B. Deubelly, J. Riede and G. Müller, *J. Organomet. Chem.*, 336, 1987, C37.
170. H.H. Karsch, B. Deubelly, J. Riede and G. Müller, *Angew. Chem., Int. Ed. Engl.*, 26, 1987, 673.
171. H.H. Karsch, B. Deubelly, J. Riede and G. Müller, *Angew. Chem., Int. Ed. Engl.*, 26, 1987, 674.
172. A.L. Balch and D.E. Oram, *Inorg. Chem.*, 26, 1987, 1906.
173. A.M. Arif, A.H. Cowley, R.A. Jones and J.M. Power, *J. Chem. Soc., Chem. Commun.*, 1986, 1446.
174. K. Jurkschat, H.-P. Abicht, A. Tzschach and R. Mahieu, *J. Organometal. Chem.*, 1986, 309, C47.
175. P. Jutzi and B. Hampel, *J. Organometal. Chem.*, 1986, 301, 283.
176. P. Jutzi, B. Hampel, M.B. Hursthouse and A.J. Howes, *J. Organometal. Chem.*, 1986, 299, 19.
177. A. Castel, P. Riviere, J. Satge, M. Ahbala and J. Jaud, *J. Organometal. Chem.*, 1986, 307, 205.
178. U. Baumeister, H. Hartung, K. Jurkschat and A. Tzschach, *J. Organometal. Chem.*, 1986, 304, 107.
179. A. Zschunke, M. Scheer, M. Völitzke and A. Tzschach, *J. Organometal. Chem.*, 1986, 308, 325.
180. H.H. Karsch and A. Appelt, *J. Organometal. Chem.*, 1986, 312, C6.
181. P.B. Hitchcock, M.F. Lappert, S.A. Thomas, A.J. Thorne, A.J. Carty and N.J. Taylor, *J. Organometal. Chem.*, 1986, 315, 37.
182. M. Onyszchuk, A. Castel, P. Riviere and J. Satge, *J. Organometal. Chem.*, 1986, 317, C35.
183. P. Riviere, A. Castel, J. Satge and D. Guyot, *J. Organometal. Chem.*, 1986, 315, 157.
184. D.L. Perry, J.L. Margrave, R.H. Hauge and P.F. Meier, *Inorg. Chim. Acta*, 1986, 116, L17.
185. K. Horchler, C. Stader and B. Wrackmeyer, *Inorg. Chim. Acta*, 1986, 117, L39.
186. M. Veith and V. Huch, *J. Organometal. Chem.*, 1986, 308, 263.
187. M. Veith, D. Käfer and V. Huch, *Angew. Chem., Int. Ed. Engl.*, 1986, 25, 375.
188. K.M. Kadish, C. Swistak, B. Boisselier-Cocolios, J.M. Barbe and R. Guillard, *Inorg. Chem.*, 1986, 25, 4336.

189. M.G.B. Drew and D.G. Nicholson, *J. Chem. Soc., Dalton Trans.*, 1986, 1543.
190. A.E. Koziol, R.C. Palenik and G.J. Palenik, *Inorg. Chim. Acta*, 1986, 116, L51.
191. H. Aghabozorg, R.C. Palenik and G.J. Palenik, *Inorg. Chim. Acta*, 1986, 111, L53.
192. K. Wieghardt, M. Kleine-Boymann, B. Nuber, J. Weiss, L. Zsolnai and G. Huttner, *Inorg. Chem.*, 1986, 25, 1847.
193. W. Wojnowski, M. Wojnowski, K. Peters, E.-M. Peters and H.G. von Schnering, *Z. anorg. allg. Chem.*, 1986, 535, 58.
194. R.T. Sanderson, *Inorg. Chem.*, 1986, 25, 1856.
195. M.J.S. Dewar, J. Friedheim, G. Grady, E.F. Healy and J.J.P. Stewart, *Organometallics*, 1986, 5, 375.
196. C. Glidewell, *Inorg. Chim. Acta*, 1986, 112, 14.
197. G. Schultz, R. Lück and L. Kolditz, *Z. anorg. allg. Chem.*, 1986, 532, 57.
198. M.J.S. Dewar and C. Jia, *Organometallics*, 6, 1987, 1486.
199. M.J.S. Dewar, G.L. Grady and E.F. Healy, *Organometallics*, 6, 1987, 186.
200. J.A. Deiters and R.R. Holmes, *J. Am. Chem. Soc.*, 109, 1987, 1686.
201. M.S. Gordon, D.R. Gano, J.S. Binkley and M.J. Frisch, *J. Am. Chem. Soc.*, 1986, 108, 2191.
202. M.S. Gordon, T.N. Truong and E.K. Bonderson, *J. Am. Chem. Soc.*, 1986, 108, 1421.
203. P.S. Neudorfl, E.M. Lown, L. Safarik, A. Jodhan and O.P. Strausz, *J. Am. Chem. Soc.*, 109, 1987, 5780.
204. I.M.T. Davidson and C.E. Dean, *Organometallics*, 6, 1987, 986.
205. M.S. Gordon, L.P. Davis, L.W. Burggraf and R. Damrauer, *J. Am. Chem. Soc.*, 1986, 108, 7890.
206. D.J. Hajdasz and R.R. Squires, *J. Am. Chem. Soc.*, 1986, 108, 3139.
207. M.R. Nimlos and G.B. Ellison, *J. Am. Chem. Soc.*, 1986, 108, 8522.
208. P. von R. Schleyer and T. Clark, *J. Chem. Soc., Chem. Commun.*, 1986, 1371.
209. B.T. Luke, J.A. Pople, M.B. Krogh-Jespersen, V. Apeloig, J. Chandrasekhar and P. von R. Schleyer, *J. Am. Chem. Soc.*, 1986, 108, 260.
210. N. Wiberg, H. Schuster, A. Simon and K. Peters, *Angew. Chem., Int. Ed. Engl.*, 1986, 23, 79.
211. E. Hengge and F. Schrank, *J. Organomet. Chem.*, 1986, 299, 1.
212. W. Wojnowski, B. Dreczewski, K. Peters and H.G. von Schnering, *Z. anorg. allg. Chem.*, 1986, 540/541, 271.
213. M. Weidenbruch, B. Blintjer, K. Peters and H.G. von Schnering, *Angew. Chem., Int. Ed. Engl.*, 1986, 23, 1129.
214. R. Jones, D.J. Williams, Y. Kabe and S. Masamune, *Angew. Chem., Int. Ed. Engl.*, 1986, 23, 173.
215. H.G. von Schnering, M. Schwarz and R. Nesper, *Angew. Chem., Int. Ed. Engl.*, 1986, 23, 566.
216. F. Shafiee, K.J. Haller and R. West, *J. Am. Chem. Soc.*, 1986, 108, 5478.
217. S. Röllner, D. Simon and M. Dräger, *J. Organomet. Chem.*, 1986, 301, 27.

218. S. Roller and M. Dräger, *J. Organomet. Chem.*, 1986, 316, 57.
219. K. Hübnerle Simon and M. Dräger, *J. Organomet. Chem.*, 1986, 312, 155.
220. R.W. Bigelow, *Organometallics*, 1986, 5, 1502.
221. K.A. Klingensmith, J.W. Downing, R.D. Miller and J. Michl, *J. Am. Chem. Soc.*, 1986, 108, 7438.
222. K. Takeda, H. Teramae and N. Matsumoto, *J. Am. Chem. Soc.*, 1986, 108, 8186.
223. G.C. Gobbi, W.W. Fleming, R. Sooriyakumaran and R. D. Miller, *J. Am. Chem. Soc.*, 1986, 108, 3624.
224. R.D. Miller, B.L. Farmer, W. Fleming, R. Sooriyakumaran and J. Rabolt, *J. Am. Chem. Soc.*, 109, 1987, 2509.
225. W.W. Schoeller and T. Dabisch, *Inorg. Chem.*, 26, 1987, 1081.
226. W.W. Schoeller, T. Dabisch and T. Busch, *Inorg. Chem.*, 26, 1987, 4383.
227. H. Matsumoto, A. Sakamoto and Y. Nagai, *J. Chem. Soc., Chem. Commun.*, 1986, 1768.
228. A. Schäfer, M. Weidenbruch, W. Saak and S. Pohl, *Angew. Chem., Int. Ed. Engl.*, 26, 1987, 778.
229. T.A. Blinka and R. West, *Organometallics*, 1986, 5, 128.
230. T.A. Blinka and R. West, *Organometallics*, 1986, 5, 133.
231. H. Püff, H. Heisig, W. Schuh and W. Schwab, *J. Organomet. Chem.*, 1986, 303, 343.
232. H. Watanabe, E. Tabei, M. Goto and Y. Nagai, *J. Chem. Soc., Chem. Commun.*, 1987, 522.
233. E.D. Jemmis, P.N.V.P. Kumar and N.R.S. Kumar, *J. Chem. Soc., Dalton Trans.*, 1987, 271.
234. C.D. Juengst, W.P. Weber and G. Manuel, S. Roller, *J. Organomet. Chem.*, 1986, 308, 187.
235. G.K. Henry, D.R. Dowd, R. Bau, G. Manuel and W.P. Weber, *Organometallics*, 1986, 5, 1818.
236. M.J. Michańczyk, M.J. Fink, K.J. Haller, R. West and J. Michl, *Organometallics*, 1986, 5, 531.
237. W. Wojnowski, K. Peters, E.M. Peters, T. Meyer and H.G. von Schnering, *Z. anorg. allg. Chem.*, 1986, 537, 31.
238. W. Ries, T. Albright, J. Silvestre, I. Bernal, W. Malisch and C. Burschka, *Inorg. Chim. Acta*, 1986, 111, 119.
239. W. Wojnowski, W. Bochenska, K. Peters, E.M. Peters, and H.G. von Schnering, *Z. anorg. allg. Chem.*, 1986, 533, 165.
240. J.A. Hawari, E.J. Gabe, F.L. Lee, M. Lesage and D. Griller, *J. Organomet. Chem.*, 1986, 299, 279.
241. F.J. Feher, *J. Am. Chem. Soc.*, 1986, 108, 3850.
242. D.M. Giolando, T.B. Rauchfuss and G.M. Clark, *Inorg. Chem.*, 26, 1987, 3080.
243. R.K. Chadha, J.E. Drake and A.B. Sarkar, *Inorg. Chem.*, 26, 1987, 2885.
244. A. Haas, H.-J. Kutsch and C. Krüger, *Chem. Ber.*, 120, 1987, 1045.
245. I. Silaghi-Dumitrescu and I. Haiduc, *Inorg. Chim. Acta*, 1986, 112, 159.
246. D.G. Anderson, A.J. Blake, S. Craddock, E.A.V. Ebsworth, D.W.H. Rankin and A.J. Welch, *Angew. Chem., Int. Ed. Engl.*, 1986, 23, 107.
247. G.H. Wiseman, D.R. Wheeler and D. Seyferth, *Organometallics*,

- 1986, 5, 146.
248. U. Kliebisch, U. Klingebiel, D. Stalke and G.M. Sheldrick, *Angew. Chem., Int. Ed. Engl.*, 1986, 23, 915.
 249. U. Kliebisch, U. Klingebiel, D. Stalke and G.M. Sheldrick, *Angew. Chem., Int. Ed. Engl.*, 1986, 23, 915.
 250. Y. Blum and R.M. Laine, *Organometallics*, 1986, 5, 2081.
 251. J.B. Lambert, J.A. McConnell and W.J. Schulz, *J. Am. Chem. Soc.*, 1986, 108, 2482.
 252. B. Tectle, A.F.M. M. Rahman and J.P. Oliver, *J. Organomet. Chem.*, 1986, 317, 267.
 253. N.H. Buttrus, C. Eaborn, S.H. Gupta, P.B. Hitchcock, J.D. Smith and A.C. Sullivan, *J. Chem. Soc., Chem. Commun.*, 1986, 1043.
 254. M.A. Guerra, T.R. Bierschenk and R.J. Lagow, *J. Am. Chem. Soc.*, 1986, 108, 4103.
 255. A.M. Arif, A.H. Cowley, T.M. Elkins and R.A. Jones, *J. Chem. Soc., Chem. Commun.*, 1986, 1778.
 256. A.G. Brook, F. Abdesaken and H. Söllradl, *J. Organomet. Chem.*, 1986, 299, 9.
 257. W.S. Rees, D.M. Schubert, C.B. Knobler and M.F. Hawthorn, *J. Am. Chem. Soc.*, 1986, 108, 5369.
 258. T.R. Bierschenk, M.A. Guerra, T.J. Juhike, S.B. Larson and R.J. Lagow, *J. Am. Chem. Soc.*, 109, 1987, 4855.
 259. J.F. Janik, E.N. Duesler and R.T. Paine, *Inorg. Chem.*, 26, 1987, 4341.
 260. D.M. Roddick, T.D. Tilley, A.L. Rheingold and S.J. Geib, *J. Am. Chem. Soc.*, 109, 1987, 945.
 261. B.K. Campion, J. Falk and T.D. Tilley, *J. Am. Chem. Soc.*, 109, 1987, 2049.
 262. J. Arnold and T.D. Tilley, *J. Am. Chem. Soc.*, 109, 1987, 3318.
 263. M. Porchia, F. Ossola, G. Rossetto, P. Zanella and N. Brianese, *J. Chem. Soc., Chem. Commun.*, 1987, 550.
 264. U. Schubert, J. Müller and H.G. Alt, *Organometallics*, 6, 1987, 469.
 265. W. Ando and T. Tsumuraya, *J. Chem. Soc., Chem. Commun.*, 1987, 1514.
 266. D.G. Anderson, J. Armstrong and S. Cradock, *J. Chem. Soc., Dalton Trans.*, 1987, 3029.
 267. D.G. Anderson, A.J. Blake, S. Cradock, E.A.V. Ebsworth, D.W.H. Rankin, H.E. Robertson and A.J. Welch, *J. Chem. Soc., Dalton Trans.*, 1987, 3035.
 268. D.G. Anderson, J. Armstrong, S. Cradock and D.W.H. Rankin, *J. Chem. Soc., Dalton Trans.*, 1987, 3061.
 269. D.W.H. Rankin and H.E. Robertson, *J. Chem. Soc., Dalton Trans.*, 1987, 785.
 270. E. Hey, P.B. Hitchcock, M.F. Lappert and A.K. Rai, *J. Organomet. Chem.*, 329, 1987, 1.
 271. A.-M. Caminade, J.-P. Majorai, R. Mathieu and Y.Y.C.Y.L. Ko, *J. Chem. Soc., Chem. Commun.*, 1987, 639.
 272. A.R. Barron and A.H. Cowley, *J. Chem. Soc., Chem. Commun.*, 1987, 1092.
 273. A.R. Barron and A.H. Cowley, *J. Chem. Soc., Chem. Commun.*, 1987, 1272.

274. G. Fritz, K. Stoll, W. Hönle and H.G. von Schnering, *Z. anorg. allg. Chem.*, **544**, 1987, 127.
275. G. Fritz and K. Stoll, *Z. anorg. allg. Chem.*, 1988, **538**, 78.
276. G. Fritz and K. Stoll, *Z. anorg. allg. Chem.*, 1988, **538**, 115.
277. G. Fritz and K. Stoll, *Z. anorg. allg. Chem.*, 1988, **539**, 65.
278. O.J. Scherer, K. Globel and J. Kaub, *Angew. Chem., Int. Ed. Engl.*, **26**, 1987, 59.
279. L. Weber and G. Meine, *Chem. Ber.*, **120**, 1987, 457.
280. V.G. Kumar Das, L.K. Mun, C. Wei and T.C.W. Mak, *Organometallics*, **6**, 1987, 10.
281. V.G. Kumar Das, L.K. Mun, C. Wei, S.J. Blunden and T.C.W. Mak, *J. Organomet. Chem.*, **322**, 1987, 363.
282. V.G. Kumar Das, L.K. Mun, C. Wei and T.C.W. Mak, *J. Organomet. Chem.*, **334**, 1987, 283.
283. S.W. Ng, C. Wei, V.G. Kumar Das and T.C.W. Mak, *J. Organomet. Chem.*, **326**, 1987, C61.
284. S.S. Al-Juaid, S.M. Dhaher, C. Eaborn, P.B. Hitchcock and J.D. Smith, *J. Organomet. Chem.*, **325**, 1987, 117.
285. Z.-T. Wang, H.-S. Wang, X.-Y. Liu, X.-K. Yao and H.-G. Wang, *J. Organomet. Chem.*, **331**, 1987, 263.
286. R.A. Howie, E.S. Paterson, J.L. Wardell and J.W. Burley, *J. Organomet. Chem.*, 1986, **304**, 301.
287. E.J. Gabe, F.L. Lee, L.E. Khoo and F.E. Smith, *Inorg. Chim. Acta*, 1986, **112**, 41.
288. J.T.B.H. Jastrzebski, G. van Koten, C.T. Knaap, A.M.M. Schreurs, J. Kroon and A.L. Spek, *Organometallics*, 1986, **5**, 1551.
289. V.G. Kumar Das V.C. Keong, N.S. Weng, C. Wei and T.C.W. Mak, *J. Organomet. Chem.*, 1986, **311**, 289.
290. H. Weichmann, J. Meunier-Piret and M. van Maerssche, *J. Organomet. Chem.*, 1986, **309**, 267.
291. S.K. Lee and B.K. Nicholson, *J. Organomet. Chem.*, 1986, **309**, 257.
292. T. Birchall and V. Manivannan, *J. Chem. Soc., Chem. Commun.*, 1986, 1441.
293. H. Puff, B. Breuer, W. Schuh, R. Sievers and R. Zimmer, *J. Organomet. Chem.*, **332**, 1987, 279.
294. S. Adams and M. Dräger, *J. Organomet. Chem.*, **323**, 1987, 11.
295. S. Adams and M. Dräger, *Angew. Chem., Int. Ed. Engl.*, **26**, 1987, 1255.
296. H. Puff, C. Bach, W. Schuh and R. Zimmer, *J. Organomet. Chem.*, 1986, **312**, 313.
297. S. Adams, M. Dräger and B. Mathiasch, *Z. anorg. allg. Chem.*, 1986, **532**, 81.
298. M.M. Amini, E.M. Holt and J.J. Zuckerman, *J. Organomet. Chem.*, **327**, 1987, 147.
299. P. Ganis, G. Valle, D. Furlani and G. Tagliavini, *J. Organomet. Chem.*, 1986, **302**, 165.
300. J.S. Tse, M.J. Collins, F.L. Lee and E.J. Gabe, *J. Organomet. Chem.*, 1986, **310**, 189.
301. J.N. Spencer, R.B. Beiser, S.R. Moyer, R.E. Haines, M.A. DiStravalo and C.H. Yoder, *Organometallics*, 1986, **5**, 118.
302. Y. Farhangi and D.P. Graddon, *J. Organomet. Chem.*, 1986, **317**, 153.

303. F. Sakai, H. Fujiwara and Y. Sasaki, *J. Organomet. Chem.*, 1986, 310, 293.
304. G. Matsubayashi, R. Shimizu and T. Tanaka, *J. Chem. Soc., Dalton Trans.*, 1987, 1793.
305. K. Shimizu, G.E. Matsubayashi and T. Tanaka, *Inorg. Chim. Acta*, 1986, 122, 37.
306. M. Austin, K. Gebreyes, H.G. Kuivila, K. Swami and J.A. Zubieta, *Organometallics*, 6, 1987, 834.
307. D. Tudela, V. Fernandez, J.D. Tornero and A. Vegas, *Z. anorg. allg. Chem.*, 1986, 532, 215.
308. V.G. Kumar Das, C. Wei, Y.C. Keong and T.C.W. Mak, *J. Organomet. Chem.*, 1986, 299, 41.
309. V.G. Kumar Das, Y. Chee-Keong and P.J. Smith, *J. Organomet. Chem.*, 327, 1987, 311.
310. V.G. Kumar Das, Y. Chee-Keong, C. Wei, P.J. Smith and T.C.W. Mak, *J. Chem. Soc., Dalton Trans.*, 1987, 129.
311. G. Valle, R. Ettore, U. Vettori, V. Peruzzo and G. Piazzogna, *J. Chem. Soc., Dalton Trans.*, 1987, 815.
312. V.I. Shcherbakov, I.K. Grigor'eva, G.A. Razuvaev, L.N. Zakharov, R.I. Bochkova and Yu.T. Struchkov, *J. Organomet. Chem.*, 319, 1987, 41.
313. C.H. Yoder, D. Mokrynka, S.M. Coley, J.C. Otter, R.E. Haines, A. Grushow, L.J. Ansel, J.W. Hovick, J. Mikus, M.A. Shermak and J.N. Spencer, *Organometallics*, 6, 1987, 1879.
314. M. Newcomb, A.M. Madonik, M.T. Blanda and J.K. Judice, *Organometallics*, 6, 1987, 145.
315. W. Clegg, C.M.J. Grievson and K. Wade, *J. Chem. Soc., Chem. Commun.*, 1987, 969.
316. S.E. Denmark, B.R. Henke and E. Weber, *J. Am. Chem. Soc.*, 109, 1987, 2512.
317. S. Dietzel, K. Jurschat, A. Tzschach and A. Zschunke, *Z. anorg. allg. Chem.*, 1986, 537, 183.
318. K.C. Molloy, T.G. Purcell, E. Hahn, H. Schumann and J.J. Zuckerman, *Organometallics*, 1986, 5, 85.
319. R.R. Holmes, R.O. Day, V. Chandrasekhar, J.F. Vollano and J.M. Holmes, *Inorg. Chem.*, 1986, 25, 2480.
320. P.J. Smith, R.O. Day, V. Chandrasekhar, J.M. Holmes and R.R. Holmes, *Inorg. Chim. Acta*, 1986, 118, 2495.
321. D.R. Senn, J.A. Gladysz, K. Emerson and R.D. Larsen, *Inorg. Chem.*, 26, 1987, 2739.
322. K.C. Molloy, K. Quill and I.W. Nowell, *J. Chem. Soc., Dalton Trans.*, 1987, 101.
323. V.G. Kumar Das, C. Wei, S.W. Ng and T.C.W. Mak, *J. Organomet. Chem.*, 322, 1987, 33.
324. F. Weller and A.-F. Shihada, *J. Organomet. Chem.*, 322, 1987, 185.
325. S. Adams, M. Dräger and B. Mathiasch, *J. Organomet. Chem.*, 326, 1987, 173.
326. T.P. Lockhart, J.C. Calabrese and F. Davidson, *Organometallics*, 6, 1987, 2479.
327. T.P. Lockhart and F. Davidson, *Organometallics*, 6, 1987, 2471.
328. S.W. Ng, C. Wei, V.G. Kumar Das and T.C.W. Mak, *J. Organomet. Chem.*, 334, 1987, 295.

329. C. Sreelatha, D.K. Srivastava, V.D. Gupta and H. Nöth, *J. Chem. Soc., Dalton Trans.*, 1987, 407.
330. E.R.T. Tiekink, *J. Organomet. Chem.*, 1986, 302, C1.
331. A.G. Davies, A.J. Price, H.M. Dawes and M.B. Hursthouse, *J. Chem. Soc., Dalton Trans.*, 1986, 297.
332. A.G. Davies, J.P. Goddard, M.B. Hursthouse and N.P.C. Walker, *J. Chem. Soc., Dalton Trans.*, 1986, 1873.
333. G. Poll, C.J. Cheer and W.H. Nelso, *J. Organomet. Chem.*, 1986, 306, 347.
334. S. Dondi, M. Nardelli, C. Pelizzi, G. Pelizzi and G. Predieri, *J. Organomet. Chem.*, 1986, 308, 185.
335. A. Glowacki, F. Huber and H. Preut, *J. Organomet. Chem.*, 1986, 308, 9.
336. E.R.T. Tiekink and G. Winter, *J. Organomet. Chem.*, 1986, 314, 85.
337. O.S. Jung, Y.S. Sohn and J.A. Ibers, *Inorg. Chem.*, 1986, 25, 2273.
338. H. Weichmann, J. Meunier-Piret and M. van Maerssche, *J. Organomet. Chem.*, 1986, 309, 273.
339. C. Silvestru, I. Haiduc, S. Klima, U. Thewalt, M. Gielen and J.J. Zuckerman, *J. Organomet. Chem.*, 327, 1987, 181.
340. H. Berwe and A. Haas, *Chem. Ber.*, 120, 1987, 1175.
341. R. Hämmäläinen and U. Turpeinen, *J. Organomet. Chem.*, 333, 1987, 323.
342. V. Chandrasekhar, C.H. Schmid, S.D. Burton, J.M. Holmes, R.O. Day and R.R. Holmes, *Inorg. Chem.*, 26, 1987, 1050.
343. R.R. Holmes, C.G. Schmid, V. Chandrasekhar, R.O. Day and J.M. Holmes, *J. Am. Chem. Soc.*, 109, 1987, 1408.
344. R.O. Day, J.M. Holmes V. Chandrasekhar and R.R. Holmes, *J. Am. Chem. Soc.*, 109, 1987, 940.
345. K.C.K. Swamy, R.O. Day and R.R. Holmes, *J. Am. Chem. Soc.*, 109, 1987, 5548.
346. T. Birchall, R. Faggiani, C.J.L. Lock and V. Manivannan, *J. Chem. Soc., Dalton Trans.*, 1987, 1875.
347. M. Porchia, U. Casellato, F. Ossola, G. Rossetto, P. Zanella and R. Graziana, *J. Chem. Soc., Chem. Commun.*, 1986, 1034.
348. T.M. Arkhireeva, B.M. Bulychov, A.N. Protsky, G.L. Soloveichik and V.K. Belsky, *J. Organomet. Chem.*, 1986, 317, 33.
349. F.W.B. Einstein, R.K. Pomeroy and A.C. Willis, *J. Organomet. Chem.*, 1986, 311, 257.
350. N. Viswanathan, E.D. Morrison, G.L. Geoffroy, S.J. Geib and A.L. Rheingold, *Inorg. Chem.*, 1986, 25, 3100.
351. C.B. Lagrone, K.H. Whitmire, M.R. Churchill and J.C. Fetting, *Inorg. Chem.*, 1986, 25, 1080.
352. H.-J. Kneuper, E. Herdtweck and W.A. Herrmann, *J. Am. Chem. Soc.*, 109, 1987, 2508.
353. T.P. Lockhart and W.F. Manders, *J. Am. Chem. Soc.*, 109, 1987, 7015.
354. R.K. Harris and A. Sebald, *J. Organomet. Chem.*, 331, 1987, C9.
355. R.E. Wasylshen and N. Burford, *J. Chem. Soc., Chem. Commun.*, 1987, 1414.
356. S.J. Blunden and R. Hill, *J. Organomet. Chem.*, 333, 1987,

- 317.
357. A. Lycka, J. Jirman, A. Kolonicny and J. Holocek, *J. Organomet. Chem.*, **333**, 1987, 305.
358. K.B. Dillon and A. Marshall, *J. Chem. Soc., Dalton Trans.*, 1987, 315.
359. H. Rüegger and P.S. Pregosin, *Inorg. Chem.*, **26**, 1987, 2912.
360. R. Barbieri, G. Alonzo and R.H. Herber, *J. Chem. Soc., Dalton Trans.*, 1987, 789.
361. J.R. Ascenso, R.K. Harris and P. Granger, *J. Organomet. Chem.*, **331**, 1987, C9.
362. T. Lockhart and W.F. Manders, *Inorg. Chem.*, 1986, **25**, 1068.
363. T. Lockhart and W.F. Manders, *Inorg. Chem.*, 1986, **25**, 583.
364. T. Lockhart, W.F. Manders and E.M. Holt, *J. Am. Chem. Soc.*, 1986, **108**, 6811.
365. T. Lockhart and W.F. Manders, *Inorg. Chem.*, 1986, **25**, 892.
366. J. Holocek and A. Lycka, *Inorg. Chim. Acta*, 1986, **118**, L15.
367. K.C. Molloy, K. Guill, S.J. Blunden and R. Hill, *J. Chem. Soc., Dalton Trans.*, 1986, 875.
368. E. Liepins, I. Zicmane and E. Lukevics, *J. Organomet. Chem.*, 1986, **306**, 327.
369. J. Holocek, M. Nadvornik, K. Handlik and A. Lycka, *J. Organomet. Chem.*, 1986, **315**, 299.
370. C. Picard, P. Tisnes and L. Cazaux, *J. Organomet. Chem.*, 1986, **315**, 277.
371. S.J. Blunden, D. Searle and P.J. Smith, *Inorg. Chim. Acta*, 1986, **119**, L31.
372. B. King, H. Eckert, D.Z. Kenney and R.H. Herber, *Inorg. Chim. Acta*, 1986, **122**, 45.
373. W.L. Wilson, R.W. Rudolph, L.L. Lohr, R.C. Taylor and P. Pyykko, *Inorg. Chem.*, 1986, **25**, 1535.
374. R.G. Wheeler, K. Laihing, W.J. Wilson, J.D. Allen, R.B. King and M.A. Duncan, *J. Am. Chem. Soc.*, 1986, **108**, 8101.